Transplantation of Mouse Embryonic Stem Cell-Derived Dopaminergic Neurons in a Unilateral 6-Hydroxydopamine Lesion Rat Model of Parkinson's Disease: Characterisation of the Fate of the Engrafted Cells and the Host Responses

Dissertation

in partial fulfilment of the requirements
for the degree of Dr. rer. nat.
in the Neuroscience Program
at the Georg August University Göttingen,
Faculty of Biology

submitted by

Keneuoe Hycianth Thinyane

born in

Leribe, Lesotho

Göttingen 2004

I hereby declare that I prepared the doctoral thesis entitled, "Transplantation of mouse embryonic stem cell-derived dopaminergic neurons in a unilateral 6-hydroxydopamine lesion rat model of Parkinson's disease: characterisation of the fate of the engrafted cells and the host responses" independently and with no other sources and aids than quoted.

……. Göttingen, September 20th, 2004

Keneuoe Hycianth Thinyane

This study was supported financially by the BMBF co-operative group grant *Dopamine producing cells in experimental models of Parkinson's Disease* (01 GN 0101) and the DFG GRK 632 *Neuroplasticity: From Molecules to Systems*.

Advisor, first member of FAC:	Prof. Dr. Walter Paulus
Second member of FAC:	Prof. Dr. Eberhard Fuchs
Third member of FAC:	Prof. Dr. Friedrich-Wilhelm Schürmann
Date of submission of the thesis:	20th September, 2004
Thesis defense:	4th November, 2004

Table of contents

List of Abbreviations

5-HT:	5-hydroxytryptamine (serotonin)
6-OHDA:	6-hydroxydopamine
BCIP/NBT:	5-bromo-4-chloro-3-indolyl phosphate/nitroblue tetrazolium
CR3:	complement receptor 3
CsA:	cyclosporine A
DA:	dopaminergic
DAB:	3,3'-diaminobenzidine
DAT:	dopamine transporter
ES:	embryonic stem (cells)
GFAP:	glial fibrillary acidic protein
i.p.:	intraperitoneal
MFB:	medial forebrain bundle
MHC:	major histocompatibility complex
MPTP:	1-methyl-4-phenyl-1,2,3,6-tetrahydropyridine
Nurr1:	nuclear receptor related-1
PD:	Parkinson's disease
PET:	positron emission tomography
s.c.:	subcutaneous
SDIA:	stromal cell line derived inducing activity
SNpc:	substantia nigra pars compacta
SNpr:	substantia nigra pars reticulata
SPE(C)T:	single photon emission (computerised) tomography
TH (+):	tyrosine hydroxylase (positive)
VM:	ventral mesencephalon
VMAT:	vesicular monoamine transporter

Chapter 1: Introduction

1. 1. Introduction to Parkinson's Disease

1.1.1. Histopathology and Symptoms

Parkinson's disease (PD) is a progressive neurodegenerative disorder characterised by tremor, akinesia and rigidity. Cognitive deficits and psychiatric disturbances are also common in advanced stages of the disease. The pathological hallmark of PD is the loss of nigrostriatal dopaminergic (DA) neurons in the substantia nigra pars compacta (SNpc) (Feldman et al., 1997; Betarbet et al., 2002; Dauer and Przedborksi, 2003). The nigrostriatal system is essential for the control of normal motor function and its degeneration leads to striatal dopamine deficiency which is believed to account for the motor impairments in PD (Fig.1.1) (Feldman et al., 1997; De Long, 2000; Chase et al., 1998). Generally, PD symptoms do not begin to appear until the striatal dopamine content is reduced by about 70 to 80% - a phenomenon thought to be due to adaptive neural responses which include increased activity of the remaining nigral dopaminergic neurons and changes in the density and/or sensitivity of striatal dopamine receptors (Feldman et al., 1997; Dunnett and Björklund, 1999). Another morphological feature of PD is the presence of intraneuronal inclusions known as Lewy bodies. In PD, Lewy bodies are found in all affected brain areas including the substantia nigra, the limbic areas and the cortex (Dauer and Przedborksi, 2003; von Bohlen und Halbach et al., 2004). In advanced PD, additional neuronal systems including noradrenergic and serotonergic neurons are also affected (Feldman et al., 1997; Dauer and Przedborski, 2003).

1.1.2. Aetiology and Pathogenesis

Parkinson's disease occurs typically in people over 50 years. The majority of PD cases (about 95%) are sporadic and do not result from any obvious genetic defects (Dauer and Przedborski, 2003). In the remaining cases, patients have a familial form which is often marked by earlier

onset and linked to mutations in genes encoding proteins such as α-synuclein and parkin which accumulate in Lewy bodies (Lotharius and Brundin, 2002; Gasser, 2003). The mechanisms involved in the degeneration of nigrostriatal dopaminergic neurons in PD are not completely understood but a range of factors including the misfolding and aggregation of proteins, mitochondrial dysfunction and oxidative stress have been implicated (Lotharius and Brundin, 2002; Dauer and Przedborski, 2003; von Bohlen und Halbach et al., 2004)

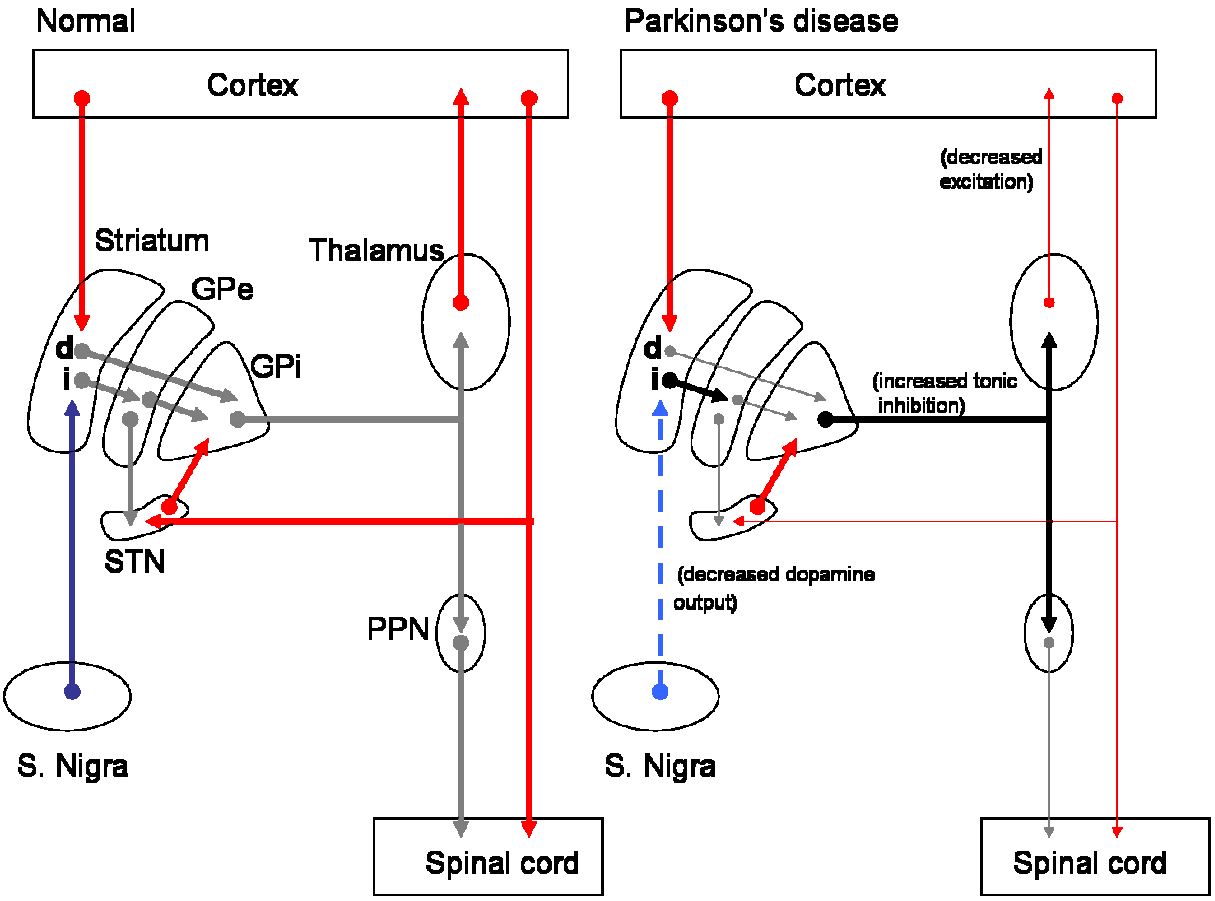

Fig. 1.1. Schematic of the basal ganglia-thalamocortical circuitry under normal conditions and in Parkinson's disease. Inhibitory connections are shown as gray and black arrows, excitatory connections as red arrows. The blue arrows represent the nigrostriatal dopaminergic pathway. Under normal conditions, dopamine action on striatal dopamine receptors initiates a cascade of events via the direct **(d)** or indirect **(i)** striatopallidal pathway leading ultimately to reduced inhibition of thalamocortical neurons and facilitation of movements initiated in the cortex. Degeneration of the nigrostriatal pathway in Parkinson's disease leads to differential changes in activity in the two striatopallidal projections, indicated by changes in the darkness or width of the connecting arrows (darker arrows indicate increased neuronal activity and lighter/thinner arrows decreased neuronal activity). The net result is increased inhibition of the thalamocortical neurons that otherwise facilitate initiation of movement. GPe – external segment of the globus pallidus; GPi – internal segment of the globus pallidus; PPN – pedunculopontine nucleus; STN – subthalamic nucleus. Adapted from Kandel et al., Principles of Neural Science (2000).

1.1.3. Clinical Treatment

Pharmacotherapy in Parkinson's disease aims to replace the dopamine that is lost as the dopaminergic neurons degenerate. Administration of the immediate dopamine precursor, levodopa (L-DOPA) is the mainstay treatment for PD patients. L-DOPA is converted to dopamine in the brain leading to replenishment of striatal dopamine levels and improvement in parkinsonian motor deficits. L-DOPA therapy is typically effective in managing the early stages of the disease. Prolonged use however commonly leads to response fluctuations, dyskinesias and the development of dopaminergic psychoses (Jenner, 2003; Rascol et al., 2003). In general, current PD medication offer symptomatic relief but none halt or retard the neurodegenerative process. There is therefore a need for the development of new therapeutic strategies for PD. Several approaches ranging from deep brain stimulation to the grafting of dopamine-producing cells have been tested with varying degrees of success in animal models of PD and in PD patients (Olanow and Brin, 2001; Dunnett and Björklund, 1999).

1.2. Overview of Animal Models of Parkinson's Disease

Animal models are essential for studying the pathogenesis of and testing new therapeutic strategies for Parkinson's disease. PD does not arise spontaneously in animals (Dunnett, 1991), thus the pathological and behavioural changes have to be mimicked by administration of neurotoxins which induce destruction of nigrostriatal dopaminergic neurons or by genetic manipulations (von Bohlen und Halbach et al., 2004). PD has been modelled in several species including non-human primates, rodents and drosophila (summarised in Table 1.1) (Betarbet et al., 2002; Dauer and Przedborski, 2003; von Bohlen und Halbach et al., 2004).

1.2.1. The 6-Hydroxydopamine (6-OHDA) Model

Intracerebral injection of the catecholaminergic neurotoxin 6-hydroxydopamine (Ungerstedt, 1968) is commonly employed to produce animal models of PD. 6-OHDA is taken up by

membrane transporter molecules and transported into the cell bodies and fibres of both dopaminergic and noradrenergic neurons (Luthman et al., 1989). Relative selectivity for the nigrostriatal dopaminergic system is achieved by injecting the 6-OHDA into the substantia nigra pars compacta, the medial forebrain bundle (MFB) - which carries the axons of the nigrostriatal tract - or the striatum and pre-treating animal test subjects with desipramine, a noradrenaline transporter blocker that inhibits the uptake of the neurotoxin into noradrenergic neurons (Feldman et al., 1997; Betarbet et al., 2002). 6-OHDA is an effective toxin for dopaminergic neurons in primates and rodents (Beal, 2001). The 6-OHDA rat model is widely used for testing novel therapeutic strategies such as cell transplantation because of relatively low maintenance costs (c.f. primates) and a more complex behavioural repertoire (c.f. mice).

Bilateral lesion of the rat nigrostriatal dopaminergic pathway with 6-OHDA produces a syndrome of severe bradykinesia that closely resembles the symptoms of PD. However bilaterally lesioned rats are akinetic, aphagic and adipsic and are thus difficult to maintain especially during the first few days after the lesion (Feldman et al., 1997; Dunnett, 1991). The standard rat model of PD is therefore produced by a unilateral stereotactic injection of 6-OHDA into the SNpc, the MFB or striatum, with the intact hemisphere serving as a control (Betarbet et al., 2002; von Bohlen und Halbach et al., 2004). Following 6-OHDA administration into the SNpc or MFB, dopaminergic neurons start degenerating within 24 hours and striatal dopamine is depleted 2 -3 days later (Jeon et al., 1995; Betarbet et al., 2002). The mechanism of 6-OHDA-induced cell death is not completely understood although the formation of free radicals which mediate cell injury has been proposed (Betarbet et al., 2002). In addition to the selective loss of nigrostriatal dopaminergic neurons, 6-OHDA neurotoxicity models some of the adaptive neural responses following loss of dopaminergic input to the striatum including heightened activity of nigral dopaminergic neurons and dopaminergic receptor upregulation in the denervated striatum (Zigmond et al., 1990a, b; Feldman et al.,

1997). The 6-OHDA model does not mimic all the features of PD: there is no formation of Lewy bodies and other brain regions such as the locus coeruleus are not affected. Furthermore, the acute nature of dopaminergic neuron degeneration in this model differs from the slow progressive nature of human PD (Betarbet et al., 2002; von Bohlen und Halbach et al., 2004).

Unilaterally-lesioned (hemiparkinsonian) rats exhibit a variety of symptoms including a spontaneous postural bias to the side ipsilateral to the 6-OHDA lesion and a quantifiable asymmetric circling behaviour (rotation) in response to dopaminergic drugs (Dunnett, 1991; Dauer and Przedborski, 2003). Indirectly acting dopamine agonists like amphetamine elicit ipsilateral rotational behaviour while dopamine receptor agonists such as apomorphine cause contralateral rotation (Fig. 1.2) (Dunnett, 1991; Feldman et al., 1997; von Bohlen und Halbach et al., 2004). This syndrome is generally viewed as analogous to the sensorimotor deficits observed in PD. The magnitude of the drug-induced rotation can be correlated with the extent of the nigrostriatal lesion (Ungerstedt, 1968; Schwarting et al., 1996; Beal, 2001) making this model suitable for evaluating the efficacy of therapeutic strategies such as cell transplantation and anti-Parkinsonian agents (Dauer and Przedborski, 2003).

1.2.2. The MPTP Model

Systemic administration of the neurotoxin 1-methyl-4-phenyl-1,2,3,6-tetrahydropyridine (MPTP) in humans produces a syndrome remarkably similar to idiopathic PD (Feldman et al., 1997; Betarbet et al., 2002; Dauer and Przedborski, 2003). MPTP toxicity in primates and mice leads to a selective degeneration of nigrostriatal dopaminergic neurons (Betarbet et al., 2002; von Bohlen und Halbach et al., 2004). Rats are relatively resistant to MPTP toxicity (Giovanni et al., 1994). In primates, depending on the treatment regimen employed, MPTP toxicity can produce an irreversible and severe parkinsonian syndrome that mimics nearly all

the behavioural deficits of PD including tremor, rigidity and freezing (Dauer and Przedborski, 2003). The MPTP model is valuable for studying the molecular mechanisms of PD pathogenesis and assessing novel therapeutic strategies for PD (Dauer and Przedborski, 2003).

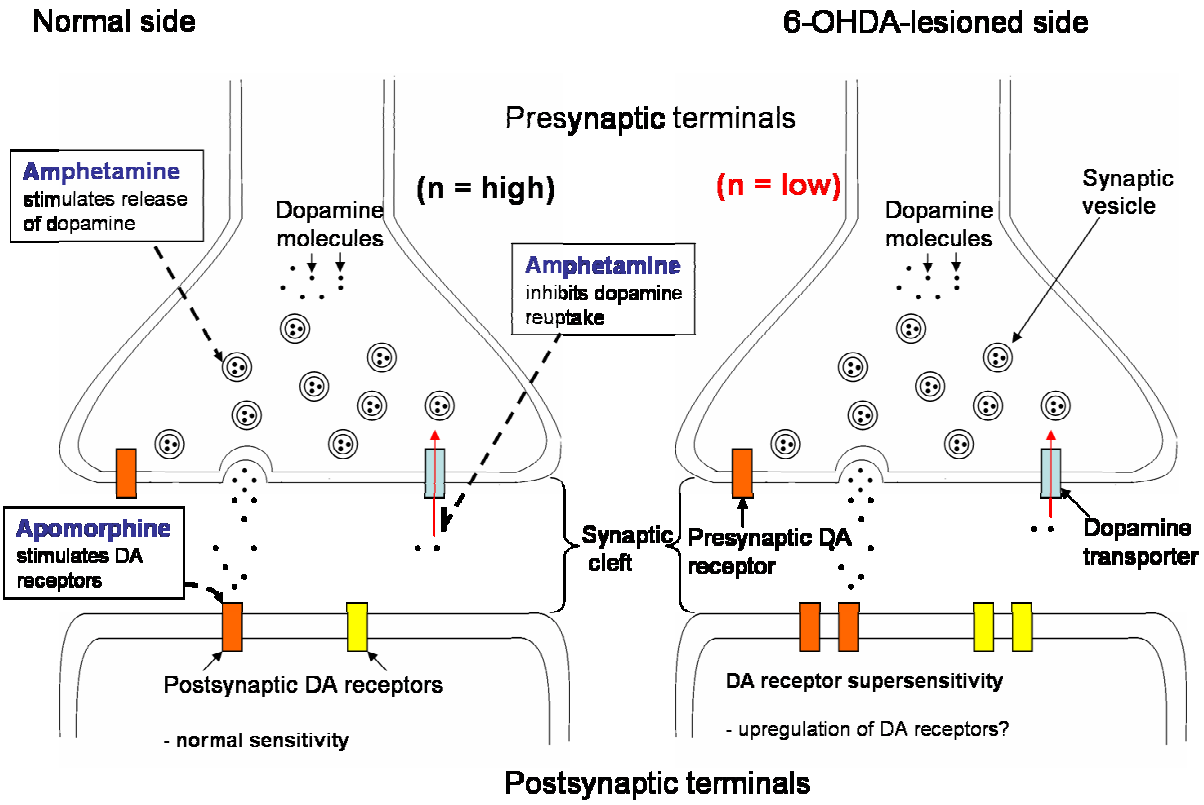

Fig. 1.2. Schematic representation of dopaminergic synapses in animals with a unilateral 6-OHDA lesion of the nigrostriatal pathway. Dopamine released from presynaptic terminals acts on postsynaptic dopamine receptors. Synaptic dopamine is taken up into presynaptic terminals by the dopamine transporter. Presynaptic dopamine receptors regulate the firing rate of the neurons and dopamine release. Denervation induces supersensitivity of dopamine receptors and this physiological imbalance between the lesioned and unlesioned striatum leads to quantifiable behavioural changes: rats will rotate contralaterally to the hemisphere in which dopamine receptor stimulation is stronger. Amphetamine therefore induces rotations ipsilateral to the lesioned side while apomorphine induces contralateral rotations.

1.2.3. The α–Synuclein Model

The discovery of PD genes has enabled the generation of novel etiologic animal models of PD. At present, most of the data come from α–synuclein-based models. Mammalian α–synuclein is located presynaptically in nerve terminals in the striatum, the substantia nigra and elsewhere (von Bohlen und Halbach et al., 2004). The physiological function of α–synuclein

is unknown. In vitro, α–synuclein protects neurons against oxidative stress and may modulate synaptic vesicle recycling (Lotharius and Brundin, 2002; von Bohlen und Halbach et al., 2004). Mutations in α–synuclein might thus promote the accumulation of dopamine in the cytoplasm leading to oxidative stress (Lotharius and Brundin, 2002). Animal models of PD have been produced by the over-expression of wild-type or mutant human α–synuclein in mice and drosophila. α–synuclein transgenic mice display neuronal atrophy and Lewy body-like α–synuclein containing inclusions. However, no mouse transgenic model has yet demonstrated a selective loss of dopamine **and** abnormal α–synuclein deposits in the substantia nigra pars compacta. Drosophila α–synuclein models are used for genetic screens to identify genes involved in α–synuclein mediated neurodegeneration (Lotharius and Brundin, 2002; Dauer and Przedborski, 2003; von Bohlen und Halbach et al., 2004).

Table 1.1. Overview of Animal Models of PD

Species	**Pathological features**	**Motor deficits**	**Applications**
MPTP-based models			
Primates	Loss of nigral dopaminergic neurons Depletion of striatal dopamine No Lewy body formation	Akinesia, rigidity, tremor, and freezing	Testing therapeutic strategies Studying the pathogenesis of Parkinson's disease
Mice		Not well characterised	
Rats	No dopaminergic neuron loss	Transient deficits after acute administration	-
6-hydroxydopamine-based models			
Primates **Rats** **Mice**	Loss of nigral dopaminergic neurons Depletion of striatal dopamine No Lewy body formation	Unilateral: spontaneous and drug-induced rotation Bilateral: bradykinesia	Testing therapeutic strategies e.g. cell transplantation, anti-parkinsonian agents
α–Synuclein-based models			
Mice	Generally: no loss of nigral dopaminergic neurons α–synuclein inclusions	Not well-characterised	Studying α–synuclein–mediated neurodegeneration
Drosophila		-	

1.3. Cell Replacement Therapy in Parkinson's Disease

One promising approach to the treatment of Parkinson's disease is the transplantation of dopamine-producing cells to restore dopaminergic neurotransmission in the striatum. Chromaffin cells of the adrenal medulla and foetal ventral mesencephalic (VM) tissue have been used in preclinical and clinical trials (Feldman et al., 1997; Isacson et al., 2003). In addition, foetal VM progenitor cells and embryonic stem (ES) cells are being investigated in preclinical studies as donors of dopaminergic neurons (Lindvall and Hagell, 2002).

1.3.1. Adrenal Medullary Cells

Although adrenal medullary chromaffin cells normally secrete mainly adrenaline and noradrenaline, they were found to produce substantial amounts of dopamine (Feldman et al., 1997). Intrastriatal grafts in hemiparkinsonian rats survived modestly, leading to amelioration of drug-induced rotation. However clinical trials showed little benefit in PD patients. Reports of serious side effects and relatively high patient morbidity led to a change of focus from these cells to foetal VM tissue (Freed et al., 1990; Kordower et al., 1997; Isacson et al., 2003.)

1.3.2. Foetal Ventral Mesencephalic Cells

Intranigral grafts of foetal VM tissue survive and restore dopamine agonist-induced rotation in hemiparkinsonian rodents (Nikkhah et al., 1994; Yurek, 1997) but fail to reinnervate the denervated striatum (Björklund et al., 1983; Nikkhah et al., 1994). Standard transplantation paradigms designed to restore dopaminergic neurotransmission therefore target the site of dopamine release, the striatum. Intrastriatal foetal VM grafts can survive and alleviate many of the 6-OHDA lesion-induced motor deficits in rats (Fisher and Gage, 1993). Despite their ectopic location, the grafted dopaminergic neurons reinnervate the host striatum and form synaptic contacts with host neurons. Furthermore they receive afferent inputs from the host and display relatively normal electrical activity (Feldman et al., 1997; Dunnett, 1991).

Over 400 PD patients have received intrastriatal grafts of human foetal VM tissue. In the most successful cases, dramatic improvement occurred and patients were able to reduce their dependence on L-DOPA treatment (Olanow et al., 1996; Piccini et al., 1999; Lindvall and Hagell, 2002). Survival of grafted dopaminergic neurons was confirmed by positron emission tomography (PET) which showed increased uptake of fluorodopa in the grafted structures up to 10 years post-grafting indicating that the grafted dopaminergic neurons were not affected by the ongoing disease process (Piccini et al., 1999; Isacson et al., 2003). [Fluorodopa is taken up by presynaptic dopaminergic terminals. The PET signal reflects the presence of dopamine in the healthy striatum, its loss in PD and its replacement by dopamine-producing neurons in transplanted patients (Barker and Dunnett, 1999)]. Post mortem histology showed robust reinnervation of the host striatum by the grafted cells (Kordower et al., 1995; 1996; 1998).

A significant number of patients have shown only a modest or transient improvement in clinical response followed by relapse and worsened condition within a year or more after grafting (Freed et al., 2001; 2003; Olanow et al., 2003). In two cases that came to autopsy, the number of surviving dopaminergic neurons was considerably lower than in previous cases where the clinical response had been more pronounced (Kordower et al., 1995; 1998). Dyskinesias have also been observed during the off-phases (periods of increased PD disability) in some transplanted patients and were proposed to be due to excessive growth of grafted dopaminergic neurons (Lindvall and Hagell, 2002). However, Hagell et al. (2002) found that the severity of post-operative dyskinesias was not related to the magnitude of graft-derived dopaminergic reinnervation. These results support the idea that restoration of dopaminergic neurotransmission by the transplantation of dopamine-producing cells can offer symptomatic relief in PD patients. The number of surviving dopaminergic neurons is a critical factor in determining the magnitude of the clinical response. The low in vivo survival rate of foetal VM-derived dopaminergic neurons (5 – 10%) means that tissue from several donors (six or

more) is needed for each PD patient to induce significant clinical improvement (Lindvall and Hagell, 2002). Technical problems associated with finding enough donors as well as ethical concerns about the need for a continuous supply of large amounts of human foetal tissue restrict the clinical application of this therapy (Lindvall, 1994; Björklund and Lindvall, 2000).

1.3.3. Foetal Ventral Mesencephalic Progenitor Cells

Committed progenitor cells from the foetal ventral mesencephalon can be expanded in vitro and induced to generate large numbers of dopaminergic neurons (Studer et al., 1998; Studer, 2001). The dopaminergic neurons survive intrastriatal grafting into hemiparkinsonian rats and alleviate some of the 6-OHDA lesion-induced motor deficits. However, the survival rate obtained with expanded progenitor cells was lower compared to that obtained with grafts of primary foetal VM tissue (Studer et al., 1998; Lindvall and Hagell, 2002).

1.3.4. Embryonic Stem Cells

ES cells are self-renewing, pluripotent cells derived from the inner cell mass of preimplantation blastocysts (Czyz et al., 2003). At present, ES cell lines have been generated from several species including mouse and human (Wobus et al., 1984; Thomson et al., 1998). Mouse ES cells are characterised by unlimited proliferation and the capacity to differentiate into all cell types of the body spontaneously or under the influence of inductive agents (Wobus et al., 1984; Doetschman et al., 1985; Bain et al., 1995; Fraichard et al., 1995). Attempts to establish pluripotent rat ES cell lines have so far failed (Buehr et al., 2003) necessitating the use of mouse ES cells for transplantation in rat models of PD. Naïve mouse ES cells differentiate into functional dopaminergic neurons after transplantation into hemi-parkinsonian rats. However, a large proportion of the grafted animals developed teratomas (Deacon et al., 1998; Björklund et al., 2002). It has been hypothesised that differentiation of ES cells prior to grafting might eliminate the risk of tumour formation in host brains.

Several groups have published protocols for the generation of dopaminergic neurons from mouse ES cells in vitro (Kawasaki et al., 2000; Lee et al., 2000; Chung et al., 2002; Barberi et al., 2003). The transcription factor nuclear receptor related-1 (Nurr1), which is expressed in post-mitotic dopaminergic neurons of the midbrain (Zetterström et al., 1996; Saucedo-Cardenas et al., 1998) is able, through its over-expression to improve the efficiency of generation of differentiated dopaminergic neurons from mouse ES cells in vitro (Kim et al., 2002; Chung et al., 2002). Kawasaki et al. (2000) identified a stromal cell-derived inducing activity (SDIA) that promotes neural differentiation of mouse ES cells with a high proportion of dopaminergic neurons. Mouse ES cell-derived dopaminergic neurons synthesize and release dopamine (Kawasaki et al., 2000; Kim et al., 2002; Barberi et al., 2003) and display normal electrophysiological activity in vitro (Barberi et al., 2003). These neurons survive intrastriatal implantation in hemiparkinsonian rodents and alleviate 6-OHDA lesion-induced motor deficits (Kawasaki et al., 2000; Kim et al., 2002; Morizane et al., 2002; Barberi et al., 2003; Baier et al., 2004). Moreover, no teratoma formation was observed in transplanted animals up to 8 weeks post-grafting - the longest survival time employed in these studies (Kim et al., 2002; Barberi et al., 2003; Baier et al., 2004).

1.4. Aim of the Thesis

The aim of this thesis was to study the survival and integration of mouse embryonic stem cell-derived dopaminergic neurons transplanted in hemiparkinsonian adult rats. Self renewing and pluripotent ES cells are a promising source of dopaminergic neurons for cell replacement therapy in PD. Undifferentiated ES cells cause teratomas when grafted into host brains (Deacon et al., 1998; Björklund et al., 2002). Until now, no tumour formation was reported following the transplantation of dopaminergic neurons derived from Nurr1-over-expressing ES cells (Kim et al., 2002). However, the use of cells expressing transgenes raises concerns about the long term safety.

We adopted the method described by Kawasaki et al. (2002) for the induction of dopaminergic neurons from mouse ES cells. SDIA-induced dopaminergic neurons were shown to survive transplantation in hemiparkinsonian mice (Kawasaki et al., 2000; Morizane et al., 2002) but no data exist on the survival, efficacy and tumourigenicity of these cells over long periods in animal models of PD. In this project, we sought to address these questions: SDIA-treated mouse ES cells were implanted intrastriatally in hemiparkinsonian adult rats. Standard histological techniques were used to analyse the survival and integration of the grafted dopaminergic neurons and the host responses after grafting. Receptor autoradiography was carried out to study lesion- and graft-induced changes in striatal D1 receptor and dopamine transporter binding. The extent of the lesion and when possible, the functional effects of the grafted cells were assessed with drug-induced rotation behaviour.

The first study **(chapter 3.1)** was undertaken to establish a unilateral 6-OHDA rat model for PD in our laboratory. We evaluated drug-induced rotation and the loss of tyrosine hydroxylase immunoreactivity in the nigrostriatal dopaminergic system post-lesioning. In the following study **(chapter 3.2)**, we transplanted pre-differentiated mouse ES cells in non-immunosuppressed hemiparkinsonian adult rats and studied the survival and functional effects of the grafted cells and the host immune response to the grafted cells. For the third study **(chapter 3.3)**, transplanted rats were immunosuppressed with cyclosporine A. We analysed the phenotype of the grafted cells, changes in the survival, distribution and morphology of the grafted dopaminergic neurons over time and the tumourigenic potential of the grafted cells. In **chapter 3.4**, I describe the host astrocytic and vascular reactions following the transplantation of pre-differentiated ES cells and examine the relationship between transplant vascularisation and grafted dopaminergic neuron viability. In the final study **(chapter 3.5),** we characterised the striatal D1 receptor and dopamine transporter binding sites and investigated the effects of denervation and transplantation of dopamine-producing cells on these parameters.

Chapter 2: Materials and Methods

2.1. Differentiation and Preparation of Embryonic Stem Cells

2.1.1. Embryonic Stem Cell Differentiation

Induction of neural differentiation was performed as described (Kawasaki et al., 2002; Baier et al., 2004). Briefly, undifferentiated mouse ES cells (MPI I) were maintained on gelatine-coated dishes in Glasgow Minimal Essential medium (G-MEM) containing 1% foetal calf serum, 10% knockout serum replacement (KSR), 2mM glutamine, 0.1mM nonessential amino acids, 1mM sodium pyruvate, 2000U/ml LIF (all from Gibco-Invitrogen; Germany) and 0.1mM 2-mercaptoethanol (2-ME) (Sigma-Aldrich; Germany). For differentiation, ES cells were cultured on mitomycin C-inactivated PA6 feeder cells (Riken cell bank; Japan) in G-MEM medium supplemented with 10% KSR, 2mM glutamine, 1mM sodium pyruvate, 0.1mM nonessential amino acids and 0.1mM 2-ME for eight days. Medium change was performed on day 4 and every other day following that. After 8 days, ES cells were cultured in induction medium [G-MEM medium with N-2 supplement, 200µM ascorbic acid, 2mM glutamine, 1mM sodium pyruvate, 0.1mM nonessential amino acids, 0.1mM 2-ME and 100µM tetrahydrobiopterin (Sigma-Aldrich)] for an additional 6 days. On day 14 of the protocol, cells were analyzed by immunocytochemistry or dissociated with Accutase™ (PAA Laboratories; Austria) for transplantation and quantification.

2.1.2. Quantification of Dopaminergic Neurons

200 randomly chosen colonies were screened for β-III-tubulin (Tuj1) and tyrosine hydroxylase (TH) labelling. Colonies containing a significant amount of Tuj1 and TH double-labelled cells were counted as positive and the percentages of positive colonies calculated. To determine cell survival after dissociation and viability before transplantation, differentiated cells were washed with phosphate-buffered saline (PBS) and exposed to Accutase™ for 20

minutes at 37°C. The enzyme was then diluted with PBS and the cells mechanically dissociated by pipetting gently up and down. Single cells were replated on gelatine-coated flask slides and cultured in induction medium for 24 hours before immunohistochemical staining using primary antibodies against Tuj1 (Babco; USA) and TH (Chemicon; USA). Using an Olympus BX60 microscope and the imaging software Analysis® (Soft Imaging System GmbH; Germany), Tuj1 positive (Tuj1+) and TH+ cells were counted in 10 randomly chosen microscopic view fields and the percentage of double-positive cells calculated.

2.1.3. Labelling of Dissociated Cells for Transplantation

After dissociation, cells were labelled with PKH26 (PKH26 Fluorescent Cell Linker Kit; Sigma-Aldrich) and resuspended in G-MEM medium supplemented with 100U/ml penicillin and 100µg/ml streptomycin (both from Gibco-Invitrogen).

2.2. Animals

The experiments were performed on male rats of the Wistar strain (average body weight approx. 300g at the beginning of the experiments). The animals were housed in pairs in ventilated sound-attenuated rooms under a 12h light/12h dark schedule at an ambient temperature of 21-23°C with food and water available *ad libitum*. Animal experiments were conducted in accordance with the European Council Directive of November 24, 1986 (86/EEC) and were approved by the Government of Lower Saxony, Germany. The minimum number of animals required to obtain consistent data was employed.

2.3. Unilateral 6-Hydroxydopamine Lesion

Before anaesthesia animals were pretreated with desipramine hydrochloride (DMI; 25mg/kg body weight i.p.) to protect noradrenergic neurons from 6-OHDA toxicity. Surgery was performed under deep i.p. ketamine:xylocaine anaesthesia (40mg/kg:5mg/kg body weight).

Each animal was placed in a stereotaxic operation frame (TSE-Systems; Homburg; Germany). Through a burr hole (position: A +2.8 mm and L +2.0 mm relative to the bregma – stereotactic coordinates according to the atlas of Paxinos and Watson, 1998), a metal canula (∅: 0.47mm; depth + 8.6mm relative to the dura) was introduced close to the medial forebrain bundle (represented schematically in Fig. 2.1). 30 - 45 minutes after DMI injection, 6-OHDA [4µl of 3.75mg/ml 6-OHDA (Sigma-Aldrich) in 0.1% ascorbic acid] was instilled at a rate of 0.5µl/min. The needle remained *in situ* for a further 4 minutes and was then slowly retracted.

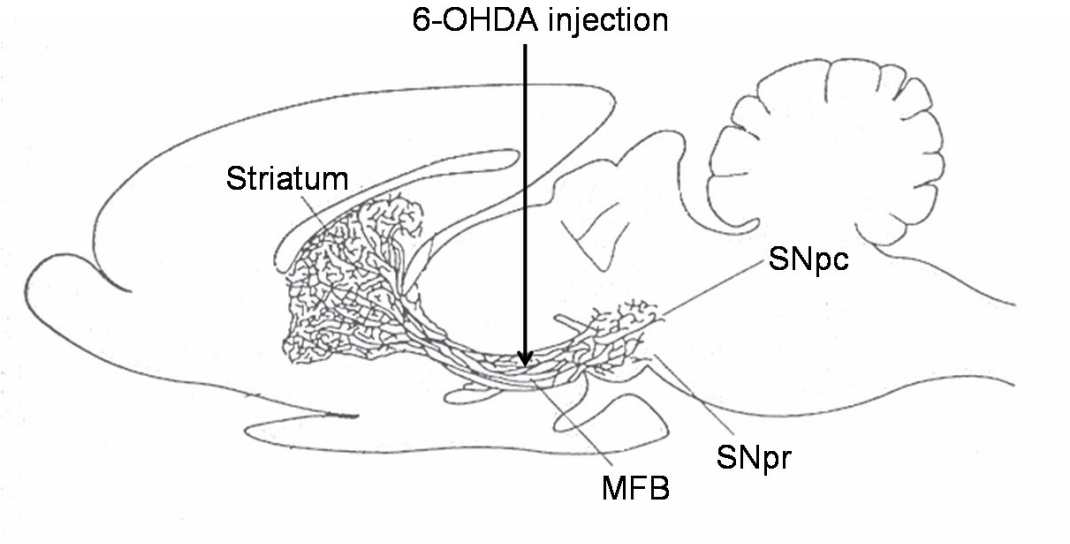

Fig. 2.1. Schematic representation of the 6-OHDA injection into the medial forebrain bundle (MFB). SNpc – substantia nigra pars compacta; SNpr – substantia nigra pars reticulata. Adapted from Feldman et al., Principles of Neuropharmacology (1997).

2.4. Behavioural Testing

The unilateral 6-OHDA lesion was evaluated with amphetamine- (AMP; Sigma-Aldrich; 1mg/kg body weight i.p.) and apomorphine- (APO; Sigma-Aldrich; 0.25mg/kg body weight s.c.) induced rotational testing on days 23 and 25 post-lesioning, respectively. Animals were placed in an automated rotameter bowl and left and right full-body turns counted. AMP net rotations over a period of 60 minutes, starting 30 minutes after injection and APO net rotations over a period of 30 minutes, starting 5 minutes after injection were determined and

the mean number of rotations per minute calculated. Animals that exhibited a mean ipsilateral score of 2 or more turns per minute were selected for transplantation surgery. All behavioural tests were repeated post-grafting (AMP day 27; APO day 29) to examine the functional effect of the implanted ES cells.

Statistical Analysis

Statistical analysis was performed using the analysis program Sigma Stat 2.03. A two-factor analysis of variance (ANOVA) was applied to the results of the behavioural tests, with treatment (cell vs. sham) and condition (pre- vs. post-transplantation) as experimental factors.

2.5. Embryonic Stem Cell Transplantation

Surgery was performed under ketamine: xylocaine anaesthesia (40mg/kg: 5mg/kg body weight i.p.) on day 28 post-lesioning. Three burr holes were drilled (position of burr hole A: A -1.8mm and L +2.2 mm, burr hole B: A -0.6mm and L +4.0mm and burr hole C: A +0.6mm and L +5.2mm relative to the bregma, with the incisor bar set to –2.5mm below the interaural line – stereotactic coordinates according to the atlas of Paxinos and Watson, 1998). Through a metal canula (∅: 0.47mm) a suspension of dissociated cells (2µl per site, $5 \cdot 10^4$ cells/µl) or vehicle (G-MEM medium with 100U/ml penicillin and 100µg/ml streptomycin) was injected at a rate of 0.5µl/min at four transplantation sites (burr hole A: 5.0mm and 6.0mm, B: 6.0mm and C: 5.0mm below the bregma) with a 10µl glass microsyringe (schematic representation in Fig. 2.2). The needle was left in situ for a further two minutes to allow the cells to diffuse. Animals received daily injections of cyclosporine A (10mg/kg body weight i.p.; Sandimmun; Novartis; Switzerland) starting 24 hours before grafting or no immunosuppressive treatment.

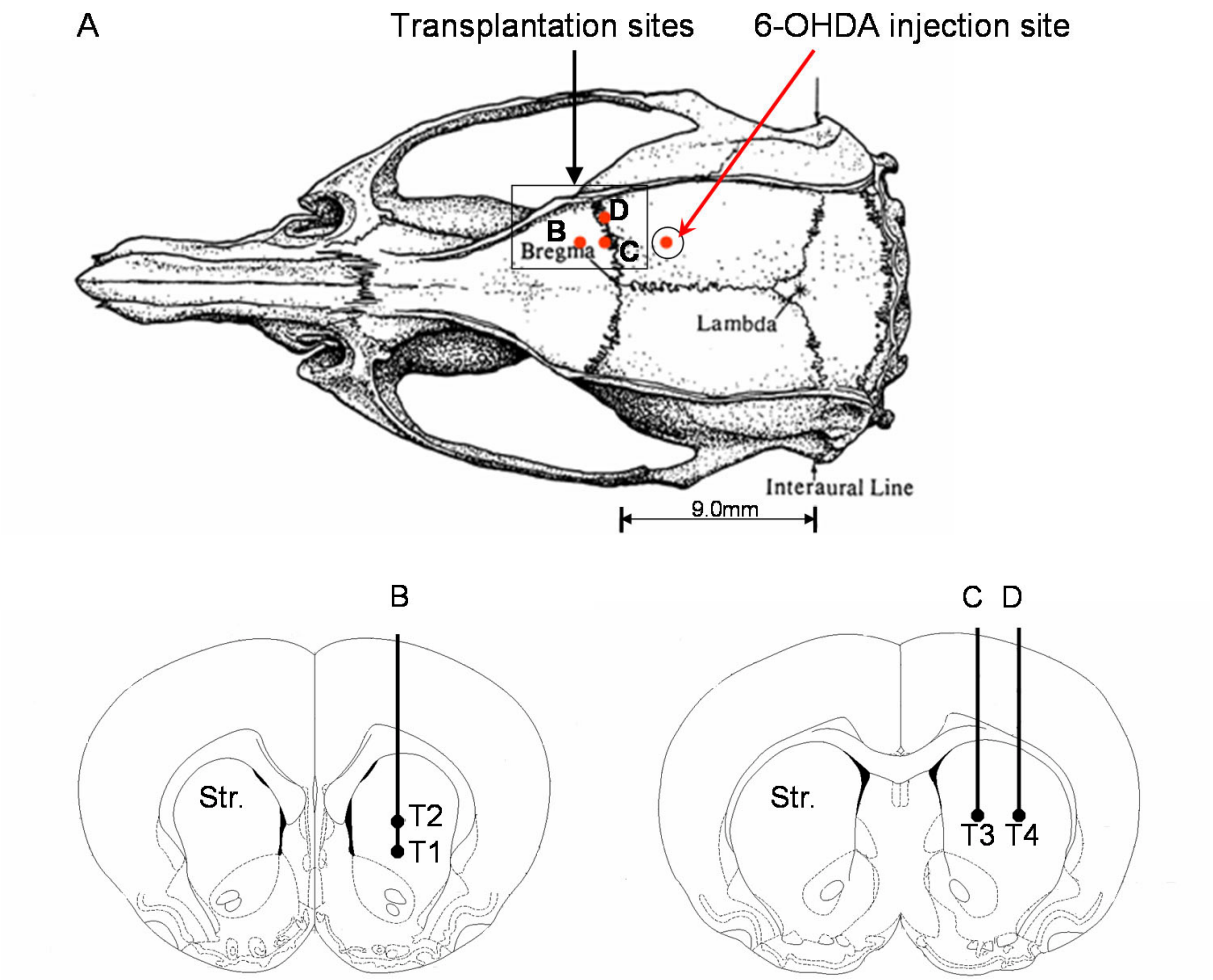

Fig. 2.2. Schematic of the rat brain. A: positions of the burr holes for transplantation (B, C and D) and 6-OHDA administration. The coronal sections depict the four transplantation sites (T1, T2, T3 and T4) within the striatum. Str – striatum. Adapted from Paxinos and Watson (1998).

2.6. Histology

2.6.1. Tissue Preparation and Histological Procedures

Animals were terminally transcardially perfused under deep ketamine anaesthesia (80mg/kg body weight) with 100ml saline for 2 minutes, followed by 200ml paraformaldehyde (4% PFA in PBS) for 8 minutes. Brains were post-fixed overnight in the same fixative, immersed in sucrose (30% in PBS) at 4°C until they sank and frozen. The brains were serially sectioned in the coronal plane at 30µm on a cryostat throughout the striatum. Six series of sections were collected and stored in PBS at 4°C. Selected sections were mounted on gelatine-coated slides for direct PKH26 visualization or Nissl staining.

2.6.1.1. Immunohistochemistry with ABC-DAB Colour Development

Free-floating tissue sections were rinsed in PBS (pH 7.2), pre-treated with 3% hydrogen peroxide in PBS for 30 minutes and incubated in 3% normal goat serum for one hour. After rinsing in PBS, sections were incubated overnight at 4°C in the primary antibodies listed in Table 2.1 followed by one hour incubation in the corresponding biotinylated secondary antibodies – goat anti-mouse or goat anti-rabbit (1:100; Vector Lab.; USA). Colour development was achieved using the Vectastain ABC and 3,3'-diaminobenzidine (DAB) kits (Vectastain ABC Kit Elite; DAB kit; Vector Lab.), used according to the manufacturer's instructions. Controls with omission of the primary antibody were performed on selected sections to verify the specificity of the primary antibodies. Immunostained sections were mounted onto gelatine-coated glass slides, coverslipped and the staining evaluated using a Zeiss Axioplan light microscope.

2.6.1.2. Visualisation of Blood Vessels

Sections were incubated in 5-bromo-4-chloro-3-indolyl phosphate/nitroblue tetrazolium (BCIP/NBT; Vector Lab.), a substrate for alkaline phosphatase in endothelial cells, for one hour. The staining was evaluated using a Zeiss Axioplan light microscope.

2.6.1.3. Immunofluorescence Studies

For single and double immunofluorescence labelling, sections were incubated overnight at 4°C in the primary antibodies (Table 2.1) followed by one hour incubation in the corresponding fluorescent-tagged antibodies – goat anti-rabbit, goat anti-mouse, rabbit anti-goat (1:200; Alexa® - Molecular Probes; USA). Fluorescence staining was examined using a Zeiss LSM 5 Pascal confocal microscope.

Table 2.1. List of Primary Antibodies

Antibody	Firm	Dilution	Antigen
Mouse anti-NeuN	Chemicon; USA	1:2000	Neuronal nuclear protein in neurons
Rabbit anti-5-HT	Zymed Laboratories; Austria	1:200	5-HT in serotonergic neurons
Mouse anti-DBH	Chemicon	1:2000	Dopamine beta hydroxylase in noradrenergic neurons
Rabbit anti-TH	Biotrend; Germany	1:500	Tyrosine hydroxylase in catecholaminergic neurons
Mouse anti-TH	Chemicon	1:5000	Tyrosine hydroxylase in catecholaminergic neurons
Rabbit anti-calbindin	Chemicon	1:2000	Calbindin in neurons
Rabbit anti VMAT-2	Chemicon	1:2000	Vesicular monoamine transporter in monoaminergic neurons
Mouse anti-GFAP	Sigma-Aldrich; Germany	1:5000	Glial fibrillary acidic protein in astrocytes
Mouse anti-ED-1	Serotec; UK	1:300	ED1 in activated microglia/macrophages
Mouse anti-OX-6	Serotec	1:80	MHC class II in activated microglia/ macrophages
Mouse anti-OX-18	Serotec	1:2000	MHC class I in activated (and a few resting) microglia/macrophages
Mouse anti-OX-42	Serotec	1:80	Complement receptor 3 (CR3) in activated microglia/macrophages
Goat anti-Ki67	Santa Cruz Biotechnology; USA	1:100	Ki67 in dividing cells

2.6.2. Quantitative Analyses

2.6.2.1. Cell Counting

Graft-derived TH+ neurons in the striatum were counted on every sixth section using a Zeiss Axioplan light microscope with a x20 lens. An approximation of the total graft cell number was calculated according to the formula of Abercrombie (1946): $P = (1/f) \times A \times [M/ (D + M)]$, where P is the corrected number of TH+ cell profiles in the grafts; f - the frequency of sections selected for immunohistochemical analysis; A – the raw count of the cell profiles; M

- section thickness in micrometers and D - average cell profile diameter in micrometers. Profile cell diameters were determined by picking one graft deposit from each section and randomly picking three TH-immunoreactive cell profiles from that deposit. The longest and shortest diameters of each profile were measured using the Stereoinvestigator 3.16 software (Microbrightfield Inc.; USA) and averaged to give the average profile diameter.

2.6.2.2. Cytomorphological Analyses

Brain sections from ≈ 1/3 of the ES cell recipients with viable grafts (n = 3 after one week; n = 4 after five weeks) were selected for a detailed light microscopic analysis. For each animal, we randomly selected 15 TH+ cells from 3 different sections throughout the graft (giving a total of 45 neurons after one week and 60 neurons after five weeks). The Stereoinvestigator 3.16 software (Microbrightfield Inc.) was used to study the following morphological parameters: size of the soma, expressed as the soma profile area, number of neurites emerging from an individual soma and the combined neurite length per soma. Morphological parameters were not assessed across multiple sections but within a single section.

2.6.2.3. Statistical Analysis

Quantitative immunohistochemical data are expressed as means ± SEM. For statistical evaluation, data were subjected to an unpaired two-tailed t-test (one week vs. five weeks survival period). For all statistical tests the significance level was set at $p < 0.05$.

2.7. In vitro Receptor Autoradiography

2.7.1. Tissue Preparation and Autoradiography

Rats were anaesthetised with ketamine and sacrificed by decapitation. The brains were rapidly removed and frozen over liquid nitrogen. 10µm coronal sections were cut at -18°C on a cryostat, thaw-mounted onto gelatine-coated slides and stored at -80°C until use. Prior to

binding experiments, sections were thawed overnight at 4°C under vacuum. Incubations were carried out as described (Mijnster et al., 1999; Isovich et al., 2000) with minor modifications.

2.7.1.1. D1 Receptor Binding

Sections were preincubated in 50mM Tris-HCl, pH 7.4 for 20 minutes at room temperature and then incubated for 90 minutes in [^{3}H]-SCH23390 (specific activity 85Ci/mmol; NEN-Dupont; MA; USA) in concentrations ranging from 0.1 – 10.0nM. The incubation buffer consisted of 50mM Tris-HCl pH 7.4, 120mM NaCl, 5mM KCl, 2mM $CaCl_2$, 1mM $MgCl_2$, 0.1% ascorbic acid and 10µM pargyline (Sigma-Aldrich) to remove endogenous serotonin. 1µM mianserin (Sigma-Aldrich) was added to the incubation buffer to prevent the binding of the ligand to 5-$HT_{2a/c}$ and α_2 binding sites. Non-specific binding was determined on consecutive sections in the presence of 5µM *cis*-(Z)-flupenthixol (RBI; MA; USA). Sections were washed 2 x 10 minutes in ice-cold distilled water and dried in a stream of cold air.

2.7.1.2. Dopamine Transporter Binding

Sections were preincubated in 50mM Tris HCl, pH 7.4 containing 120mM NaCl and 0.1% bovine serum albumin for 20 minutes at 4°C and then incubated for 2h in [^{3}H]-WIN35428 (2 beta-carbomethoxy-3beta-(4-fluorophenyl)-N-methyl-3H tropane; specific activity 84.5Ci/mmol; NEN-Dupont) in concentrations ranging from 0.1 – 15.0nM. Non-specific binding was determined on consecutive sections in the presence of 100µM (-) cocaine hydrochloride (Sigma-Aldrich). Sections were washed 2 x 1 minute in ice-cold buffer, dipped in ice-cold distilled water (30s) and dried in a stream of cold air.

2.7.1.3. Autoradiographic Film Development

All sections for autoradiographic studies were placed in light-proof cassettes and co-exposed to [^{3}H]-sensitive films (Kodak Biomax MR Film; Kodak; USA) with [^{3}H]-microscale

standards (Amersham Corp; USA) at 4°C for 10 weeks. Films were developed in Kodak GBX developer for 5 minutes at room temperature, rinsed for 30 seconds in water and fixed for 5 minutes (Kodak GBX fixer). After a final rinsing in water, films were allowed to dry.

2.7.2. Densitometry

Densitometric analysis of autoradiograms was performed with a computerised image analysis system (MCID; Imaging Inc; St. Catherines; Canada). Using calibration data from the co-exposed radioactive standards, optical densities of films were converted to tissue equivalent radioactivity and then to the number of binding sites (expressed as fmol/mg tissue). For each rat, levels of non-specific binding (as determined with *cis*-(Z)-flupenthixol or (-) cocaine) were subtracted from the total binding in order to calculate levels of specific binding.

2.7.3. Statistical Analysis

A saturation curve for [^{3}H]-SCH23390 binding was constructed using specific binding values for each ligand concentration. Non-linear regression analysis for one site binding was performed using Prism software (Graph Pad Inc.; CA; USA) to determine the maximal number of binding sites (B_{max}) and the equilibrium dissociation constant (K_d) of the D1 receptor binding sites. For [^{3}H]-WIN32548 binding, non-saturating ligand concentrations were used and the data analysed qualitatively.

Chapter 3: Results

3.1. Immunohistochemical and Behavioural Changes Induced by a Unilateral Injection of 6-Hydroxydopamine in the Rat Nigrostriatal Dopaminergic System

3.1.1. Introduction

Unilateral injection of 6-hydroxydopamine can be employed to produce animal models of PD (Betarbet et al., 2002). When injected into the medial forebrain bundle in rats (in the presence of a noradrenaline transporter blocker), 6-OHDA is transported into the cell bodies and fibres of dopaminergic neurons where it induces extensive degeneration of the dopaminergic cell bodies and nerve terminals of the substantia nigra and the striatum respectively. The extent of the lesion is dependent on the total dose of 6-OHDA injected and the stereotactic coordinates of the site of injection (Betarbet et al., 2002; von Bohlen und Halbach et al., 2004).

Neuronal death induced by the administration of a neurotoxin is followed by the activation of glial cells (Marty et al., 1991; Dusart et al., 1989; Kohutnicka et al., 1998; Cicchetti et al., 2002). Activated microglia and macrophages are involved in the removal of neuronal debris (Marty et al., 1991; Cicchetti et al., 2002). However activated microglia can release free radicals and other molecules detrimental to the survival of neurons (Fawcett and Asher, 1999; Depino et al., 2003). Since we aim to transplant pre-differentiated mouse ES cells into 6-OHDA hemi-lesioned rats in future studies, characterisation of the 6-OHDA lesion-induced inflammatory response may be beneficial in determining the optimal time for ES cell transplantation post-lesioning.

The present study was undertaken to establish a unilateral 6-hydroxydopamine lesion rat model for late-stage Parkinson's disease in our laboratory. Following stereotactic injection of 6-OHDA into the right medial forebrain bundle in rats, we quantified amphetamine- and apomorphine-induced rotation and performed immunohistochemistry for tyrosine hydroxylase to assess the extent of the lesion. We also studied the microglial and astrocytic response to the 6-OHDA-induced degeneration of dopaminergic cell bodies and nerve terminals in the substantia nigra and striatum respectively.

3.1.2. Materials and Methods

Fig. 3.1 shows the experimental design employed. 6-OHDA lesioning, behavioural tests and immunohistochemistry for TH, GFAP and ED1 were performed as described in chapter 2.

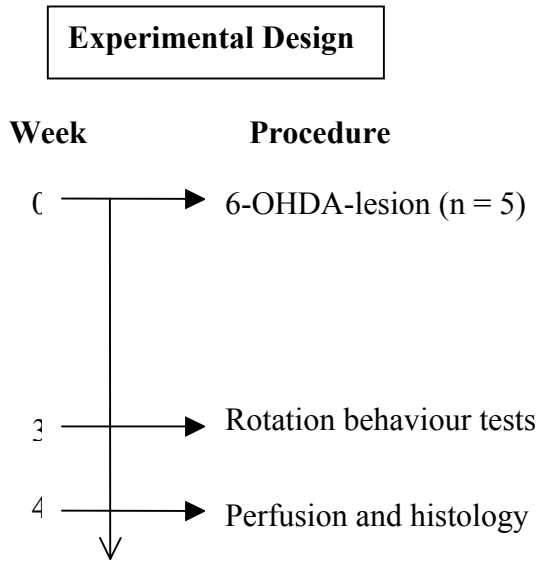

Fig.3.1. Overview of the sequence of procedures conducted during this study.

3.1.3. Results

TH Immunoreactivity

Fig. 3.2A shows TH-immunoreactivity in the substantia nigra at four weeks post-lesion. Dense clusters of TH+ cell bodies and processes are found in the substantia nigra pars

compacta (SNpc) and pars reticulata (SNpr) contralateral to the 6-OHDA lesion (C). The loss of dopaminergic cell bodies in the ipsilateral SNpc (D) was associated with a loss of TH+ terminals in the ipsilateral striatum (B). We estimated that over 90% of the striatal TH+ nerve terminals had been eliminated by the lesion.

ED1 Immunoreactivity

The ED1 antibody labels a cytoplasmic antigen found in activated microglia and macrophages. No ED1+ cells were found within the contralateral brain hemisphere (data not shown). In the ipsilateral substantia nigra, there was a high density of ED1+ cells in the pars compacta region and virtually no ED1 staining in the SN pars reticulata (Fig. 3.3A and B). Very few ED1+ cells were detected within the ipsilateral striatum (Fig. 3.3C and D).

GFAP Immunoreactivity

The GFAP antibody binds to glial fibrillary acidic protein – a type of intermediate filament found in astrocytes. When activated, astrocytes react by upregulating production of GFAP and undergoing morphological changes which include shortening of the cytoplasmic processes and nuclear enlargement. We did not detect any differences in the intensity of GFAP labelling between the ipsilateral and contralateral striatum and/or substantia nigra (data not shown).

Drug-Induced Rotation Behaviour

Table 3.1 shows the scores for amphetamine- and apomorphine-induced rotation behaviour for individual animals. The average net rotation score for the group was 1.89 ± 0.07 for amphetamine- and 4.20 ± 0.62 for apomorphine-induced rotation.

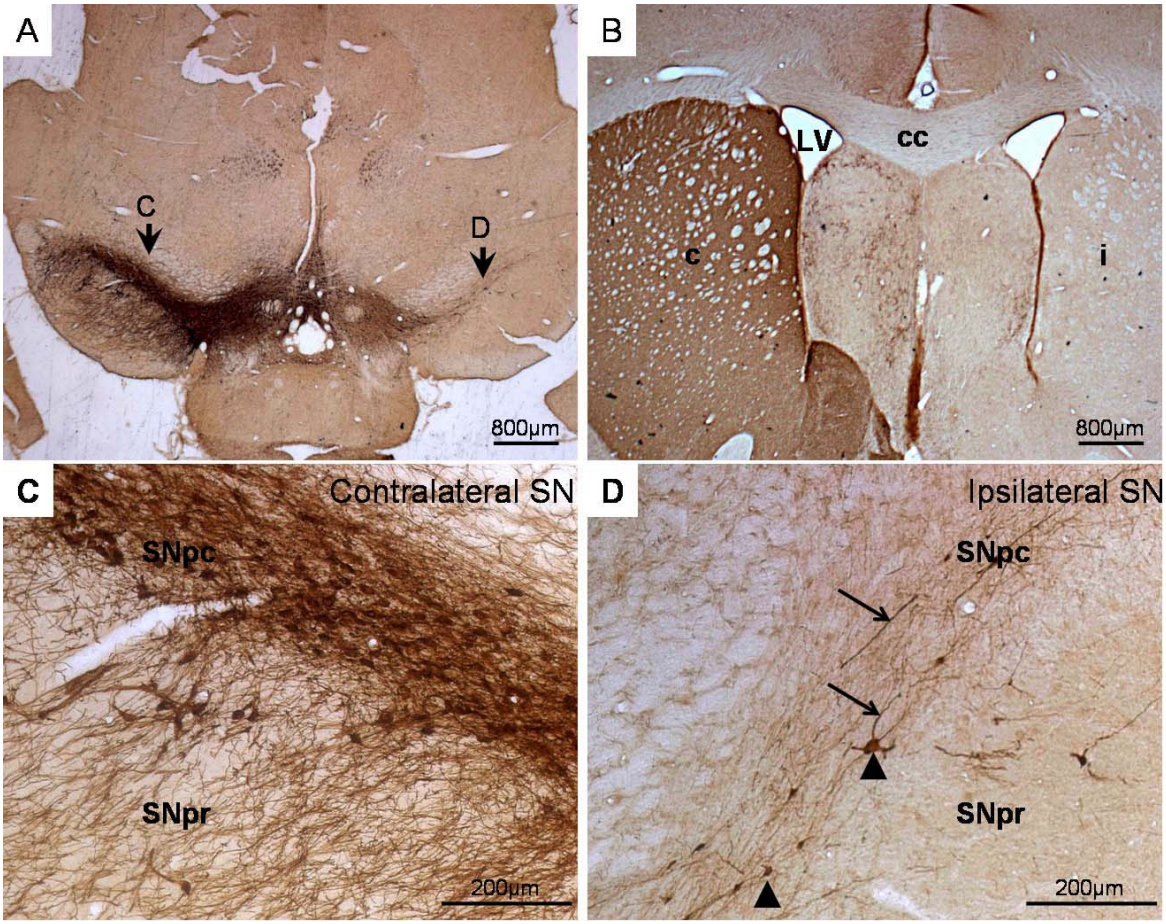

Fig. 3.2. TH-immunoreactivity in the substantia nigra (A, and at a higher power, C and D) and the striatum (B) four weeks after a unilateral 6-OHDA lesion of the nigrostriatal dopaminergic pathway in rats. (C) shows preservation of TH immunoreactivity in the substantia nigra (SN) contralateral to the 6-OHDA lesion. D: TH staining in the ipsilateral substantia nigra. Arrowheads indicate TH+ cell bodies and arrows TH+ neurites. There is a corresponding loss of TH+ nerve terminals in the ipsilateral striatum (B). SNpc – substantia nigra pars compacta; SNpr – substantia nigra pars reticulata; cc – corpus callosum; LV – lateral ventricle; c – contralateral; i – ipsilateral.

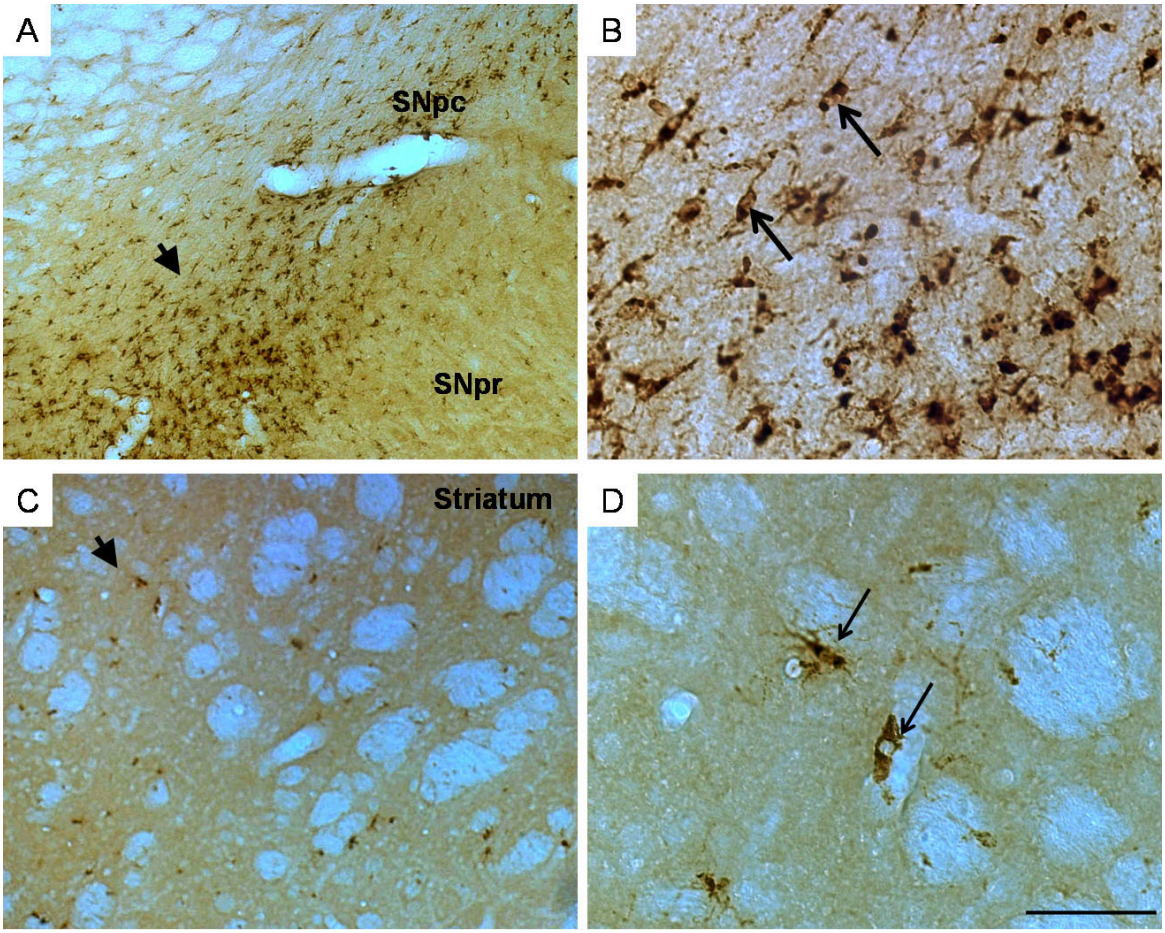

Fig. 3.3. ED1 immunoreactivity four weeks after a unilateral 6-OHDA lesion of the nigrostriatal dopaminergic pathway in rats. A: many ED1+ microglia/macrophages were found within the ipsilateral SN pars compacta (shown at a higher magnification in B) but not in the pars reticulata region. Very few ED1+ cells were found in the ipsilateral striatum (C, and at a higher power, D). Arrows in (B) and (D) indicate individual ED1+ cells. Scale bar: A, C – 200µm; B, D – 50µm.

Table 3.1. Amphetamine- and Apomorphine-Induced Rotation

Animal	AMP-induced rotation (net rotations/min)	APO-induced rotation (net rotations/min)
1	1.88	6.52
2	2.06	3.66
3	1.78	3.88
4	1.99	2.81
5	1.68	4.14
Mean ± SEM	**1.89 ± 0.07**	**4.20 ± 0.62**

Animals were challenged with amphetamine and apomorphine three weeks post-lesion. The data show the net numbers of full body turns for individual animals and the mean rotation scores for the group (n = 5).

3.2. Transplantation of Pre-differentiated Mouse Embryonic Stem Cells in Non-Immunosuppressed Hemiparkinsonian Adult Rats: Grafted Cell Survival and Host Responses[1]

3.2.1. Introduction

In a pilot study, we transplanted pre-differentiated mouse embryonic stem cells intrastriatally in 6-OHDA hemi-lesioned adult rats. Five weeks post-grafting, none of the graft recipients had surviving TH+ cells. Although the brain is an immunologically privileged transplantation site (Dunnett, 1991), intracerebral neural grafts are rejected whenever there is immunological incompatibility between donor and host tissue (Finsen et al., 1991; Duan et al., 1995).

Allogeneic grafts induce a weaker activation of the host immune response and show better survival than xenogeneic grafts (Duan et al., 1995). Until now, all attempts to establish rat ES cell lines have failed (Buehr et al., 2003) necessitating the use of mouse ES cells for transplantation in rat models of PD. Administration of the immunosuppressant cyclosporine A (CsA) can improve the survival of cross-species neural grafts (Brundin et al., 1985; Dunnett, 1995). However CsA increases locomotor activity in hemiparkinsonian rats, and may thus interfere with the locomotor effects observed following neural transplantation in conjunction with CsA immunosuppression (Borlongan et al., 1996).

We studied the survival of graft-derived dopaminergic neurons at 2, 7 and 35 days after the intrastriatal grafting of pre-differentiated mouse ES cells in non-immunosuppressed,

[1] Parts of this study have been published in: Baier PC, Schindehutte J, Thinyane K, Flugge G, Fuchs E, Mansouri A, Paulus W, Gruss P and Trenkwalder C. Behavioral changes in unilaterally 6-hydroxy-dopamine lesioned rats after transplantation of differentiated mouse embryonic stem cells without morphological integration. *Stem Cells* 22 (3):396-404, 2004.

hemiparkinsonian adult rats. Dopaminergic neuron survival was evaluated using immunohistochemistry for tyrosine hydroxylase, the rate-limiting enzyme for dopamine synthesis in dopaminergic synaptic terminals. We also characterised the host responses to the grafted cells using antibodies directed against the following antigenic structures: ED1 (in activated microglia and macrophages), complement receptor 3 (CR3, in resting and activated microglia and macrophages), major histocompatibility complex (MHC) class I and class II and GFAP. Amphetamine- and apomorphine-induced rotation behaviour was evaluated at four weeks post-grafting to assess the therapeutic benefit of the grafted cells.

3.2.2. Materials and Methods

The experimental design is shown in Fig. 3.4. Surgery, behavioural testing and histology were performed as described in chapter 2.

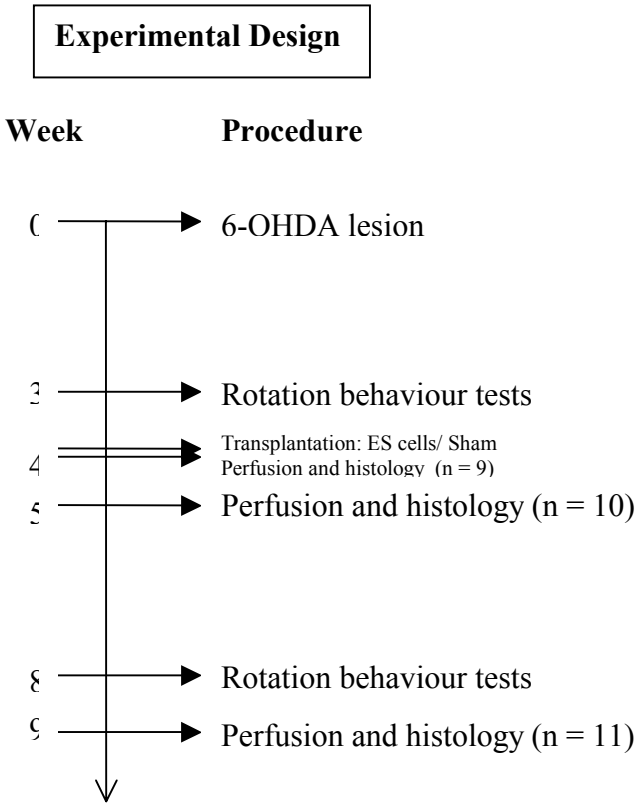

Fig. 3.4. Overview of the sequence of procedures conducted during this study. Animals were perfused at 2, 7 and 35 days post-grafting. For each survival period, 4 – 6 animals received sham- or pre-differentiated ES cell transplants.

3.2.3. Results

Detection of Transplanted Cells

We detected PKH26 fluorescence in the corpora striata of all ES cell recipients up to five weeks post-grafting (Fig. 3.5). Nissl staining revealed that at all time points, ES cell grafts exhibited a higher cell density than the surrounding host tissue (Fig. 3.5). It was not possible to distinguish between graft-derived neurons and infiltrating host immunostimulatory cells.

TH Immunoreactivity after 2 and 7 Days

2 days after grafting, 2 out of 4 ES cell recipients had grafts with < 10 TH+ neurons. After one week, 2 out of 5 ES cell recipients had viable grafts with several TH+ cells (< 100 per striatum). These cells had a neuron-like morphology with distinct TH+ cell bodies and short neurites which did not extend into the surrounding striatal tissue (inset, Fig. 3.6B).

Immunohistochemistry after Five Weeks

After five weeks, 3 out of 6 ES cell recipients had viable grafts. The TH+ cell bodies in these grafts formed clusters at the graft core and did not possess any neurites (Fig. 3.6A and at a higher power, B). It was not possible to identify or count individual cell bodies. At this time point, reactive astrocytes – characterised by hypertrophied cell bodies and short, thick processes - formed a tight glial scar surrounding the grafted cells (Fig. 3.6C and D).

Host Immune Responses: Sham vs. Cell-Transplanted Animals

We studied the nature and time course of the development of the rat immune response to the intrastriatal implantation of pre-differentiated mouse ES cells. Sections from sham animals were used to assess the immune response to the injury caused by the needle during grafting. Extracellular molecules released following central nervous system (CNS) injury lead to activation of microglia which react by enhancing their expression of surface markers like

complement receptor 3 and MHC class I (Jensen et al., 1997; Kullberg et al., 2001). At later time points, activated microglia express MHC class II antigens which is indicative of the induction of the host immune response. Due to technical problems we did not evaluate CR3, MHC class I and MHC class II immunoreactivity after 2 days. Although the general pattern of activation and recruitment of immunostimulatory cells was common to sham- and ES cell-grafted animals, all responses were more pronounced and persisted for a longer period in mouse ES cell recipients than in sham animals.

Astroglial Reactions

One week post-grafting, astrocytes in the ipsilateral striatum displayed increased GFAP immunoreactivity. Several astrocytes were found within grafts but we could not determine whether they were graft- or host-derived (Fig. 3.7A). After five weeks, reactive astrocytes formed a tight glial scar at the graft border (Fig. 3.7C). Sham animals showed reduced astrogliosis at both time points (Fig. 3.7B and D).

Detection of Activated Microglia/Macrophages: ED1 Immunoreactivity

2 days post-grafting, ED1+ cells were found mainly within grafts. There were no detectable differences in the number and/or distribution of infiltrating cells between ES cell recipients and sham animals (Fig. 3.8A and B). After one week, ED1+ cells were distributed over a larger area of the ipsilateral striatum with the highest density of stained cells within grafts and in the adjacent host tissue (Fig. 3.8C and D). In some animals, ED1 immunoreactivity was detected in the overlying cortex close to the canula track (data not shown). At five weeks post-grafting, the number of ED1+ cells was reduced (Fig. 3.8E and F). No ED1 staining was detected in the contralateral brain hemisphere.

Detection of Microglia/Macrophages: Complement Receptor 3 Immunoreactivity

The OX42 antibody binds to the CR3 antigen expressed by resting and activated microglia and macrophages. Resting microglia have small cell bodies and irregular, angular processes. In contrast, activated microglia are round, non-branched and indistinguishable from macrophages (Kullberg et al., 2001). Fig. 3.9 shows OX42 immunoreactivity in sham animals and ES cell recipients. After one week there was extensive infiltration of microglia-like CR3-epxressing cells into grafts. Several round cells resembling macrophages were also detected. Increased staining for CR3 persisted up to five weeks post-grafting.

MHC Class I and Class II Immunoreactivity

The OX18 and OX6 antibodies bind to MHC class I and class II antigens respectively. One week after grafting, ES cell recipients exhibited large numbers of macrophage-like MHC class I-expressing cells in and around grafts. MHC class I-expressing cells with a microglial morphology were detected in graft recipients after five weeks and in sham animals at both time points (Fig. 3.10). After one week, the majority of MHC class II-expressing cells within ES cell grafts had a macrophage-like morphology. Microglia-like cells were predominant in sham animals at one week and after five weeks in both sham and ES cell-transplanted animals (Fig. 3.11).

Drug-Induced Rotation Behaviour

The majority of the grafted animals showed a significant reduction in amphetamine-induced rotation at four weeks post-grafting (mean rotation score: pre-grafting - 4.33 $\pm$ 0.5; post-grafting 3.7 $\pm$ 1.9 net rotations per minute). In contrast, all sham-operated animals displayed an increase in this parameter (mean rotation score: pre-grafting - 4.0 $\pm$ 0.3; post-grafting - 6.4 $\pm$ 0.4 net rotations per minute). There was no significant change in either group in apomorphine-induced rotation (Fig. 3.12).

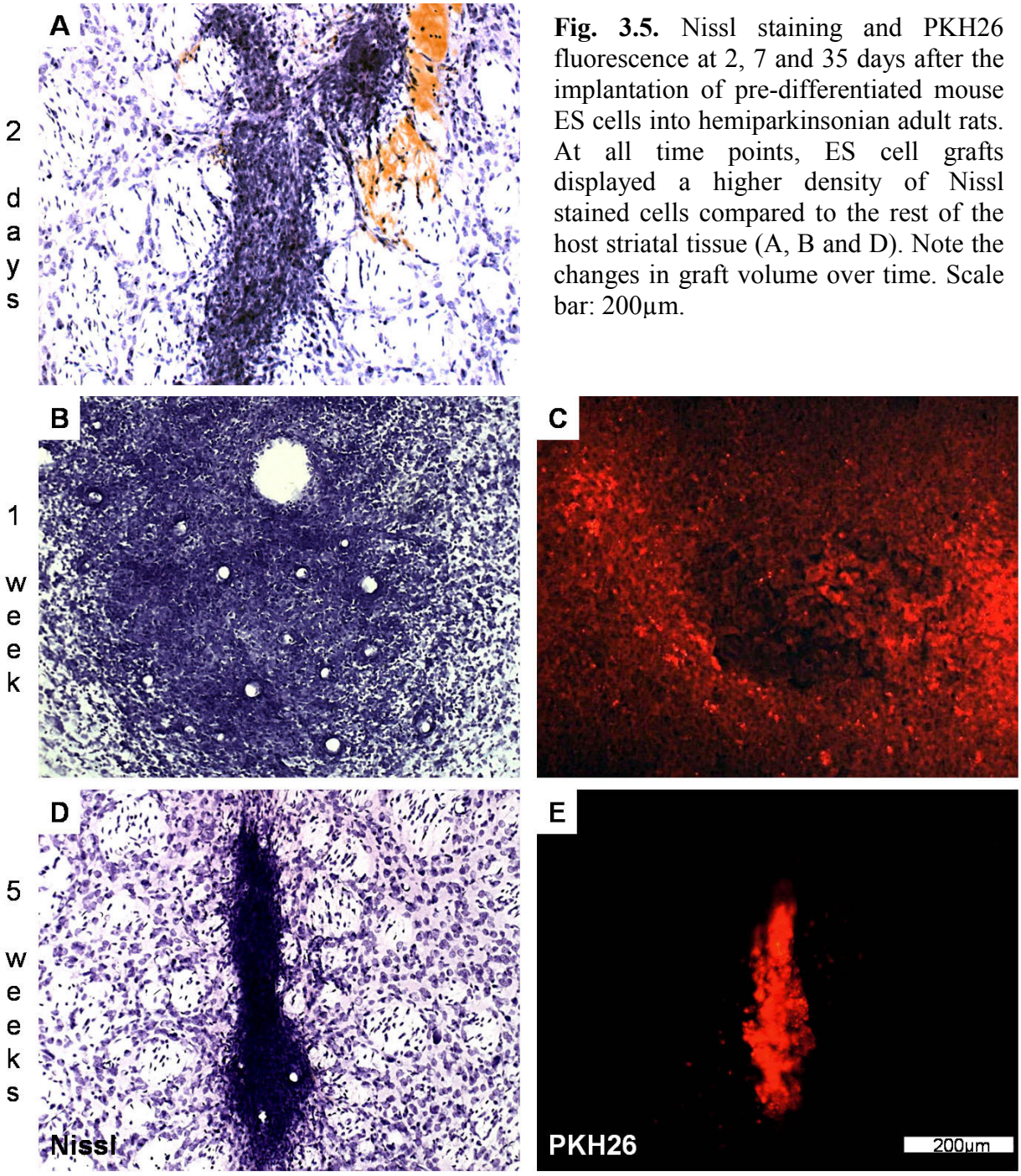

Fig. 3.5. Nissl staining and PKH26 fluorescence at 2, 7 and 35 days after the implantation of pre-differentiated mouse ES cells into hemiparkinsonian adult rats. At all time points, ES cell grafts displayed a higher density of Nissl stained cells compared to the rest of the host striatal tissue (A, B and D). Note the changes in graft volume over time. Scale bar: 200µm.

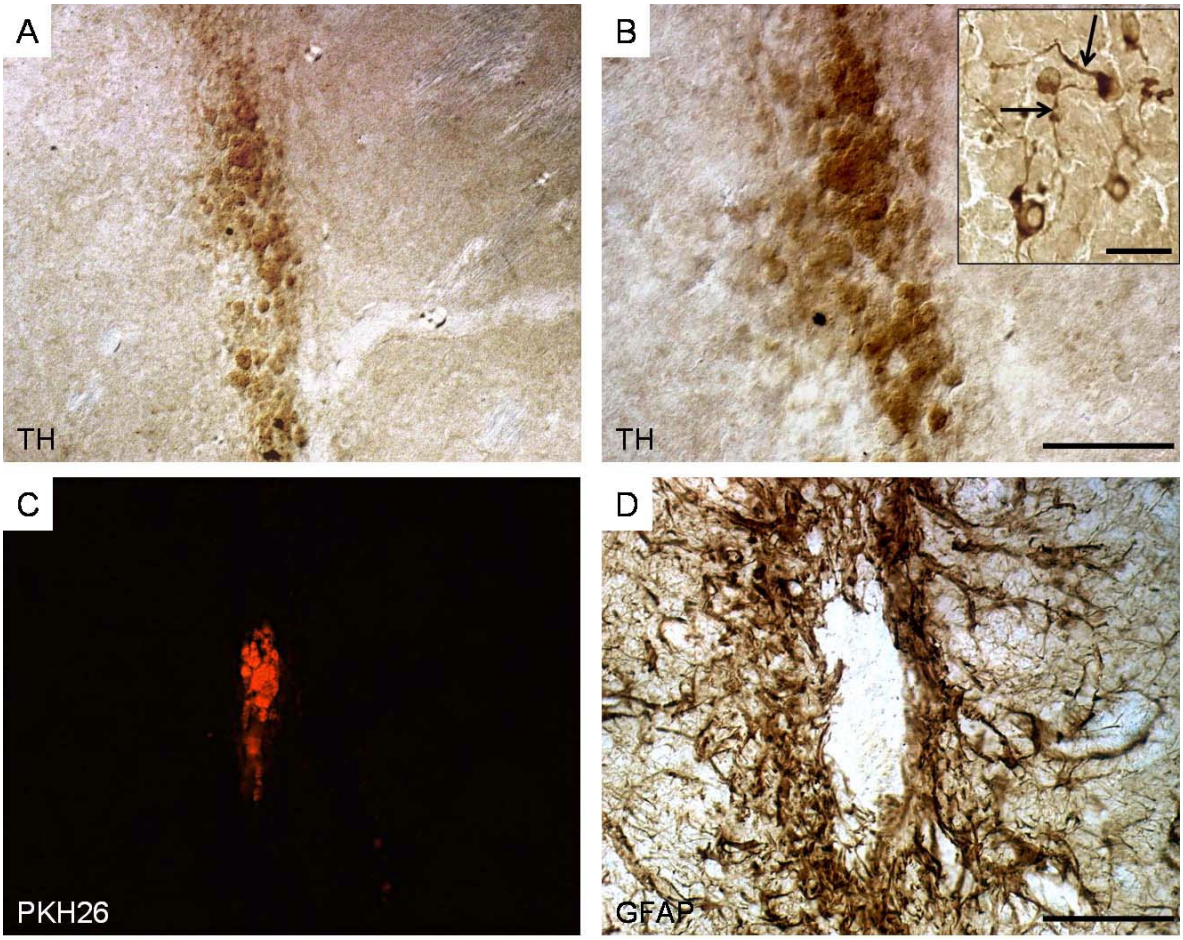

Fig. 3.6. Five weeks after the intrastriatal transplantation of pre-differentiated mouse ES cells in hemiparkinsonian adult rats. Clusters of TH+ cell bodies occupy the core of the graft (A, and at a higher power, B). These cells do not possess neurites characteristic of mature dopaminergic neurons. The inset in (B) shows TH+ neurons at one week post-grafting – arrows indicate TH+ neurites. After five weeks, reactive astrocytes formed a glial scar at the host-graft interface. No PKH26 labelling was detected outside this scar (C and D). Scale bars: A, C, D – 100μm; B and inset – 50μm.

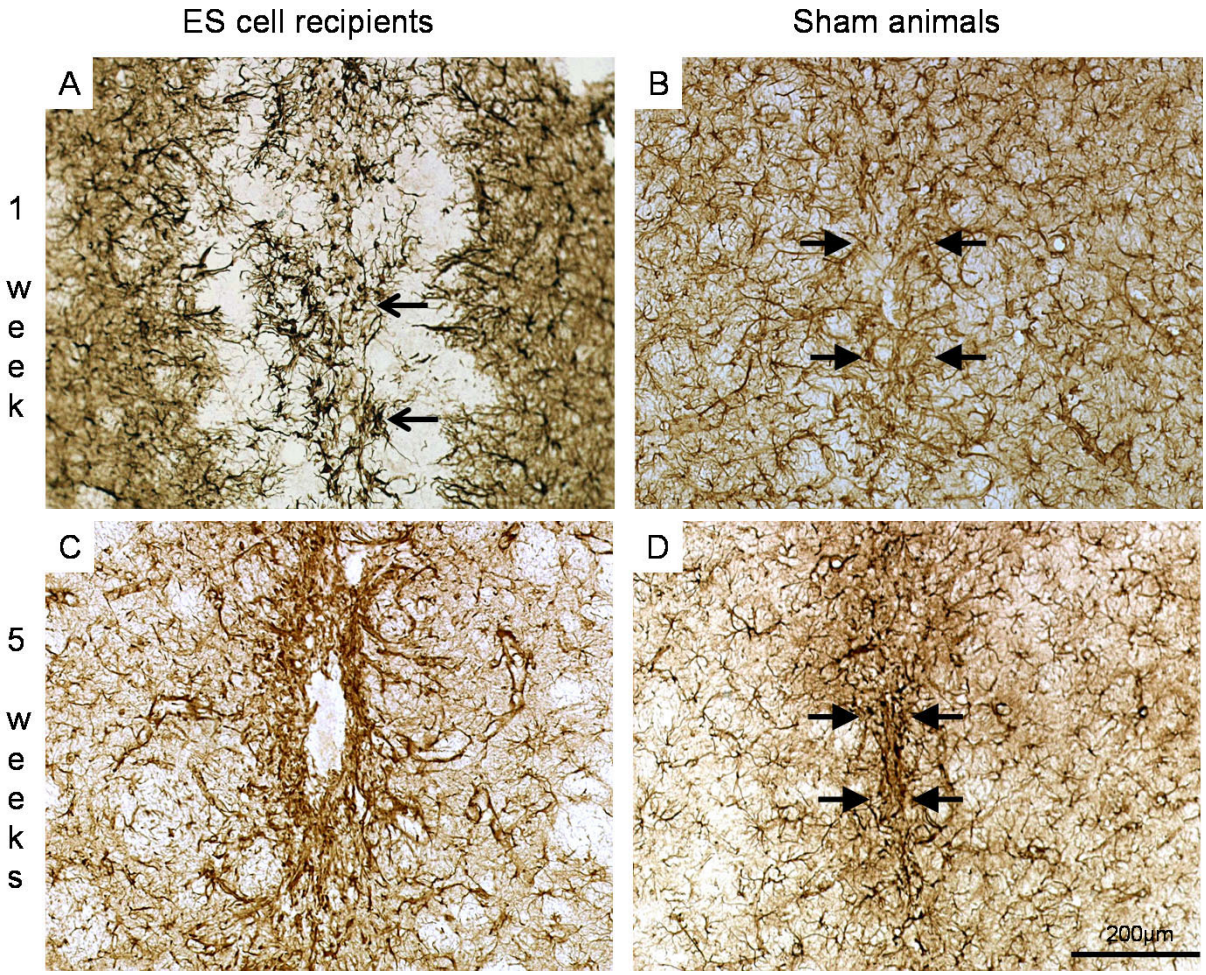

Fig. 3.7. GFAP-immunoreactivity in cell recipients and sham animals at one and five weeks after the intrastriatal implantation of pre-differentiated mouse ES cells/vehicle respectively in hemiparkinsonian adult rats. A: after one week, the number of reactive astrocytes had increased around the transplantation site and within the ipsilateral striatum. Several astrocytes were also detected within grafts (open arrows in A). After five weeks, astrocytes formed a glial scar around the graft (C). Sham animals showed reduced astrogliosis at both time points (B and D). Closed arrows in (B) and (D) indicate the outline of the transplantation sites. Scale bar: 200µm.

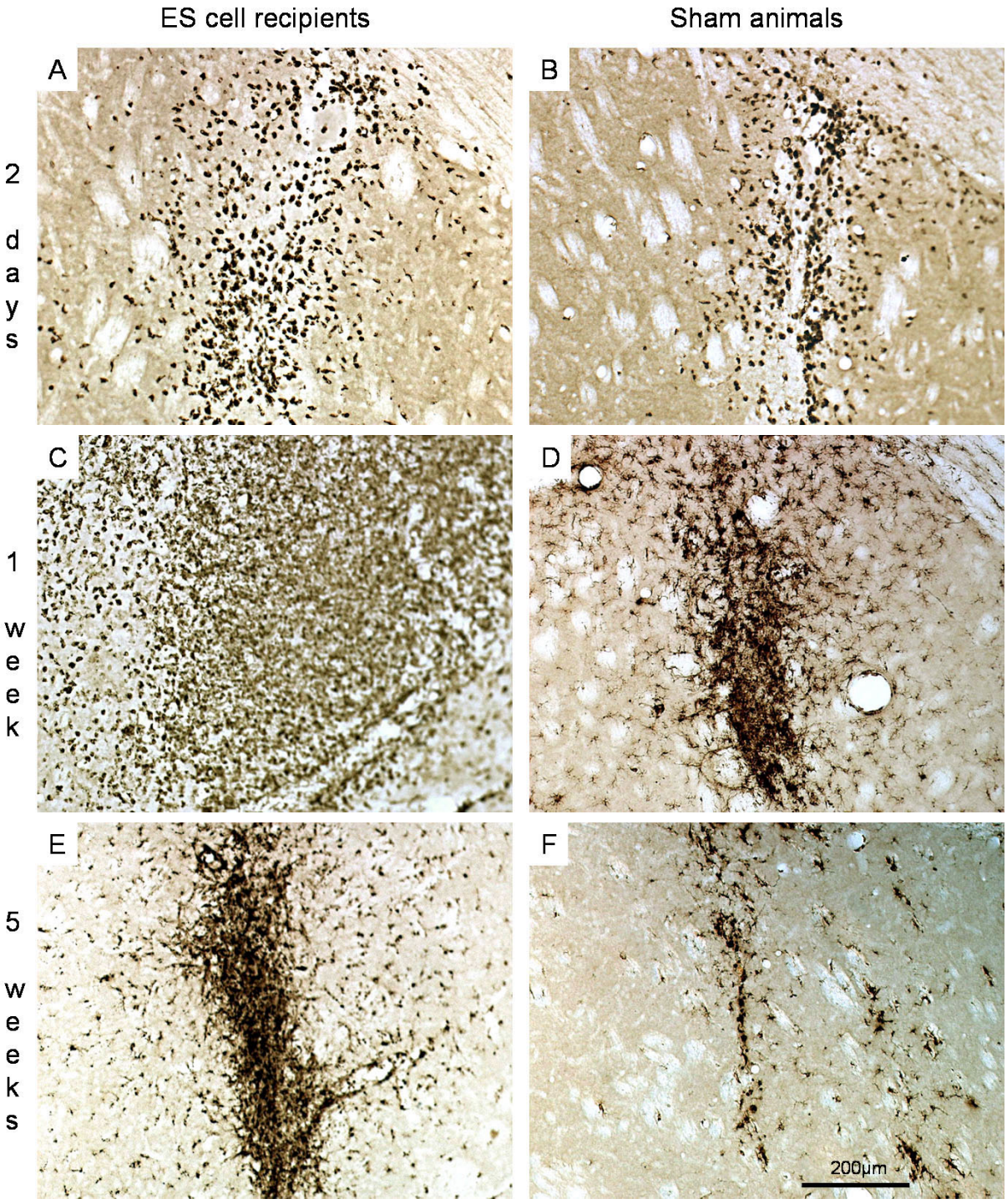

Fig. 3.8. ED1-immunoreactivity in cell recipients and sham animals after the intrastriatal implantation of pre-differentiated mouse ES cells/vehicle respectively in hemi-parkinsonian adult rats. ED1 labelling was detected at the implantation site as early as two days post-grafting. Note the differences in the density and distribution of ED1+ microglia/macrophages between sham animals and ES cell recipients and the changes in these parameters over time. Scale bar: 200µm.

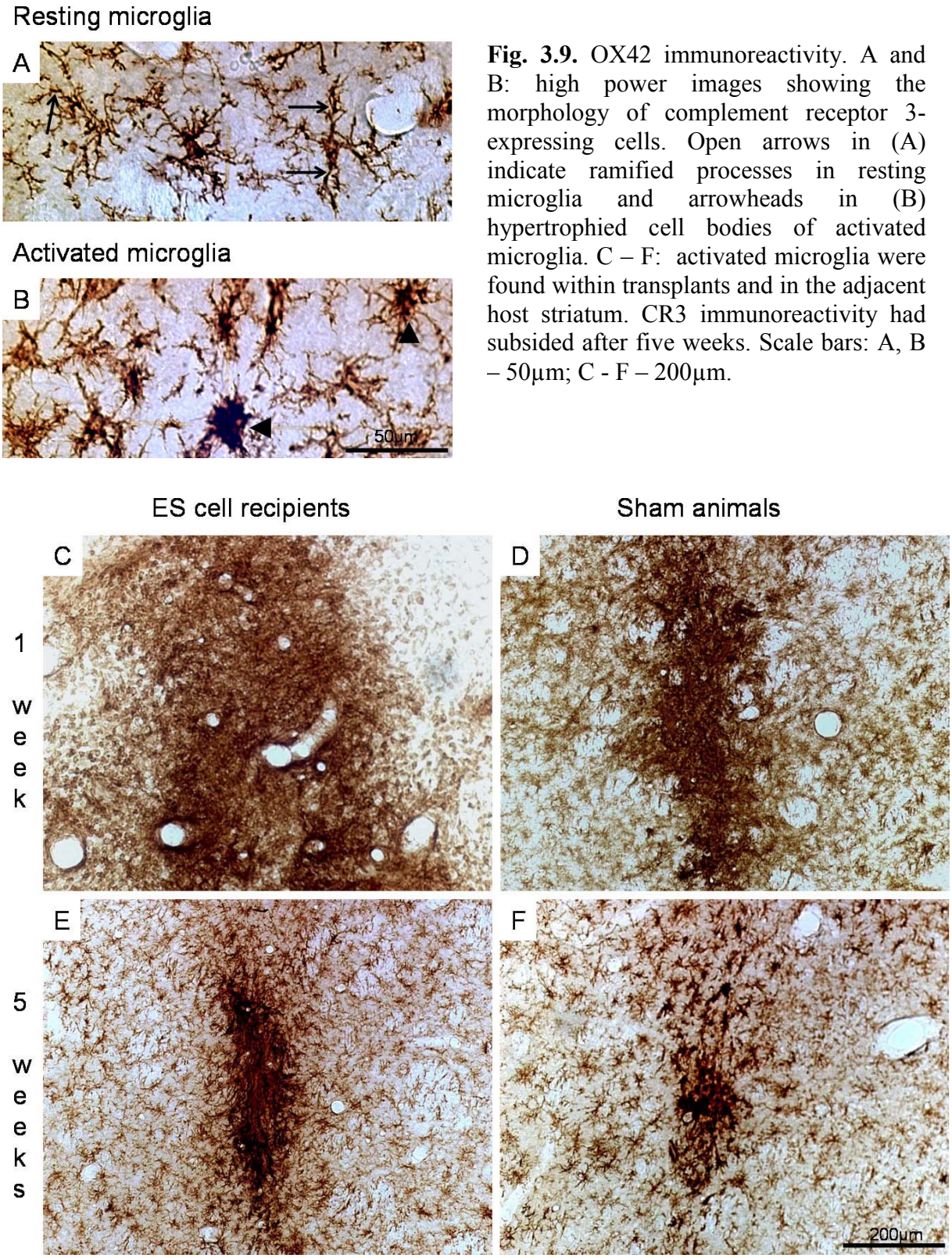

Fig. 3.9. OX42 immunoreactivity. A and B: high power images showing the morphology of complement receptor 3-expressing cells. Open arrows in (A) indicate ramified processes in resting microglia and arrowheads in (B) hypertrophied cell bodies of activated microglia. C – F: activated microglia were found within transplants and in the adjacent host striatum. CR3 immunoreactivity had subsided after five weeks. Scale bars: A, B – 50µm; C - F – 200µm.

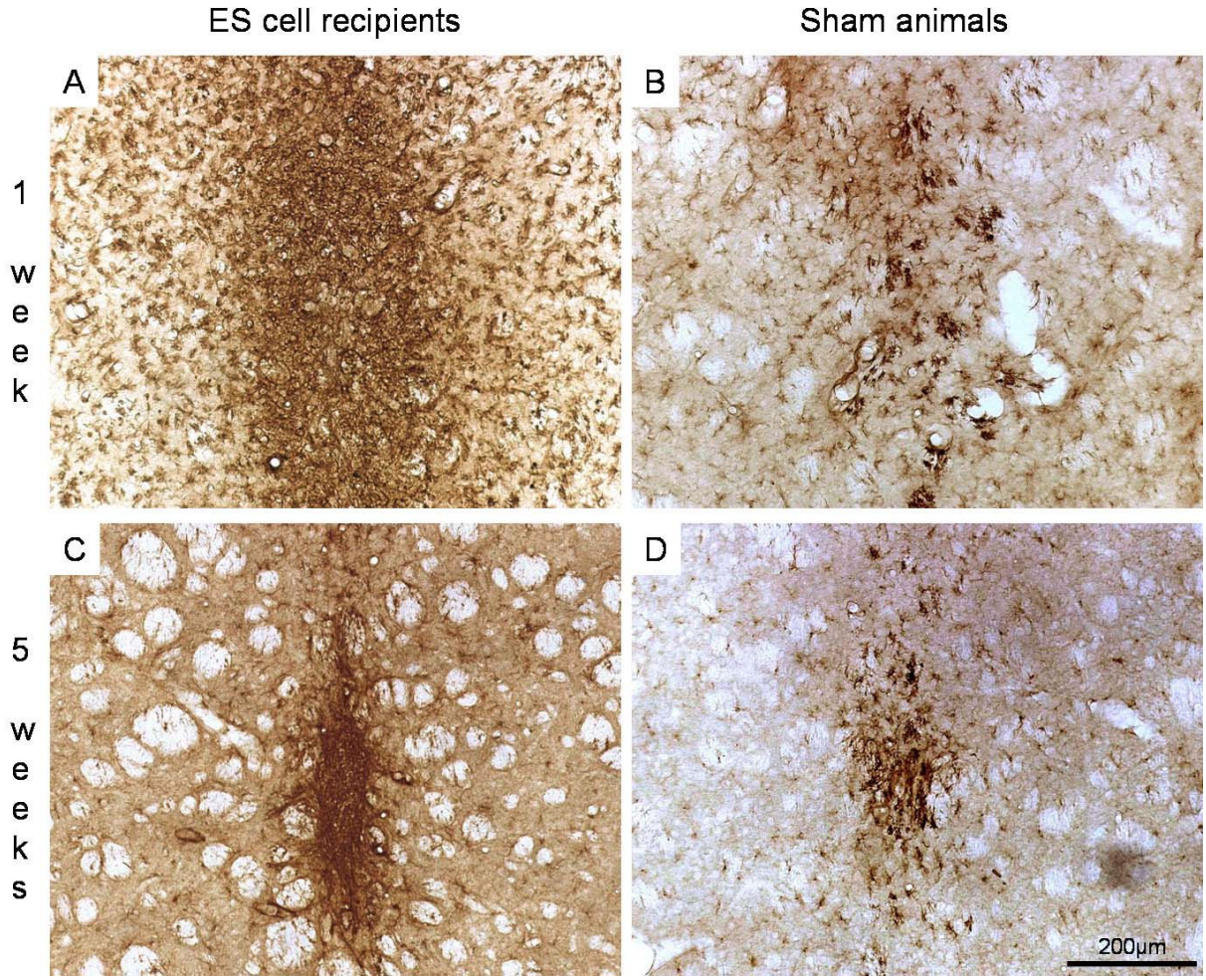

Fig. 3.10. OX18 immunoreactivity at one and five weeks post-grafting. At both time points, the number of MHC class I-expressing cells was higher in ES cell recipients than in sham animals. Scale bar: 200µm.

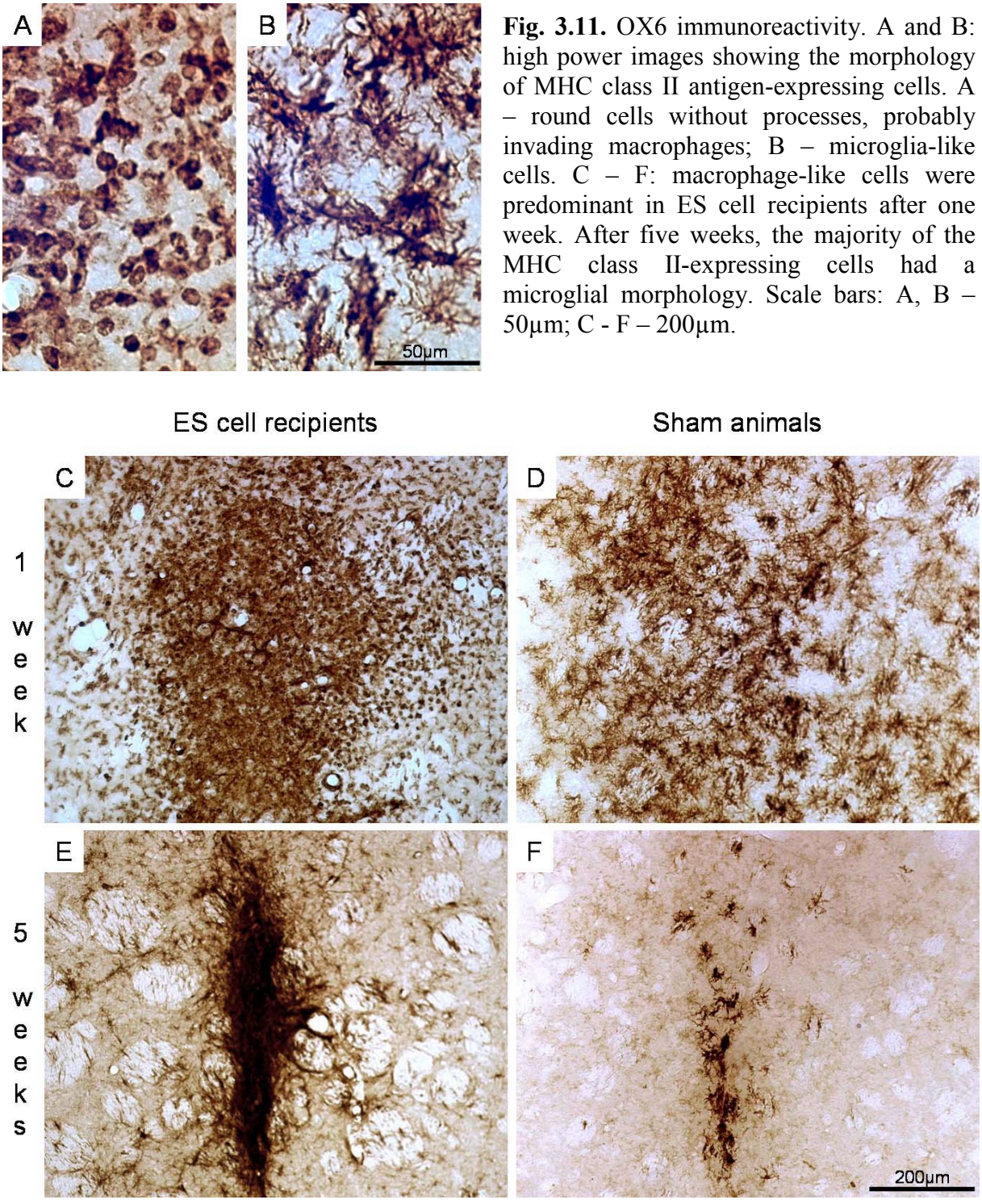

Fig. 3.11. OX6 immunoreactivity. A and B: high power images showing the morphology of MHC class II antigen-expressing cells. A – round cells without processes, probably invading macrophages; B – microglia-like cells. C – F: macrophage-like cells were predominant in ES cell recipients after one week. After five weeks, the majority of the MHC class II-expressing cells had a microglial morphology. Scale bars: A, B – 50µm; C - F – 200µm.

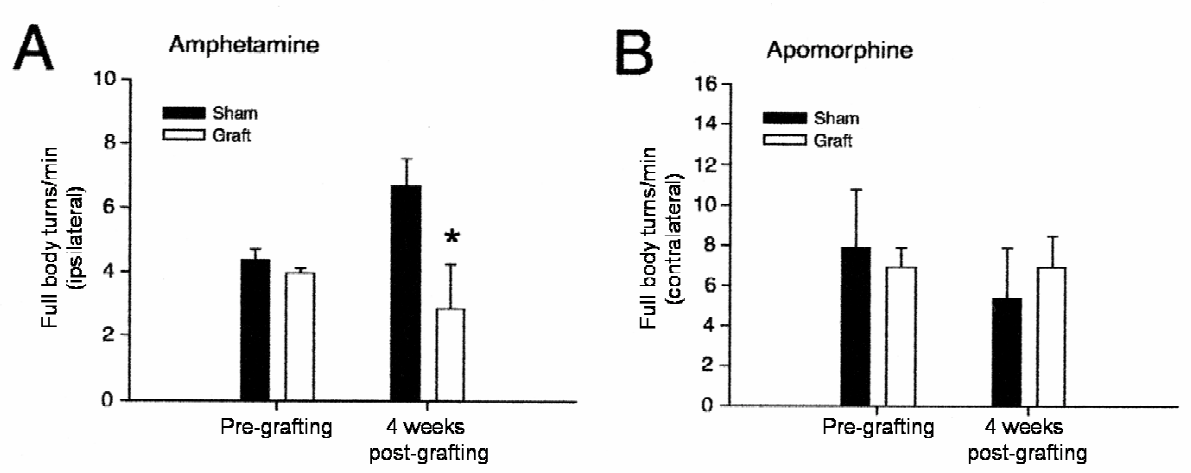

Fig. 3.12. For the pregrafting rotametry data, sham and graft refer to the data from animals that were later selected for sham- and mouse ES cell transplantation respectively. A: amphetamine (1 mg/kg i.p.)-induced rotations showed a significant difference post-transplantation between grafted and sham-operated animals with a reduction in the grafted group (n = 6), and an increase in sham-operated animals (n = 5) ($F_{1,19} = 6.537$, $P < 0.05$). B: there was no change in apomorphine (0.25 mg/kg s.c.) - induced rotation behaviour ($F_{1,19} = 1.294$, not significant). Error bars represent the standard error of the mean. From: Baier et al. (2004).

3.3. Transplantation of Pre-differentiated Mouse Embryonic Stem Cells in Immunosuppressed Hemiparkinsonian Adult Rats: Histological Characterisation of the Grafted Cells

3.3.1. Introduction

Results from a previous study showed significant recovery in amphetamine-induced rotation behaviour following the intrastriatal implantation of pre-differentiated mouse ES cells in non-immunosuppressed adult hemiparkinsonian rats. Immunohistochemical analysis at five weeks post-grafting revealed poor survival of the grafted TH+ cells, probably due to graft rejection (Baier et al., 2004). Cyclosporine A can inhibit rejection processes, leading to improved survival and function of cross-species intracerebral neural grafts (Brundin et al., 1985).

Our aim was to study the survival and integration of graft-derived dopaminergic neurons after the intrastriatal transplantation of pre-differentiated mouse ES cells in hemiparkinsonian adult rats treated with cyclosporine A for immunosuppression. We analysed the survival, distribution and morphology of graft-derived dopaminergic neurons at one and five weeks post-grafting. We also examined Nissl-stained sections for signs of tumour formation and used the mouse Ki67 antibody – which labels dividing cells – to search for proliferating cells within transplants. Amphetamine- and apomorphine-induced rotation was evaluated four weeks post-grafting to assess the functional effects of the grafted cells.

3.3.2. Materials and Methods

The experimental design is shown in Fig. 3.13. Surgery, behavioural testing and histology were performed as described in chapter 2.

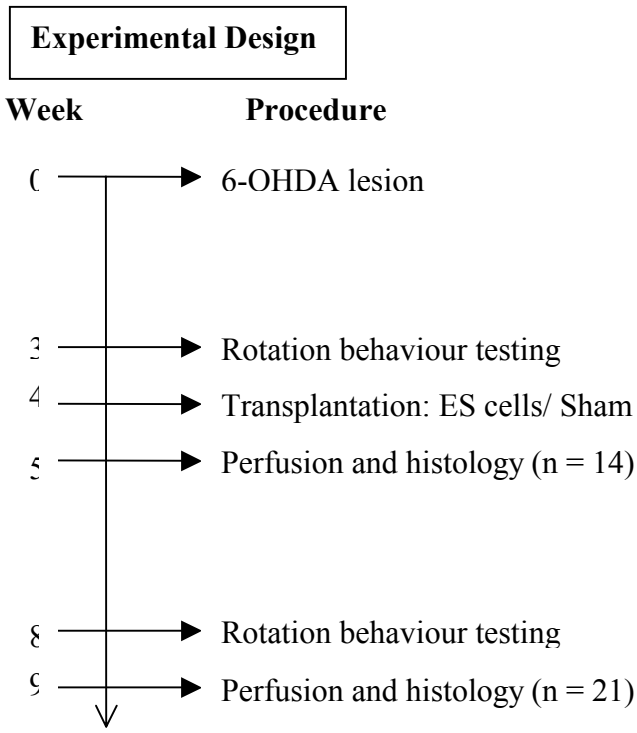

Fig. 3.13. Overview of the sequence of procedures conducted during this study. All animals were immunosuppressed with cyclosporine A (10mkg/kg, i.p.) daily, starting 24 hours before grafting. For each survival period, 4 – 6 animals received sham transplantations. The rest of the animals (n = 9, for 1 week survival and n = 15, for 5 weeks survival) received pre-differentiated mouse ES cell grafts.

3.3.3. Results

Compared to non-immunosuppressed rats (chapter 3.2), cyclosporine A-immunosuppressed graft recipients showed improved survival of TH+ neurons, increased graft size and reduced astrogliosis at the host-graft interface (with the last two most notable at five weeks post-grafting). Our results indicate that graft-derived TH+ neurons express the cellular machinery for the restoration of dopaminergic neurotransmission in the denervated host striatum and (the majority) retain the morphology of mature midbrain dopaminergic neurons up to five weeks post-grafting. Despite ES cell pre-differentiation, 2 out of 15 ES cell recipients had tumours five weeks after grafting.

Phenotype of the Grafted Cells

One week after the intrastriatal implantation of pre-differentiated mouse ES cells into hemiparkinsonian adult rats, 8 out of 9 graft recipients had viable grafts. After five weeks, one graft recipient had no viable grafts; two had developed tumours and were excluded from quantitative histological analyses. In the rest of the animals (n = 12), examination of the gross anatomy did not reveal any abnormalities in striatal tissue morphology.

Staining with the neuronal marker NeuN revealed that after five weeks, the grafts contained regions with a higher density of neurons than the surrounding striatal tissue interspersed with regions that were negative for NeuN staining. All TH+ neurons were NeuN+ (Fig. 3.14A – C). To determine whether some of the TH+ neurons within grafts were noradrenergic, we performed double-labelling for TH and DBH (the noradrenergic neuron-specific enzyme). We did not find TH+/DBH+ neurons indicating that the TH+ neurons are most likely dopaminergic (data not shown). We detected the co-expression of TH and calbindin, which is normally co-expressed with TH in the midbrain (Fig. 3.14D – F), and VMAT-2 (Fig. 3.14G – I). VMAT-2 is a marker for sites of intracellular monoamine storage and has been localised with TH in cell bodies, dendrites, and axonal terminals of midbrain DA neurons (Nirenberg et al., 1996). Many grafts also contained 5-HT+ neurons (Fig. 3.15A – C). Double labelling for 5HT and TH showed that the ratio of 5-HT+:TH+ neurons varied greatly among grafts. In general, TH+ neurons had more elaborate processes than 5-HT+ neurons (Fig. 3.15D – F).

Organisation of ES Cell Grafts

Grafted TH+ neurons had dispersed up to 1690 ± 140μm along the rostrocaudal axis at one week and 1850 ± 190μm at five weeks post-grafting (Fig. 3.16 and Table 3.2). Laterally, ES cell grafts occupied a larger area of the host striatum after five weeks. However, some grafts had fused making it difficult to identify individual graft borders for quantitative analysis at

this time point. After five weeks, the majority of TH+ neurons were found either at the graft core (Fig. 3.17A and at a higher power, C) or periphery (Fig. 3.17B and D). In general, TH+ neurites at the graft border displayed extensive neurite outgrowth (Fig. 3.17C vs. D). GFAP immunoreactivity was evaluated in parallel sections. After five weeks, very few astrocytes were found within grafts. Reactive astrocytes were found mainly at the graft border (Fig. 3.17E). In contrast, ED1+ microglia/macrophages were detected within grafts and in the adjacent host striatal tissue (Fig. 3.17D).

Survival of Grafted TH+ Cells

We estimated the number of TH+ neurons in the graft recipients after one and five weeks. The mean number of TH+ neurons in all the grafts combined was 330 ± 73 after one week and 1220 ± 400 after five weeks (Table 3.2). Rats from the latter group were transplanted in three sessions. Poor survival during one of the sessions (n = 4, mean TH+ cell count = 85 ± 15) may have led to the big intragroup variation in surviving TH+ neuron number. We used the mouse Ki67 antibody to search for proliferating cells within grafts. No cells immunoreactive for mouse Ki67 were found in ES cell recipients without tumours (data not shown). In contrast, clusters of Ki67 immunoreactive cells were found throughout some transplants in the two animals that had developed tumours at five weeks post-grafting (Fig. 3.18).

Morphology of Grafted TH+ Cells

105 TH+ neurons were used for a detailed light microscopic analysis. One week post-grafting, the majority of the TH+ neurons had medium sized cell bodies (mean soma profile area 130.9 ± 5.4μm^2) which were mostly ovoid or round in shape. More than 90% of the neurons had 1 - 3 primary processes emerging from the soma (combined neurite length per soma 55.9 ± 5.7μm/soma). Fig. 3.19 shows the morphology of graft-derived TH+ neurons after five weeks. Mean soma profile area was significantly enlarged (mean soma profile area 163.9 ± 8.1μm^2)

and there was an increase in combined neurite length per soma (69.8 ± 9.9μm/soma). However, a higher percentage of TH+ somata (38.3%) lacked neurites (Table 3.3). The data were subjected to a correlation analysis with soma profile area as the independent variable and combined neurite length per soma the dependent variable. There was no correlation between the two variables.

Drug-Induced Rotation Behaviour

Many animals demonstrated a reduction in spontaneous motor activity (compared to pre-grafting observations). There were no significant changes in amphetamine- and apomorphine-induced rotation at four weeks post-grafting. Furthermore, we did not find a correlation between the rotation scores and the number of surviving TH+ neurons for individual animals. Retrospective analysis showed that many animals had lost weight or displayed a reduced rate of weight gain [compared to non-immunosuppressed animals from the previous study (section 3.2)] following transplantation and initiation of cyclosporine A administration.

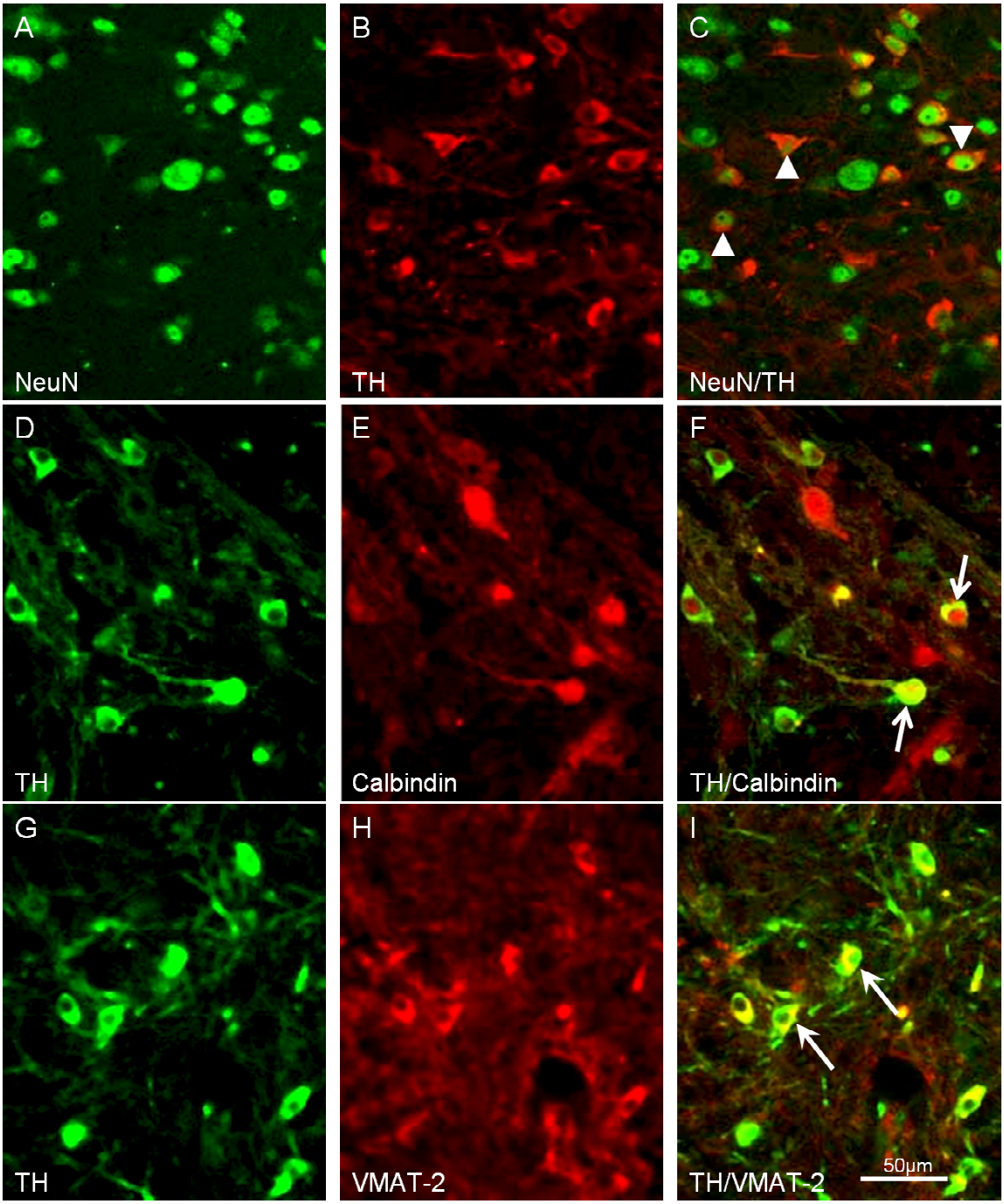

Fig. 3.14. Confocal images showing the phenotype of grafted cells five weeks after the intrastriatal implantation of pre-differentiated mouse ES cells in hemiparkinsonian adult rats. A – C: green – NeuN; red – TH. D – F: green – TH; red – calbindin. G – I: green – TH; red – VMAT-2. (C), (F) and (I) show merged pictures. All TH+ cells co-expressed the neuronal marker NeuN (C). TH+ cells also co-expressed calbindin (F) and VMAT-2 (I), which labels intracellular sites of monoamine storage. Arrowheads/arrows in (C), (F) and (I) indicate double-labelled cell bodies. Scale bar: 50µm.

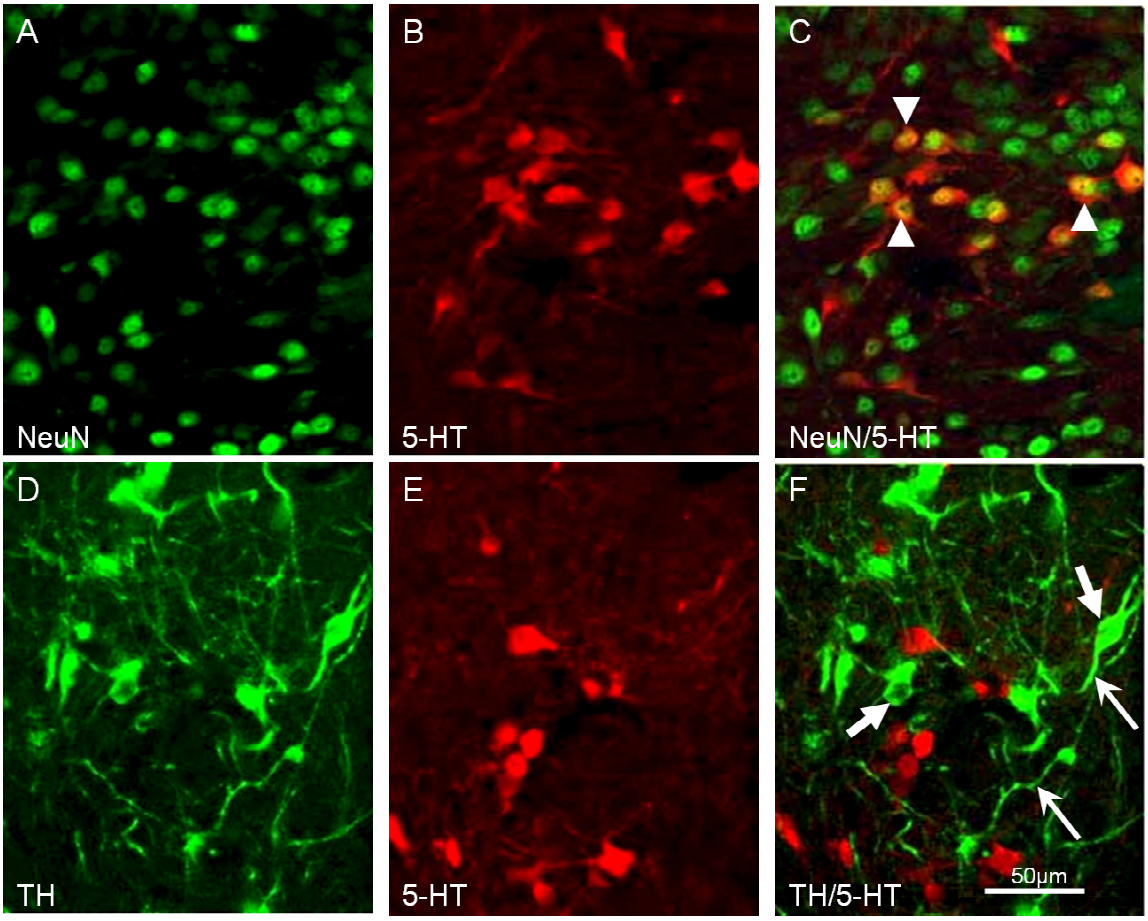

Fig. 3.15. Confocal images showing the phenotype of grafted cells five weeks after the intrastriatal implantation of pre-differentiated mouse ES cells in hemiparkinsonian adult rats. A – C: green – NeuN; red – 5-HT. Many grafts contained 5-HT+ neurons. Arrowheads in (C) indicate NeuN+/5-HT+ cell bodies. D – F: green - TH; red – 5-HT. In (F), closed arrows indicate TH+ cell bodies and open arrows TH+ neurites throughout the graft. TH+ neurons had more elaborate processes than 5-HT+ neurons. Scale bar: 50µm.

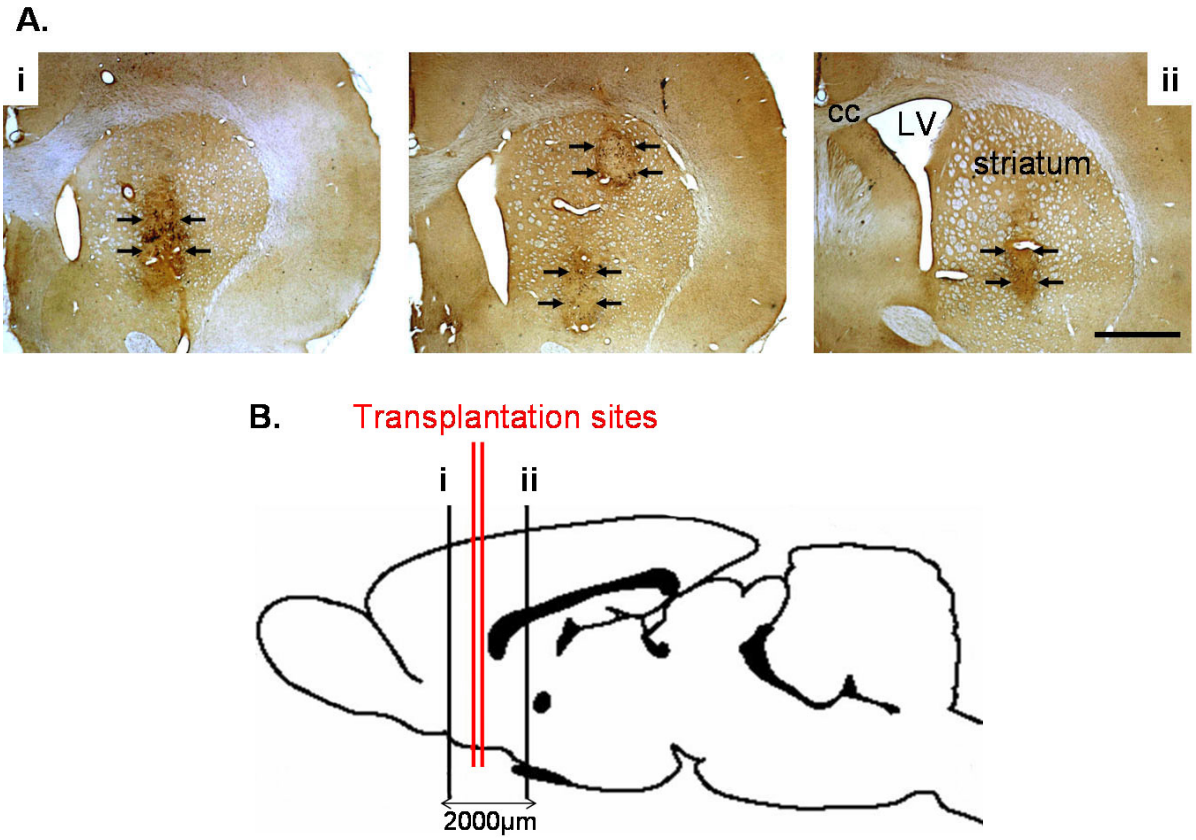

Fig. 3.16. A: TH immunoreactivity throughout a graft five weeks after the intrastriatal implantation of pre-differentiated mouse ES cells in hemiparkinsonian adult rats. Arrows in (A) indicate graft borders. In this example, TH+ neurons were found across ≈ 2000µm of host striatal tissue – represented schematically in (B). Red lines represent the posterior coordinates of the four transplantation sites. cc - corpus callosum; LV - lateral ventricle. Scale bar: 1.6mm.

Table 3.2. Survival and Distribution of Grafted TH+ Cells.

	After one week (n = 8)		***After five weeks (n = 12)***	
	Mean ± SEM	Range	Mean ± SEM	Range
No. of TH+ cells	330 ± 73	64 - 620	1220 ± 400	56 - 4376
Distribution along the rostrocaudal axis (µm)	1690 ± 140	1080 – 2160	1850 ± 190	720 – 2700

There were higher numbers of surviving TH+ cells in grafts at five weeks post-grafting than after one week but the means were not statistically different. There was no significant change in the distribution of grafted TH+ cells along the rostrocaudal axis over this time. For statistical evaluation, data were subjected to an unpaired two-tailed t-test (one week vs. five weeks). Differences were considered significant when $P < 0.05$.

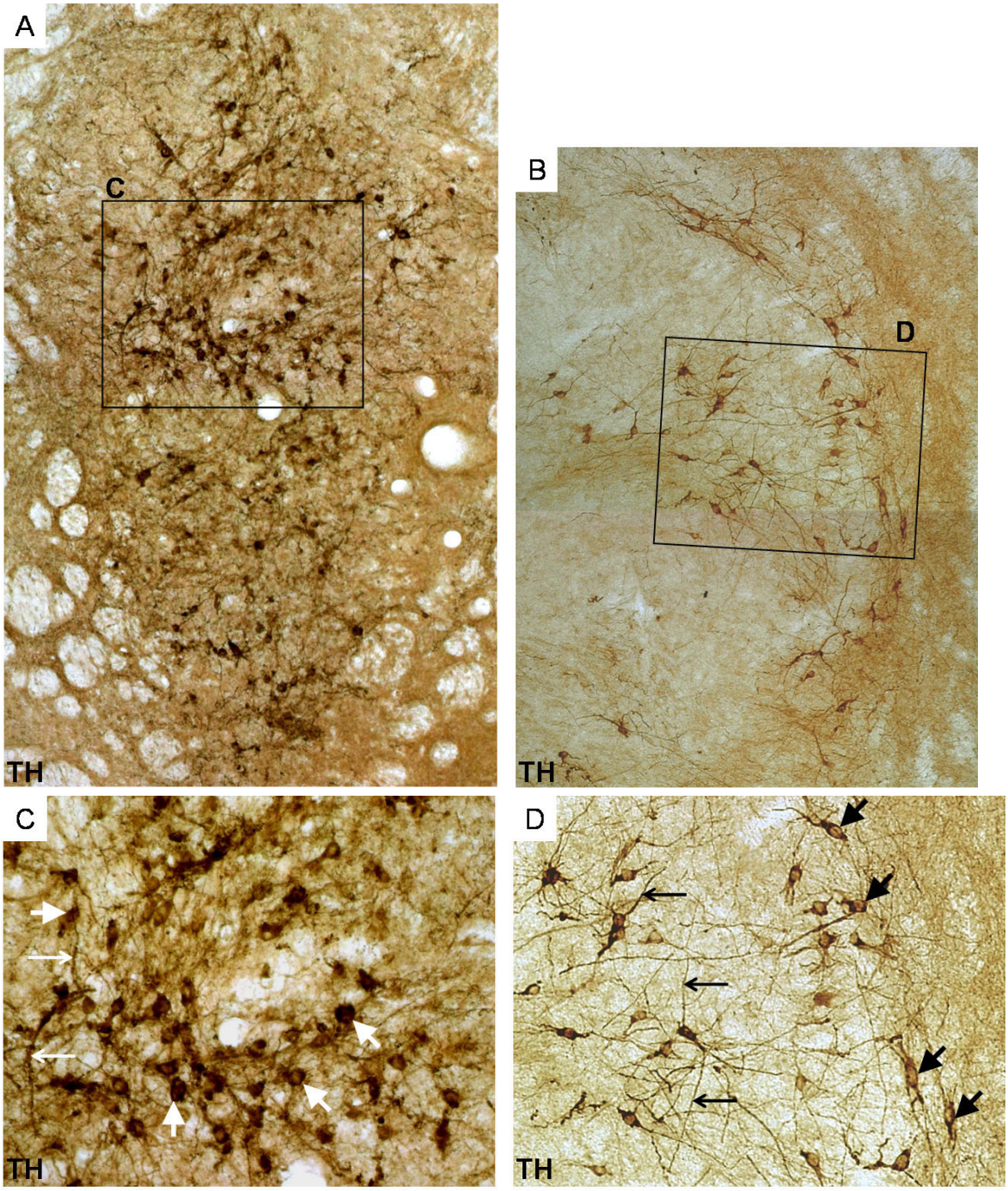

Fig. 3.17. A – D: Legend on the following page.

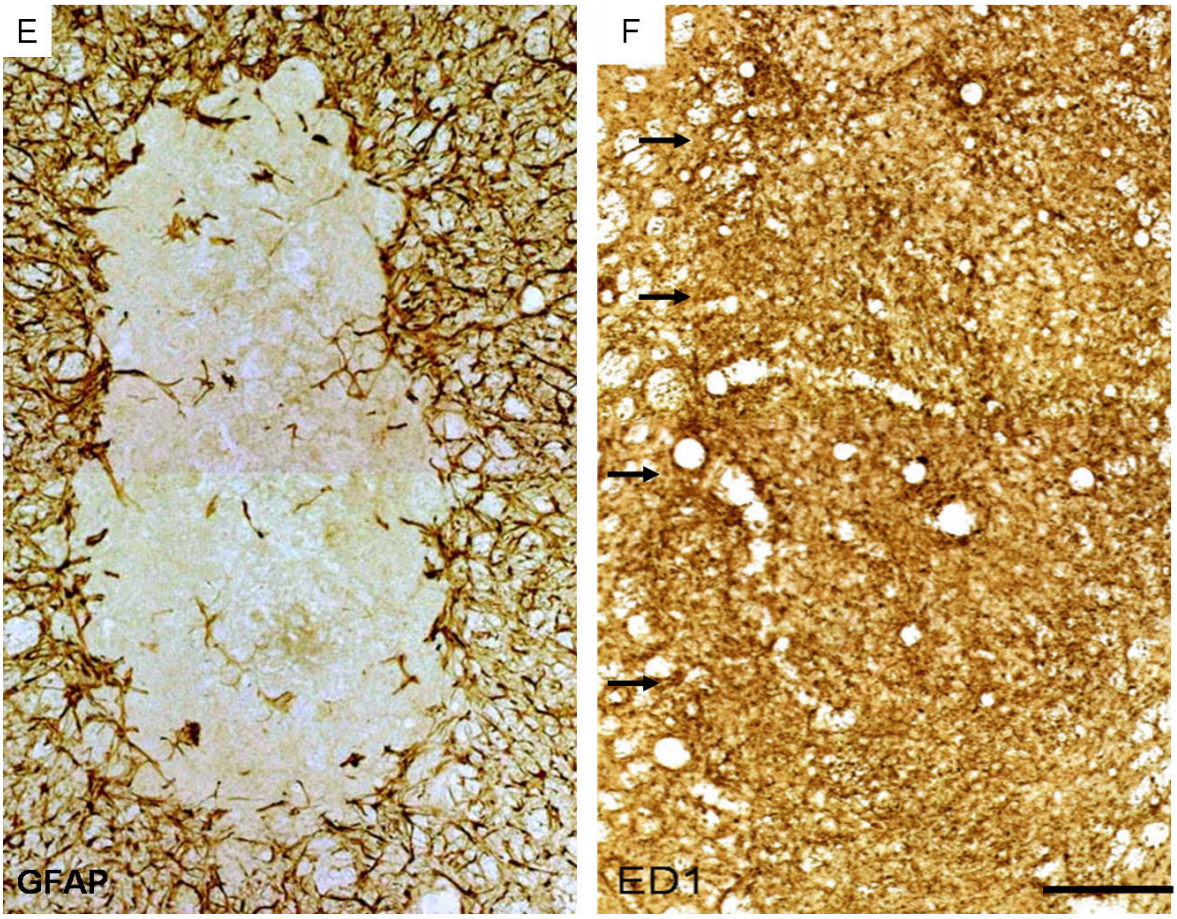

Fig. 3.17. Organisation of ES cell grafts five weeks after the intrastriatal implantation of pre-differentiated mouse ES cells in hemiparkinsonian adult rats. A: a graft with a dense core of TH+ cell bodies. B: grafted TH+ neurons were found mainly at the graft border. (C) and (D) are high power images of (A) and (B). Closed arrows indicate TH+ cell bodies and open arrows TH+ neurites. In general, there was limited penetration of TH+ neurites into the host striatal tissue. E and F: GFAP and ED1 immunostaining from parallel sections to (A). Arrows in (F) outline the graft border. Scale bar: A, B, E, F - 200µm; C, D – 100µm.

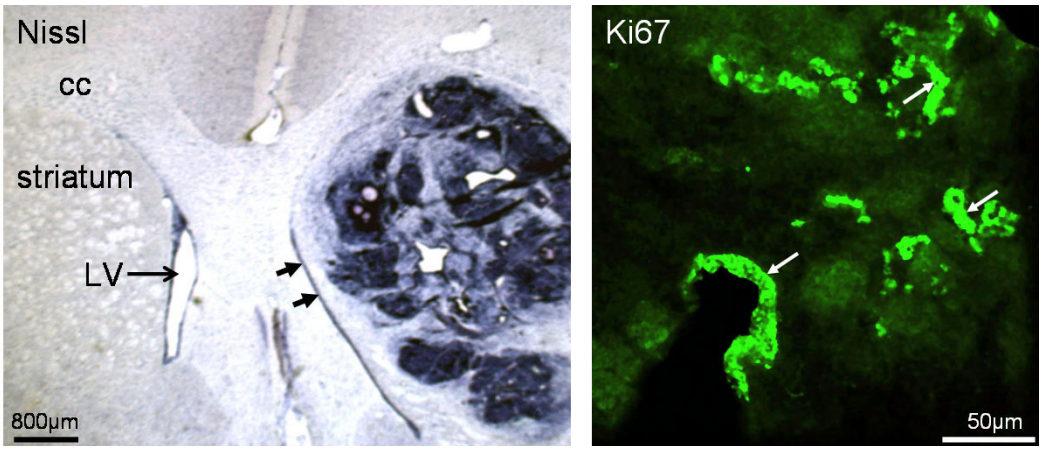

Fig. 3.18. Nissl staining and Ki67 immunoreactivity in a transplant displaying tumour formation at five weeks post-grafting. Nissl staining shows that the enlarged grafts filled and/or extended beyond the host striatal boundaries. Note compression of the right lateral ventricle (closed arrows). cc – corpus callosum; LV – lateral ventricle.

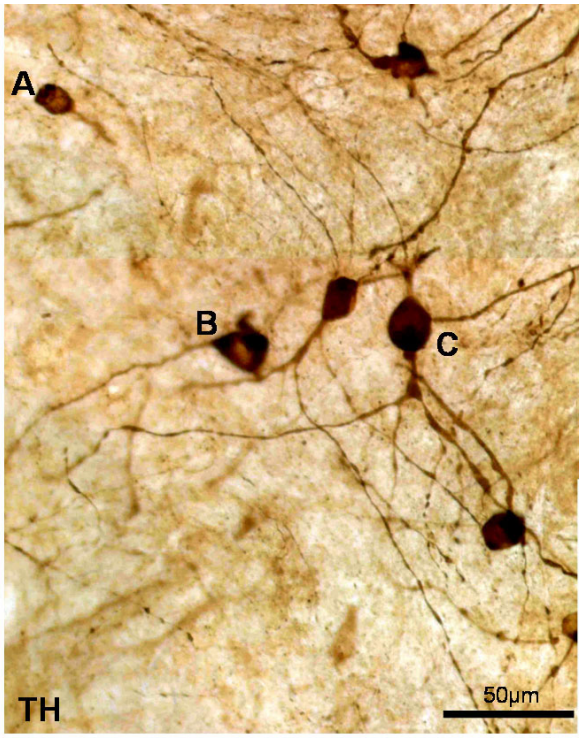

Fig. 3.19. High power image showing the morphology of graft-derived TH+ neurons five weeks after the intrastriatal implantation of pre-differentiated mouse ES cells in hemiparkinsonian adult rats. A: TH+ neuron with small, ovoid soma – probably immature or rejecting dopaminergic neuron. (B) and (C) show apparently unipolar and multipolar neurons respectively. It was not possible to distinguish between axons and dendrites. Scale bar: 50µm.

Table 3.3: Morphological Characteristics of Grafted TH+ Cells

	After 1 week	***After 5 weeks***
	Mean ± SEM	Mean ± SEM
Soma area (μm^2)	130.9 ± 5.4	163.9 ± 8.1**
Somata: n with neurites n without neurites	42 3	37 23
Combined neurite length per soma (µm/soma)	55.9 ± 5.7	69.8 ± 9.9

Between one and five weeks, mean soma profile area increased by 25.2% and combined neurite length per soma by 24.9%. The proportion of characterised cell bodies without neurites increased from 6.7% to 38.3 % over this time. ** indicate statistically significant changes (unpaired two-tailed t-test with significance level set at $P < 0.05$).

3.4. Astrocytic and Vascular Reactions Following the Intrastriatal Transplantation of Pre-differentiated Mouse Embryonic Stem Cells in Hemiparkinsonian Adult Rats

3.4.1. Introduction

The reversal of motor deficits in animal models of PD depends on graft-derived dopaminergic neurons surviving in sufficient numbers and establishing functional connections with the host striatal tissue (Dunnett, 1994; Lindvall, 1994). 80 – 95% of dopaminergic neurons derived from foetal ventral mesencephalon die following grafting (Brundin and Björklund, 1998; Emgard et al., 1999), a fate likely shared by pre-differentiated mouse ES cells (Morizane et al., 2002). Axotomy and anoxia during dissociation and grafting lead to reduced viability of the grafted cells (Schwarz et al., 1998). Anoxia may also account for neuronal loss during the immediate post-grafting period (Dunnett, 1991). The establishment of a functional vascular network is therefore crucial for the long term survival of grafted cells (Dunnett, 1991).

Earlier transplantation studies showed that grafted dopaminergic neurons are often localised at the periphery of the transplant (Mahalik et al., 1991; Emgard et al., 1999). It has been proposed that proximity to host blood vessels and access to diffusible host-derived trophic factors may favour the survival of grafted neurons in this region (Emgard et al., 1999). However, reactive astrocytes form a glial scar at the graft border and the environment of the glial scar is known to be inhibitory to axonal outgrowth (Fawcett and Asher, 1999).

We characterised the astrocytic (GFAP immunohistochemistry) and vascular (BCIP/NBT histochemistry for alkaline phosphatase in endothelial cells) reactions following the intrastriatal implantation of pre-differentiated mouse ES cells in immunosuppressed and non-

immunosuppressed hemiparkinsonian adult rats and analysed the relationship between transplant vascularisation and the distribution and viability of TH+ neurons within grafts.

3.4.2. Methods

Fig. 3.22 shows the experimental design employed.

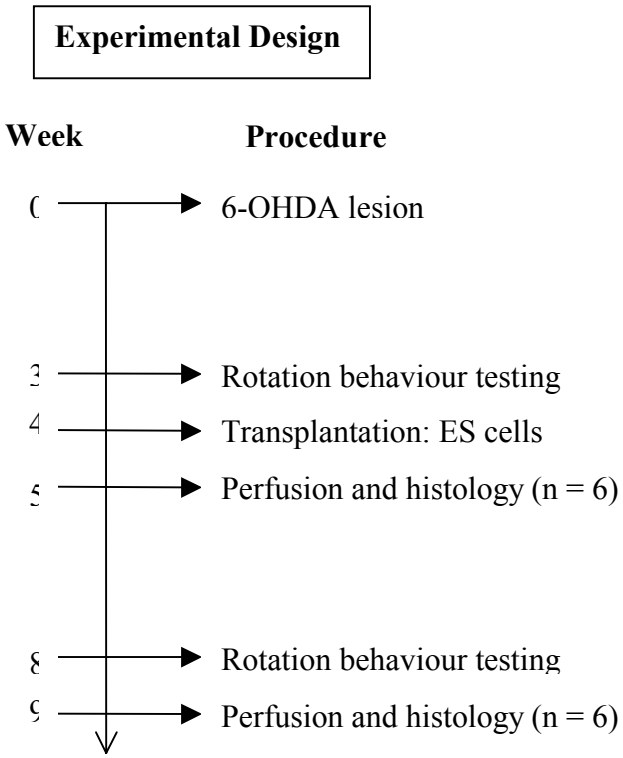

Fig. 3.20. Overview of the sequence of procedures conducted during this study. ES cell recipients received daily injections of cyclosporine A (i.p.) for immuno-suppression (starting 24 hours before grafting) or no immosuppressive treatment. For each survival period, brains from 3 immunosuppressed and 3 non-immunosuppressed ES cell recipients were analysed.

3.3.3. Results

Astrocyte Reactivity and Graft Vascularisation

Fig. 3.21 shows GFAP immunoreactivity in ES cell recipients at one and five weeks post-grafting. After one week, transplants contained numerous graft-/host-derived astrocytes. Reactive astrocytes were found at the host-graft interface and in the adjacent host striatal

tissue (A and B). After five weeks, a glial scar had formed, clearly delineating graft from host tissue. In non-immunosuppressed animals, astrocytic processes formed a continuous, tightly interwoven wall of varying thickness at the graft border (C). The astrogliosis was significantly reduced in cyclosporine A-treated animals; although reactive astrocytic processes were detected at the host-graft interface, the glial scar was in most cases narrower and discontinuous (D). BCIP/NBT histochemistry showed evidence of a sparse blood vessel network within ES cell grafts at one week post-grafting (Fig. 3.22A). Despite the presence of a seemingly impenetrable glial scar after five weeks (in non-immunosuppressed animals), several blood vessels of varying size were found within grafts at this time point (Fig. 3.22B).

Graft Vascularisation: Comparison between CsA- and Non-Immunosuppressed Animals

Fig. 3.23A shows TH immunoreactivity and blood vessels in non-immunosuppressed rats. Surviving TH+ cells occupied a small area of the host striatum and several large vessels (lumen diameter 20 – 30μm) were detected within grafts, at the host-graft interface or in the adjacent host parenchyma (B). Vascularisation throughout the rest of the ipsilateral striatum was comparable to that in the contralateral side and consisted mainly of small diameter vessels classified as capillaries (lumen diameter < 10μm). In immunosuppressed animals, viable ES cell grafts occupied a larger area of the host striatum. The vascular network was composed mainly of small vessels with a distribution similar to that found in the surrounding striatum (C and at a higher magnification, D).

Analysis of Vascularisation Patterns and TH+ Neuron Distribution within Grafts

In a previous study, we observed morphological differences between graft-derived TH+ neurons found at the graft core and those at the graft periphery in cyclosporine A-immunosuppressed animals (chapter 3.3). In this study, we characterised the vascularisation pattern in grafts with differential TH+ neuron distributions at five weeks post-grafting to

study the relationship between transplant vascularisation and TH+ neuron viability. In general, all grafts were well-vascularised with numerous small calibre blood vessels distributed evenly throughout grafts. We did not observe any preferential distribution of microvessels at the graft periphery. The TH+ neuron to vascular element ratio (analysed qualitatively) was invariably higher in high cell density regions at the graft core – thus fewer neurons in this region were in direct proximity to a blood vessel compared to the neurons at the graft border (Fig. 3.24).

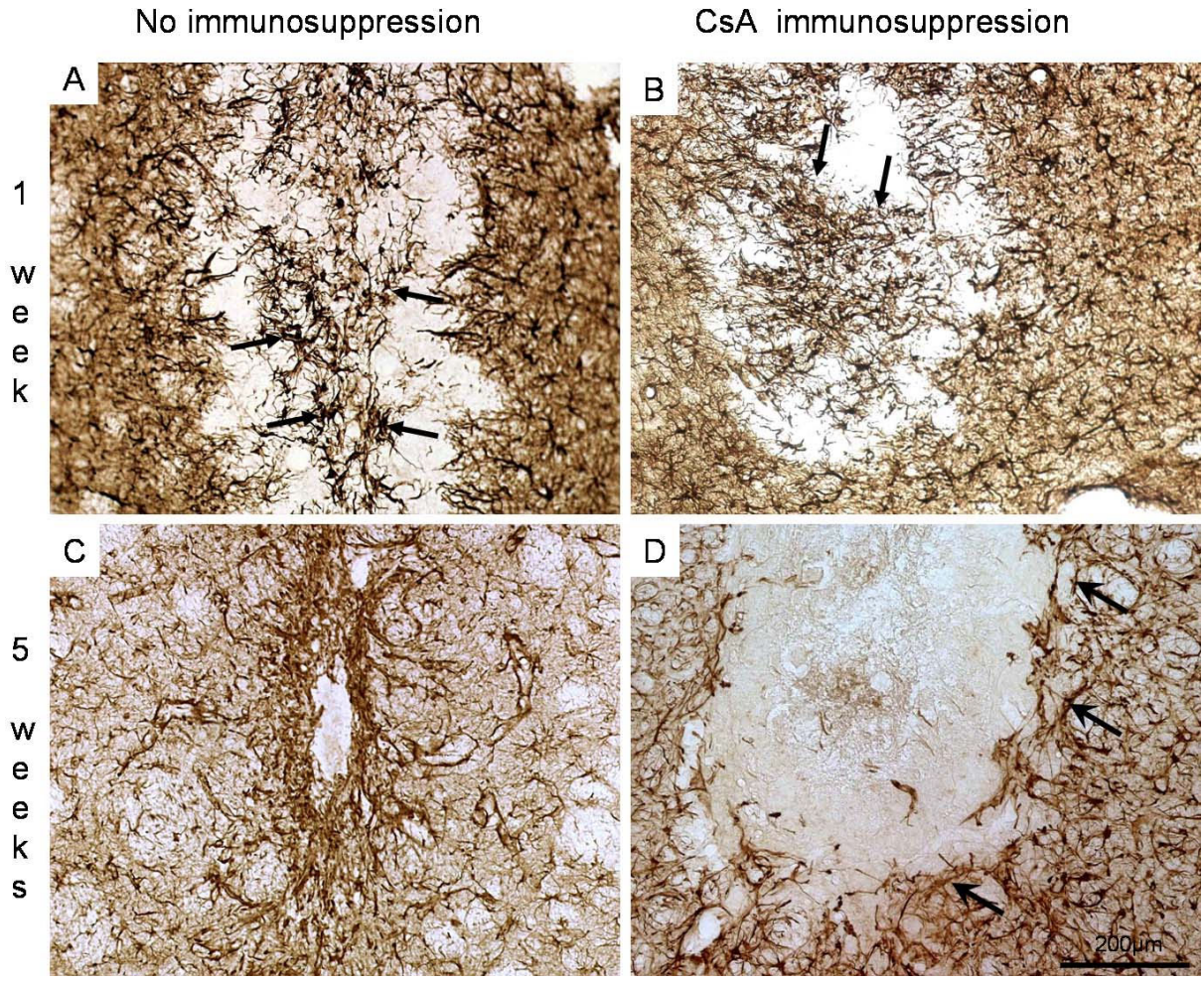

Fig. 3.21. GFAP immunoreactivity. After one week, reactive astrocytes – staining intensely for GFAP – were detected within transplants (arrows in A and B) and in the adjacent host striatal tissue. After five weeks, a tight glial scar had formed at the graft border in non-immunosuppressed animals (C). In comparison, cyclosporine A-immunosuppressed animals showed reduced astrogliosis at this time point – arrows indicate intermingling astrocytic processes (D). Note the differences in the thickness and continuity of the glial scar in (C) and (D).

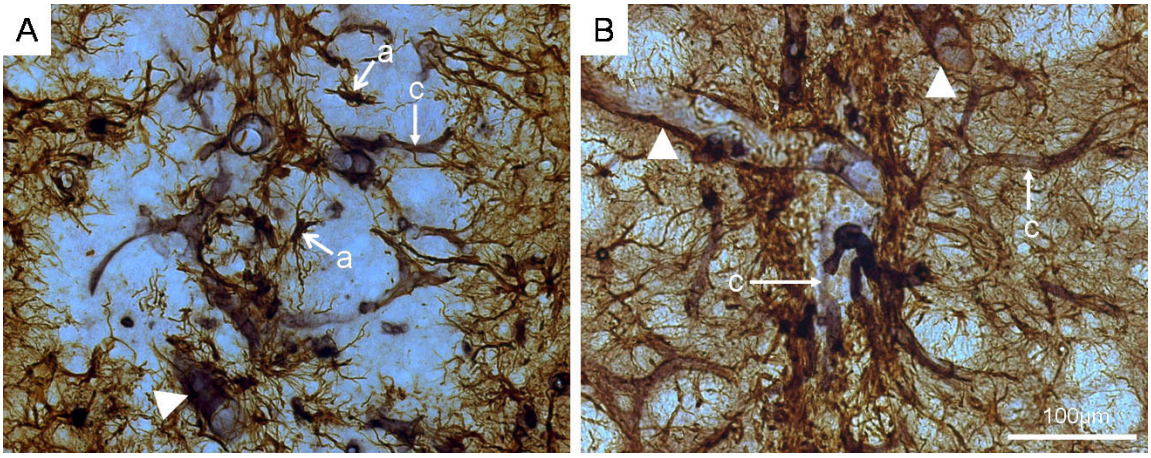

Fig. 3.22. High power image showing astrocyte reactivity (GFAP; brown) and blood vessels (BCIP/NBT substrate for alkaline phosphatase in endothelial cells; purple colour) in non-immunosuppressed rats at one (A) and five weeks (B) post-grafting. Blood vessels are found within grafts at both time points despite the astrogliosis at the graft border. a – astrocytes; c- small blood vessels, probably capillaries; arrowheads – large blood vessels.

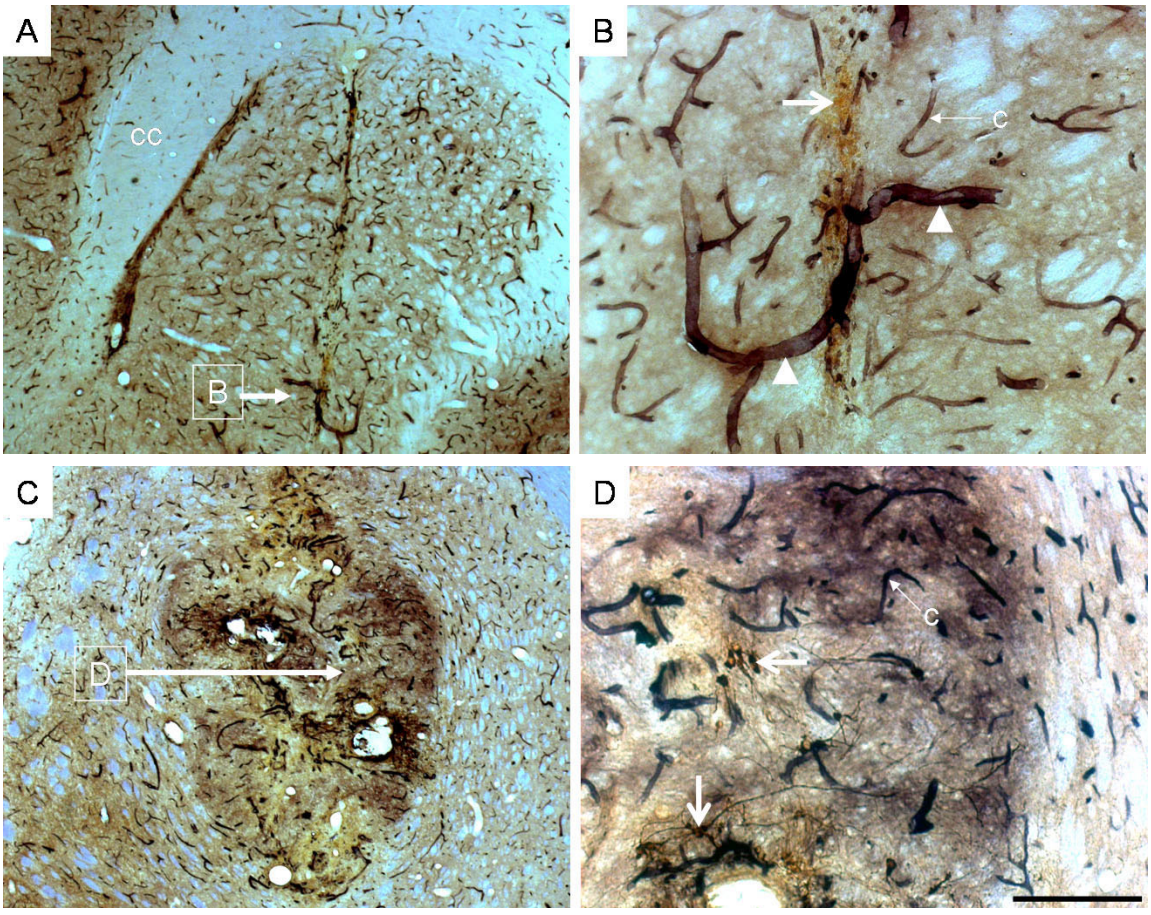

Fig. 3.23. TH immunoreactivity and transplant vascularisation in non-immunosuppressed (A, and at a higher power, B) and cyclosporine A-immunosuppressed ES cell recipients (C and D) at five weeks post-grafting. In non-immunosuppressed animals, a few large vessels are observed within transplants and in the adjacent host parenchyma. In immunosuppressed animals, transplants are well-vascularised with many small vessels. Arrowheads indicate large diameter vessels, open arrows TH+ cells and c – capillaries; cc – corpus callosum. Scale bar: A, C – 1.6mm; B, D – 200µm.

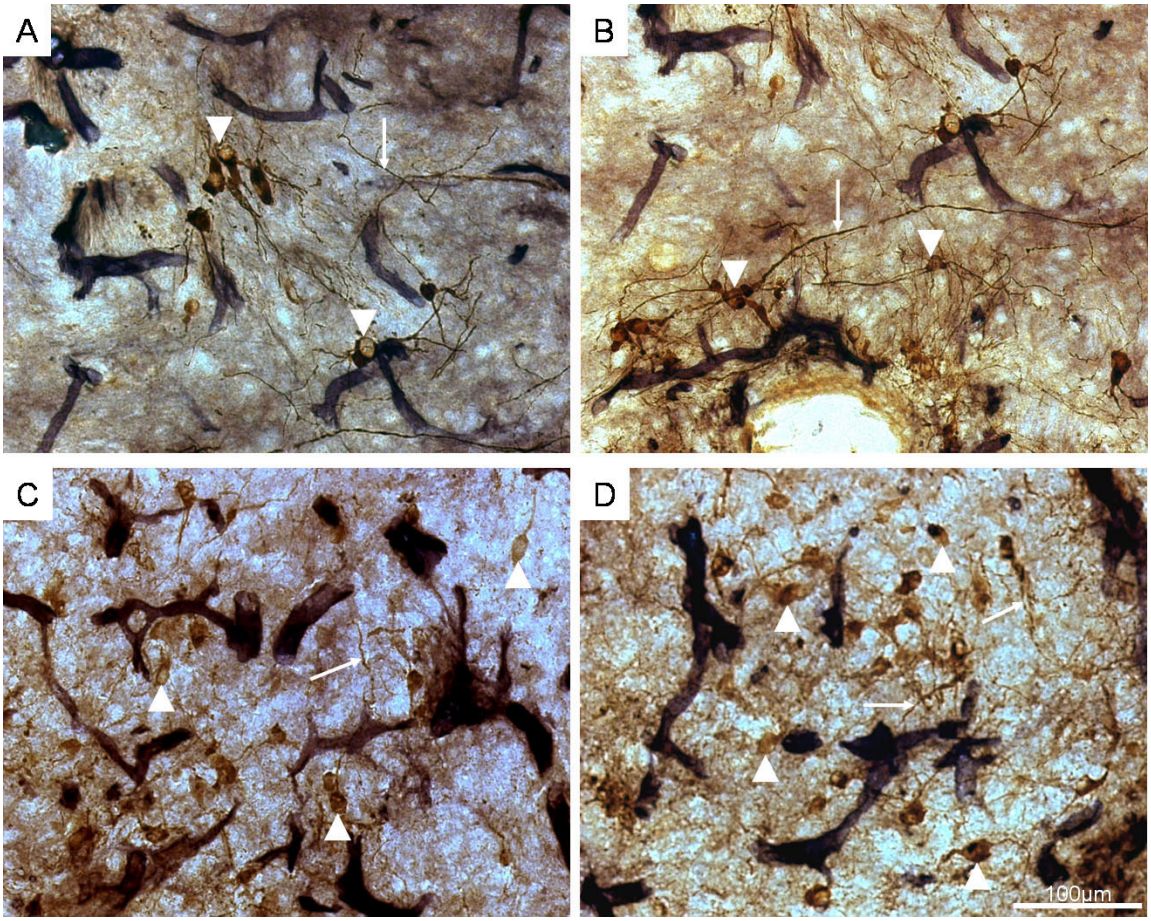

Fig. 3.24. High power photomicrographs showing the distribution of TH+ neurons (brown) and blood vessels (dark purple colour) within ES cell transplants five weeks after grafting in cyclosporine A-immunosuppressed animals. A and B: images from a graft region with a low density of TH+ neurons – TH+ neurons are found close to blood vessels. C and D: images from a high TH+ cell density region. Note differences in the ratio of TH+ neurons to vascular elements throughout the grafts. Arrowheads – TH+ cell bodies; arrows – TH+ neurites. Scale bar: 100µm.

3.5. Transplantation of Pre-differentiated Mouse Embryonic Stem Cells in Hemiparkinsonian Adult Rats: an Autoradiographic Study of the D1 Receptor and Dopamine Transporter Binding Sites using [^{3}H]-SCH23390 and [^{3}H]-WIN35428

3.5.1. Introduction

The physiological effects of dopamine are mediated by at least five G-protein coupled receptor subtypes classified as D1-like and D2-like receptors based on pharmacological and functional criteria. D1-like receptors (D1 and D5) activate adenylyl cyclase while D-2 like receptors (D2, D3 and D4) appear to inhibit adenylyl cyclase (Kandel et al., 2000). The D1 and D2 receptors are expressed postsynaptically on neurons in various brain regions including the striatum, substantia nigra and cortex with the highest level of expression found in the striatum and SN. D2 receptors are also expressed presynaptically on dopaminergic cell bodies and terminals where they regulate the firing rate of the neurons and dopamine release (Hersch et al., 1995; Kandel et al., 2000; Schmitz et al., 2002). Dopaminergic neurotransmission is terminated mainly by the uptake of synaptic dopamine into dopaminergic neurons by the plasmalemmal dopamine transporter (DAT) which is located presynaptically on dopaminergic neurons in the midbrain and elsewhere (Freed et al., 1995)

Animals with 6-OHDA-induced hemiparkinsonism rotate in the direction contralateral to the side of the lesion when challenged with directly acting dopamine receptor agonists (Dunnett, 1991). This effect has been attributed to the development of dopamine receptor supersensitivity on the denervated side (Graham et al., 1990; Dunnett, 1991). Unchanged, elevated or decreased densities of D1 and D2 receptors have been reported following a unilateral 6-OHDA lesion of the nigrostriatal dopaminergic pathway in rodents (Marshall et

al., 1989; Beresford et al., 1988; Savasta et al., 1992; Dawson et al., 1991; Graham et al., 1990). Similarly contradictory data have been reported from in vitro binding assays for D1 and D2 receptors in human parkinsonian brains (Cortés et al., 1989). Immunohistochemical and in-vivo imaging studies using single photon emission tomography (SPET) have consistently shown a dramatic loss of striatal dopamine transporter immunoreactivity/ligand binding in animal models of PD and in PD patients (Booij et al., 2002; 2003; Stanic et al., 2003b; Nutt et al., 2004). We used in vitro receptor autoradiography to evaluate changes in the binding of striatal D1 receptors and the dopamine transporter following a unilateral 6-OHDA induced degeneration of nigrostriatal dopaminergic neurons and transplantation of mouse ES cell-derived dopaminergic neurons. [^{3}H]-SCH23390 and [^{3}H]-WIN35428 were used as radioligands for the D1 receptors and the dopamine transporter respectively.

3.5.2. Materials and Methods

Fig. 3.25 shows the experimental design employed.

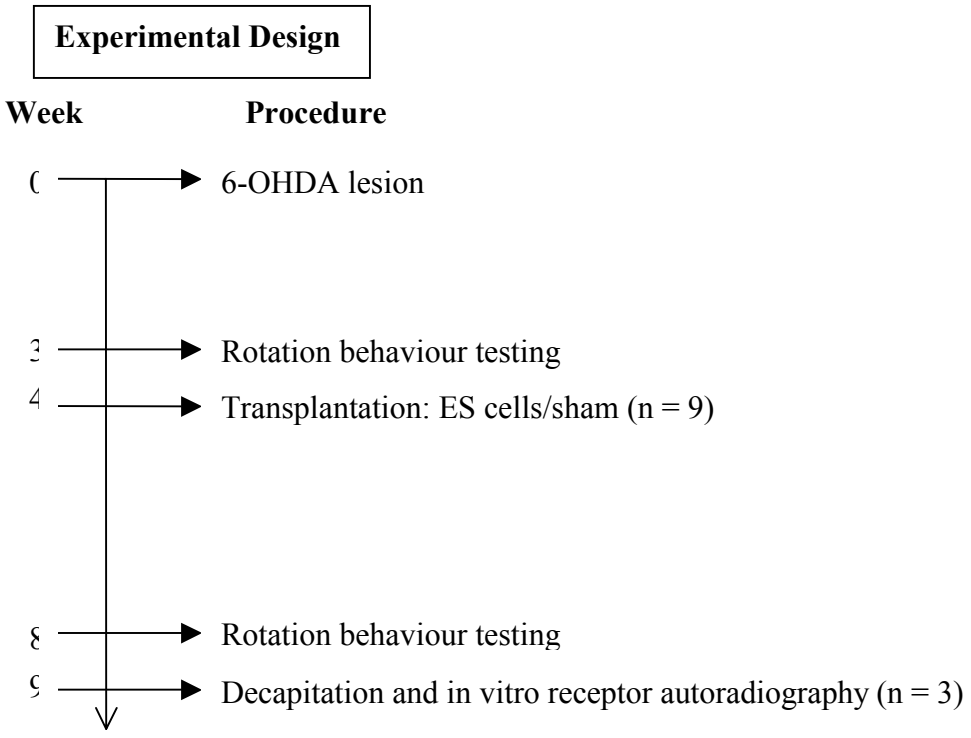

Fig. 3.25. Overview of the sequence of procedures conducted during this study. ES cell recipients received daily injections of cyclosporine A (i.p.) for immuno-suppression (starting 24 hours before grafting).

3.5.3. Results

Four animals had to be killed before the endpoint of study because of sickness. Two other ES cell recipients had developed tumours at five weeks post-grafting and were excluded from the study.

One untreated control animal was decapitated and the brain prepared for in vitro receptor autoradiography. The saturation curve for [^{3}H]-SCH23390 binding in the rat striatum was generated from binding data from one untreated control animal (Fig. 3.26). Non-linear regression analysis of the saturation binding data revealed a K_d value of 0.38 ± 0.07 and a B_{max} of 249.3 ± 10.7fmol/mg. Further quantitative densitometric analysis was carried out on autoradiographs produced from sections incubated with 4 nM [^{3}H]-SCH23390 (Fig. 3.27). For each animal, ligand binding values were calculated on both sides of the brain and the non-lesioned side of the brain treated as a control (Table 3.4). Striatal [^{3}H]-SCH23390 binding was not altered by denervation and/or intrastriatal transplantation of dopamine-producing cells.

Fig. 3.28 shows [^{3}H]-WIN32548 binding in control, sham and ES cell-transplanted animals. Due to technical problems, only non-saturating concentrations of the ligand were used. Nevertheless, the data show the loss of [^{3}H]-WIN32548 binding in the ipsilateral striatum and the lack of restoration of the DAT-like binding after the transplantation of pre-differentiated mouse ES cells.

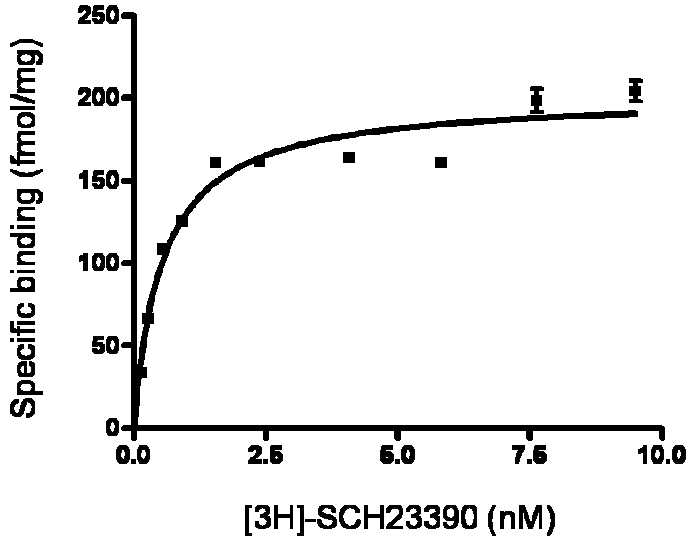

Fig. 3.26. Binding curve for D1 receptor binding sites in the striatum of one untreated control rat. Each data point represents the mean ± SEM of 2 – 3 sections. The curve was fitted by a nonlinear regression algorithm for one-site binding using Graph Pad PRISM software.

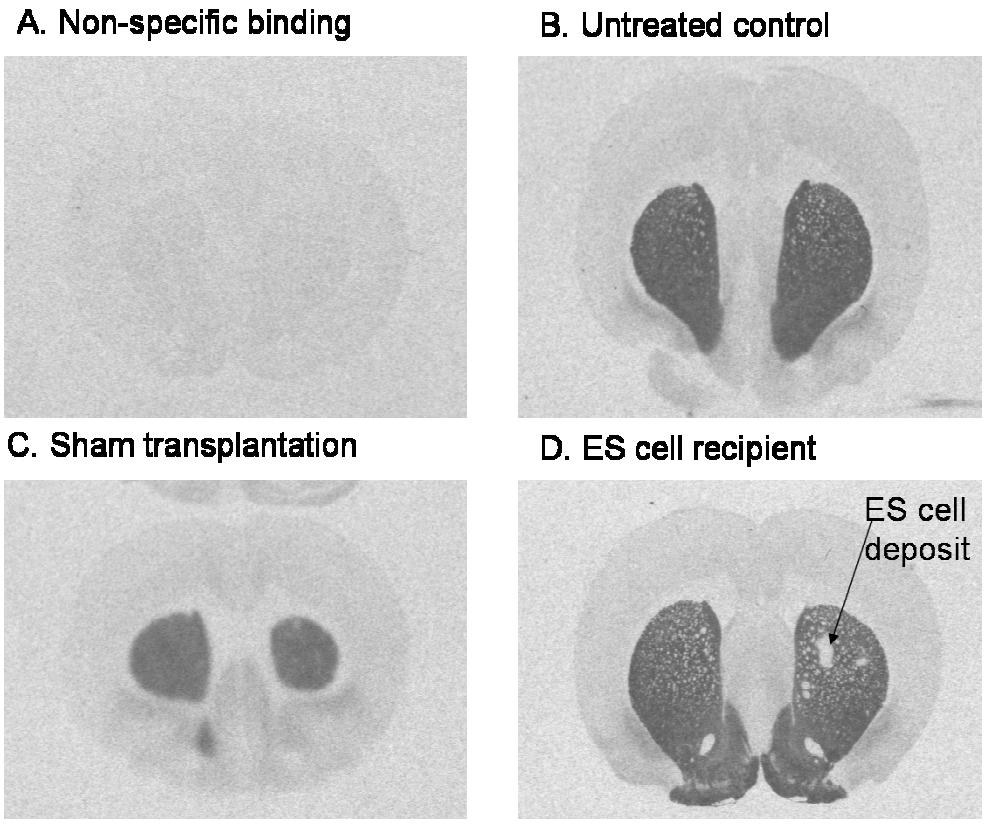

Fig. 3.27. Autoradiograms showing in (A), non specific binding and in (B - D), total binding of 4 nM [^{3}H]-SCH23390 (ligand for D1 receptor binding sites) in the rat striatum. Digitised autoradiographic images of sections were converted to TIF format and printed without modification. Non-specific binding was determined in the presence of 5 µm *cis*-(z)-flupenthixol. Sham (C) and ES cell grafting (D) were performed on the right side. Quantitative binding data are presented in Table 3.4.

Table 3.4. Striatal [^{3}H]-SCH23390 Binding

	[^{3}H]-SCH23390 binding (fmol/mg)	
Animals	Left	Right
1. Untreated	249.0 ± 24.5	257.0 ± 21.6
2. Sham	164.1 ± 0.0	155.6 ± 0.0
3. ES cell recipient	184.7 ± 7.5	185.1 ± 15.2
4. ES cell recipient	225.1 ± 5.4	210.1 ± 4.8

Ligand binding data from sections incubated with 4 nM [^{3}H]-SCH23390 to label D1 receptor binding sites. From each animal, 2 - 4 sections were analysed and the data presented as mean ± SEM of binding in fmol/mg tissue. For treated animals, 6-OHDA injection and sham/ES cell transplantation were performed on the right side with the left side acting as a control. There were no statistically significant differences in binding between the two sides following denervation and/or the transplantion of pre-differentiated mouse ES cells.

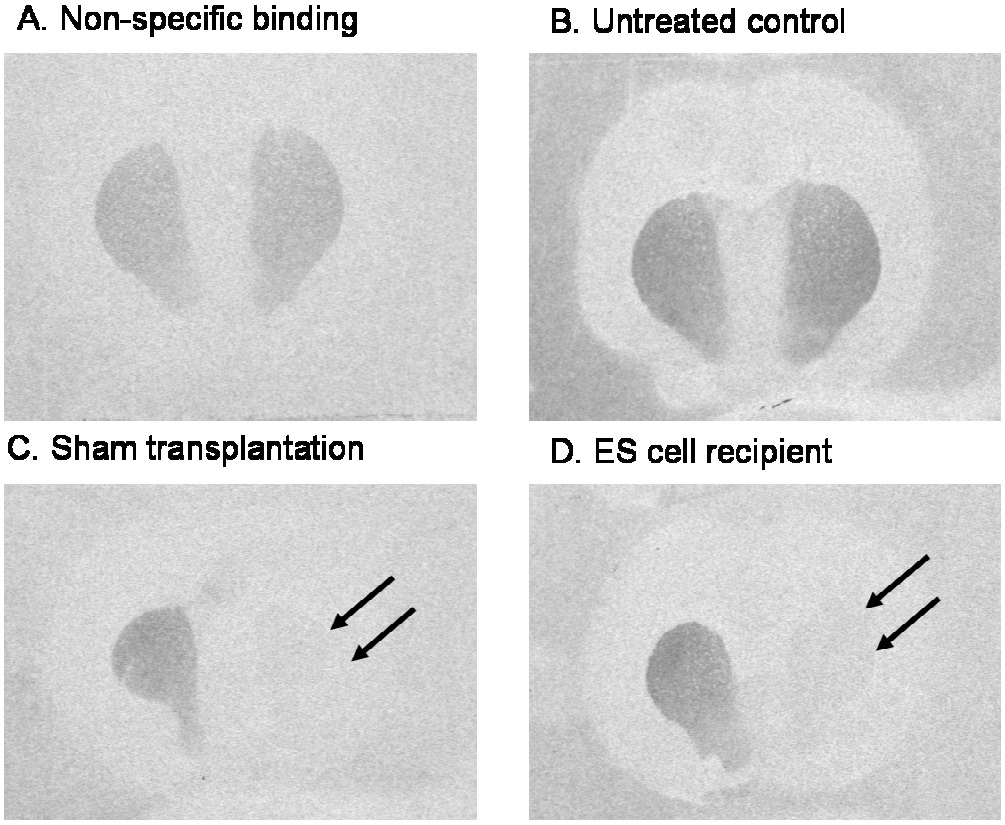

Fig. 3.28. Autoradiograms showing in (A), non specific binding and in (B – D) total binding of [^{3}H]-WIN32548 (ligand for dopamine transporter binding sites) in the rat striatum. Non-specific binding was determined in the presence of 50 μM (-) cocaine. The images demonstrate qualitatively the reduction in [^{3}H]-WIN32548 binding on the denervated side (C). Transplantation of mouse ES cell-derived dopaminergic neurons did not lead to restoration of [^{3}H]-WIN32548 binding (D). Arrows in (C) and (D) indicate the outer striatal boundary on the side ipsilateral to the 6-OHDA lesion.

Chapter 4: Discussion

The data presented in this thesis add to the characterisation of the survival and integration of mouse embryonic stem cell-derived, in vitro-generated dopaminergic neurons in animal models of Parkinson's disease (Kim et al., 2002; Barberi et al., 2003). Specifically, our results extend the findings of Kawasaki et al. (2000) and Morizane et al. (2002) by providing insight into the survival of SDIA-induced dopaminergic neurons in a mouse-to-rat transplantation model. The longer survival period employed here enabled the investigation of various time-dependent aspects of the host-graft interaction including induction of the host immune response and the subsequent xenograft rejection, transplant vascularisation, tumour formation and functional effects of grafted dopaminergic neurons.

4.1. Changes Induced by a Unilateral Injection of 6-Hydroxydopamine in the Rat Nigrostriatal Dopaminergic System

The mean amphetamine-induced rotation score at three weeks post-lesion was 1.89 ± 0.07 full body turns per minute. Stanic et al. (2003a) claim that a rotation score of this magnitude corresponds to a loss of at least 75% of the dopaminergic neurons of the substantia nigra pars compacta. Reinnervation of the denervated striatum does not occur in animals with lesions of this size (Finkelstein et al., 2000; Stanic et al., 2003a). Such animals are useful models for late stage Parkinson's disease and are suitable for the evaluation of novel therapeutic strategies including the transplantation of dopamine-producing cells.

The microglial and astrocytic reactions to the degeneration of nigrostriatal dopaminergic neurons were similar to those reported elsewhere (Cicchetti et al., 2002; Depino et al., 2003). Our results differed in that we found very few activated microglia in the striatum. Cicchetti et al. (2002) employed intrastriatal lesions and found that activated microglia persisted within

the lesion needle tract up to 28 days post-grafting. Medial forebrain bundle lesions may thus be more desirable when planning to graft cells intrastriatally at short post-lesion time points.

4.2. Detection of Transplanted Cells

Labelling donor cells prior to grafting can facilitate the analysis of the survival, distribution and integration of the cells after grafting into host tissue. Mouse ES cells were labelled with the fluorescent membrane dye PKH26 red prior to grafting. PKH26 labelling is stable and durable and has been used for the detection of transplanted cells in various organs of host animals (Catapano et al., 1999; Haas et al., 2000; Shin et al., 2000). Because of its distribution characteristics - the dye gets diluted as the cells mature over time - PKH26 labelling cannot be used for the detection of individual grafted cells after some survival time. Mouse-specific antibodies have also been used to identify grafted mouse tissue in rat host brains (Björklund et al., 2002; Kim et al., 2002). One interesting approach would be the generation of mouse ES cell lines in which the expression of green fluorescent protein (GFP) is driven by specific regulatory elements (Sawamoto et al., 2001a, b). The advantage of this method is that GFP fluorescence can be visualised easily without a need for an extra immunohistochemical analysis step. Moreover GFP-labelled cells can be isolated by fluorescence activated cell sorting to obtain ES cell populations enriched for the desired phenotype.

4.3. Survival of Grafted Dopaminergic Neurons

We transplanted 4 x 10^5 pre-differentiated mouse ES cells per striatum and found an average of 1220 ± 400 TH+ cells after five weeks in immunosuppressed animals. Other groups have reported comparable survival rates following the grafting of pre-differentiated mouse ES cells into hemiparkinsonian rodents: 4% eight weeks after transplantation of Nurr-1 transfected mouse ES cells in (immunosuppressed) rats (Kim et al., 2002) and less than 3% (Kawasaki et al., 2000; Morizane et al., 2002) 15 days after transplantation of SDIA-treated mouse ES cells

in mice (survival rates = percentage of surviving TH+ neurons in total number of grafted ES cells). Based on these results, the survival of mouse ES cell-derived, in vitro differentiated dopaminergic neurons appears to be similar or even lower than that reported for primary foetal VM grafts in animal models of PD (5 – 10%) (Dunnett, 1994).

4.3.1. The Early Phase of Neuronal Loss

ES cell grafts contained very few TH+ neurons at two days post-grafting – the earliest time tested. Earlier studies indicate that up to 95% of the dopaminergic neurons from rat foetal ventral mesencephalon (around E11 – E15 of gestation) may be lost within the first 3 days after grafting (Barker et al., 1996; Zawada et al., 1998; Emgard et al., 1999). The SDIA-method of dopaminergic neuron induction from mouse ES cells mimics the time course of the early development of the midbrain (Kawasaki et al., 2000). After 14 days of SDIA treatment – the induction time adopted in this study – mouse ES cells are likely at a similar developmental stage to that of the aforementioned VM tissue (Morizane et al., 2002). At this stage, the dopaminergic phenotype is determined and TH+ neurite outgrowth detectable but not extensive (Dunnett, 1991; Morizane et al., 2002). Injury to neurites during dissociation and grafting can lead to a reduction in grafted cell viability (Schwarz et al., 1998; Larsson et al., 1999; Morizane et al., 2002). Furthermore unfavourable conditions in the host brain in the immediate post-grafting period – e.g. the lack of oxygen and nutrients necessary for normal metabolism (Dunnett, 1991; Rosenstein, 1995), direct contact with host blood, which is known to be poorly tolerated by neurons (Rosenstein, 1995) and the release of neurotoxic factors by the injured striatal tissue (Emgard et al., 1999; Casper et al., 2003) – may lead to the loss of more dopaminergic neurons. The majority of the grafted dopaminergic neurons die by apoptosis at this early time point (Zawada et al., 1998; Schierle et al., 1999). In support of this finding, pre-treatment of foetal VM suspensions with anti-apoptotic agents was shown to improve the viability of dopaminergic neurons grafted to hemiparkinsonian rats (Schierle et

al., 1999). The pre-treatment of donor cells with glial derived neurotrophic factor and cyclosporine A was also shown to be neuroprotective (Zawada et al., 1998; Castilho et al., 2000) although the mechanisms of neuroprotection in these cases are not yet fully elucidated.

4.3.2. Effect of Transplant Vascularisation on Grafted Dopaminergic Neuron Viability

The establishment of a functional blood supply is crucial for the long term survival of grafted cells (Dunnett, 1991). Our results show that transplant vascularisation had started within 7 days post-grafting. This finding is consistent with observations made by Leigh et al. (1994) and Casper et al. (2003) following the intracerebral grafting of dissociated cell suspensions. After five weeks, transplant vascularisation in cyclosporine A-treated rats was similar to that in the contralateral striatum. Non-immunosuppressed animals displayed both small and large diameter vessels within and around grafts at this time point, a vascularisation pattern similar to that reported by Nakashima et al. (1988) and Finsen et al. (1991) during the rejection of intracerebral mouse-to-rat grafts. Large diameter vessels, interpreted as representing immature, newly formed vessels (Finsen et al., 1991) are often found within grafts during the first 1 - 3 weeks post-grafting and are replaced by capillaries at time points > 4 weeks post-grafting (Lawrence et al., 1984; Dusart et al., 1989). The continuing formation of new blood vessels in non-immunosuppressed ES cell recipients may be related to the persistence of activated microglia and macrophages both of which are known to release angiogenic factors (Polverini et al., 1977; Finsen et al., 1991). In agreement with Leigh et al. (1994), we found that graft vascularisation was not impeded by extensive astroglial scarring at the graft border.

One common observation made from various transplantation studies is that the surviving dopaminergic neurons are often localised at the periphery of the grafts (Emgard et al., 1999; Casper et al., 2003; Barberi et al., 2003). Better access to diffusible host-derived trophic factors and earlier vascularisation in this region – transplants are vascularised inward from the

host-graft border (Geny et al., 1994) – may account for this observation (Emgard et al., 1999; Casper et al., 2003). In cyclosporine A-treated animals, the distribution of blood vessels was uniform throughout all viable grafts at five week post-grafting. Grafted TH+ neurons found in high cell density regions at the graft core displayed limited neurite outgrowth compared to the TH+ neurons at the graft periphery. This difference may have several causes including: **1)** suboptimal supply of blood-derived nutrients to the cells as a result of the higher TH+ neuron: blood vessel ratio in the high cell density regions. Casper et al. (2003) recently showed that dopaminergic neurons in VM grafts were associated with blood vessels. It would be interesting to extend the topographic analysis by examining the relationship between vascular elements and dopaminergic neuron viability (including soma size and neurite outgrowth); **2)** differential access to diffusible host-derived trophic factors and **3**) effect of grafted cell density - grafted cells show better differentiation and integration into the host tissue in low than in high cell density grafts (Ostenfeld et al., 2000; Deacon et al., 1998; Björklund et al., 2002). It has been suggested that a low cell concentration may decrease contact between the grafted cells and increase the influence from the adult host striatum (Björklund et al., 2002).

4.3.3. Effect of Graft Cell Suspension Composition on Dopaminergic Neuron Survival

Prior to grafting, ES-cell derived TH+ neurons made up 25 – 30% of the total neuronal population, the rest of the cells being neuronal precursors and undifferentiated ES cells. After five weeks, many grafts contained 5-HT+ neurons. Other groups have also shown the presence of significant numbers of 5-HT+ neurons and smaller numbers of other neuronal phenotypes including γ aminobutyric acid- and glutamate decarboxylase-positive neurons after the grafting of naïve (Björklund et al., 2002) and Nurr-1 over-expressing mouse ES cells (Kim et al., 2002) in hemiparkinsonian rats. 5-HT and dopaminergic neurons are generated at the same region (on either side of the isthmic organiser) during development and their early differentiation share some features including dependency on fibroblast growth factor 8 and

sonic hedgehog (Kim et al., 2002; Rodriguez-Pallares et al., 2003). Both stimulatory (Liu and Lauder, 1992) and inhibitory (Rodriguez-Pallares et al., 2003) effects of 5-HT on the growth of dopaminergic neurons have been reported in vitro. It is not known whether 5-HT exerts the same effects in vivo. Consistent with the observations of Deacon et al. (1998), grafted TH+ neurons displayed more extensive neurites than 5-HT+ neurons suggesting that the denervated striatum is more supportive of the growth of dopaminergic neurons. It is not known whether the non-dopaminergic neurons and other cells found in pre-differentiated ES cell suspensions are important for the survival of dopaminergic neurons or whether the in vivo survival may be improved by grafting enriched ES cell suspensions. Nevertheless selection for differentiated cells is necessary for the elimination of undifferentiated ES cells.

4.4. Characterisation of the Host Glial and Immune Responses

4.4.1. The Astrocytic Response

Injury to the CNS, such as occurs during grafting, is followed by the release of extracellular signals that induce the activation of astrocytes (Fawcett and Asher, 1999). In agreement with Finsen et al. (1991), we found that (in non-immunosuppressed animals), the astrogliosis was stronger and persisted for longer periods in xenograft recipients compared to sham animals. After five weeks, grafted TH+ cells lacked neurites and were isolated from the host tissue by a gliotic scar. The glial scar can be inhibitory to axonal outgrowth, an effect attributed to the upregulation of several extracellular matrix molecules on reactive astrocytes, the main cells forming the glial scar (Fawcett, 1994; Barker et al., 1996; Fawcett and Asher, 1999). The involvement of the glial scar in determining grafted cell integration is supported by in vivo data showing that the anatomical integration of intrastriatal VM grafts is more substantial following implantation into newborn than into adult recipients (Snyder-Keller et al., 1989; Olsson et al., 1997; Englund et al., 2002). Glial scarring is weaker in neonatal brain. Astroglia

could also display growth-promoting properties by secreting neurotrophic factors (Takeshima et al., 1994; Fawcett and Asher 1999).

Immunosuppressed animals displayed reduced astrogliosis at the host-graft interface (most notable after five weeks) and many of the surviving TH+ neurons demonstrated robust neurite outgrowth at this time point. Interestingly, TH+ neurites at the graft border were oriented away from the glial wall and/or along the graft perimeter. These data support the idea that the astroglial environment is inhibitory to the growth of axons. It has also been suggested that astroglia may present a mechanical barrier to outgrowing neurites (Fawcett and Asher, 1999). Although we cannot exclude the influence of graft rejection and grafted cell density on the morphological characteristics of grafted dopaminergic neurons, our results support the hypothesis that interactions between graft and host tissue, specifically the formation of the glial scar at the graft border, are important for the anatomical integration of grafted dopaminergic neurons (Petit et al., 2002).

4.4.2. The Host Immune Response

Although the brain is an immunologically privileged transplantation site, intracerebral neural grafts are rejected whenever there is immunological incompatibility between donor and host tissue (Dunnett, 1991). The exact mechanism of graft rejection is not completely understood but major histocompatibility complex class I and class II antigens expressed on the surface of donor cells are considered a prerequisite for the induction of host immune responses (Finsen et al., 1991; Duan et al., 1995, 2001). It was reported that immature brain tissue and recently, human ES cells lack MHC class II antigens and demonstrate very low levels of MHC class I. However the expression of both antigens can be quickly induced in these cells e.g. as a result of the inflammatory reaction that occurs following grafting thus rendering the cells susceptible to destruction by the host's T cells (Finsen et al., 1991; Drukker et al., 2002).

The temporal pattern of activation of microglia and macrophages, upregulation of complement receptor 3 and induction of MHC class I and class II antigen expression observed in non-immunosuppressed graft recipients was similar to that described in earlier studies during the rejection of mouse neuronal grafts in the adult rat brain (Finsen et al., 1991; Duan et al., 1995). The accumulation of immunostimulatory cells in sham-transplanted animals after 2 and 7 days confirmed that the initial inflammatory responses were triggered by injury to the host tissue during the grafting procedure (Duan et al., 1995). We did not perform a detailed analysis of the host immune response in cyclosporine A-treated animals. ED1 immunoreactivity in these animals revealed the presence of activated microglia/macrophages within grafts and in the adjacent host tissue up to five weeks after grafting. Interestingly, there were no detectable differences in the accumulation of activated microglia/macrophages between immunosuppressed and non-immunosuppressed graft recipients. Microglia and macrophages are known to display multiple functions in the immune system. Activated microglia can release free radicals and other neurotoxic molecules (Fawcett and Asher, 1999) and are capable of presenting antigen to host lymphocytes thus inducing immune responses (Hayes et al., 1987; Poltorak and Freed, 1989). However, activated microglia can also provide a neuroprotective function through scavenging free radicals and secreting growth factors (Kreutzberg, 1996; Depino et al., 2003). The neurotoxic and neuroprotective properties may be predominant at different time points following CNS injury.

4.4.3. Strategies to Reduce the Rejection of Grafted Dopaminergic Neurons

The rejection of intracerebral neural xenografts is mainly mediated by T-lymphocytes and can be controlled with immunosuppressive drugs (Pakzaban and Isacson, 1994). Cyclosporine A, which acts by inhibiting T cells, is the most widely used immunosuppressant for neural transplantation (Dunnett, 1991). Chronic administration of CsA is necessary to prevent the rejection of xenografts (Brundin et al., 1989) and this is associated with various adverse side

effects including increased risk of opportunistic infections (Duan et al., 1996). The reduction in spontaneous motor activity following initiation of cyclosporine A administration found in this study is consistent with earlier observations made by Borlongan et al. (1996).

Non-pharmacological approaches to improving the long term survival of grafted dopaminergic neurons are based on the reduction of the host immune response to the grafted cells e.g. removal of specific T cell subpopulations and/or the reduction of donor tissue immunogenicity (Dunnett, 1991). Duan et al. (2001) showed improved graft survival following the grafting of mouse MHC class I- or class II-depleted dopaminergic neurons in rats. ES cells are likewise amenable to genetic manipulation and strategies proposed to reduce ES cell immunogenicity include deletion of the genes involved in the induction of the rejection process such as the MHC genes as described above (Czyz et al., 2003).

4.5. Tumourigenic Potential of Grafted Embryonic Stem Cells

In immunosuppressed animals, the mean number of surviving TH+ neurons was higher at five weeks compared to one week post-grafting. At the time of grafting, SDIA-treated ES cell suspensions may contain committed dopaminergic neuronal precursors which are not mature enough to express TH but differentiate into dopaminergic neurons after grafting (Morizane et al., 2002). It is not known how many TH+ neurons are generated this way. Despite the absence of Ki67 positive cells within grafts in animals which had not developed tumours, we cannot exclude the possibility of proliferation of undifferentiated ES cells at other time points.

Five weeks post-grafting, tumour formation was detected in 2 out of 15 immunosuppressed ES cell recipients but not in non-immunosuppressed animals. It is known that chronic cyclosporine A immunosuppression predisposes graft recipients to the development of lymphomas (Duan et al., 1996). However no tumours were detected in host brains following

the grafting of postmitotic foetal VM with adjunctive cyclosporine A immunosuppression (Brundin et al., 1985; Brundin et al., 1989). The formation of tumours in this study may be related to the proliferation of undifferentiated ES cells in vivo. Tumour formation after the grafting of pre-differentiated ES cells has been reported elsewhere (Blyszczuk et al., 2003). Cyclosporine A immunosuppression may increase the risk of tumourigenesis by improving the survival of the undifferentiated ES cells. Although many protocols for the induction of dopaminergic neurons from ES cells include a step for the selection of differentiated cells (Kawasaki et al., 2000; Lee et al., 2000; Chung et al., 2002), it is believed that no differentiation protocol can yield an ES cell population with 100% post-mitotic cells. At present, no reliable practical method exists for excluding undifferentiated ES cells from differentiated ES cell suspensions prior to grafting. A combination of several methods e.g. lineage selection and fluorescent activated cell sorting may be effective in eliminating undifferentiated ES cells. Other proposals include the active elimination of tumourigenic cells by directing the expression of apoptosis controlling genes in graft tissue (Czyz et al., 2003).

4.6. Implications for Functional Integration

Behavioural tests provide the simplest way of demonstrating the survival and functional integration of grafted dopaminergic neurons in animal models of PD. In non-immunosuppressed animals, graft-derived dopaminergic neurons led to a significant reduction in amphetamine-induced rotational asymmetry despite the lack of anatomical integration of the grafted TH+ cells. Reconstruction of the neural circuitry is not always a prerequisite for functional recovery after the transplantation of dopamine-producing cells in animal models of PD (Dunnett, 1991; Feldman et al., 1997; Björklund and Lindvall, 2000). Amphetamine can induce the release of dopamine from the grafted dopaminergic neurons leading to the restoration of drug-induced rotation. A synaptic integration of the transplanted cells may be necessary for the grafts to have an effect on apomorphine-induced rotation (Baier et al., 2004).

In immunosuppressed animals, grafted dopaminergic neurons did not attenuate drug-induced rotation despite the fact that after five weeks more than half of the graft recipients had a higher number of surviving TH+ neurons than the minimum number of neurons considered sufficient to induce reduction in rotation asymmetry (≈ 700) (Clarkson et al., 1998; Brundin and Björklund, 1998; Isacson et al., 2003). There was no correlation between the number of surviving TH+ neurons and changes in amphetamine-/apomorphine-induced rotation. Many animals displayed significant weight loss/reduced rate of weight gain and reduced spontaneous motor activity after the initiation of immunosuppressive treatment. It is possible that treatment effects were masked by motor impairments due to opportunistic infections.

The lack of change in the number of striatal D1 receptor binding sites following denervation and/or the transplantation of dopamine-producing cells is consistent with observations made by Graham et al. (1990). This and other studies showed no change in D1 receptor binding and an increase in striatal D2 receptor binding in hemiparkinsonian rodents (Savasta et al., 1987; Dawson et al., 1991). It has been postulated that D1 receptors may be located extrasynaptically whereas D2 receptors are positioned postsynaptically to the nigrostriatal terminals. Denervation therefore results in supersensitivity of D2 receptors but not of D1 receptors which are under normal conditions not stimulated by synaptically released dopamine (Graham et al., 1990; Caille et al., 1996). An increase in the binding sites of D2 receptors has been demonstrated by PET and SPECT studies in PD patients (Booij et al., 1999; Barker and Dunnett, 1999). The D2 receptor upregulation was reversed by the transplantation of foetal VM cells (Barker and Dunnett, 1999).

The loss of dopamine transporter binding sites following 6-OHDA-induced denervation has been reported elsewhere (Brownell et al., 1998; Chalon et al., 1999; Booij et al., 2002). In vivo imaging studies in humans show a clear loss of dopamine transporter binding in PD

(Booij et al., 1999). Recovery of DAT binding was reported following neural transplantation in hemiparkinsonian rats (Brownell et al., 1998) but not in PD patients despite a significant increase of fluorodopa uptake (Cochen et al., 2003). The latter finding suggests that clinical benefit induced by the graft may be more related to increased dopaminergic activity than improved dopaminergic innervation in the host striatum. Due to technical difficulties, we could not use the brains prepared for in vitro receptor autoradiography to perform immunohistochemistry for tyrosine hydroxylase (to confirm the survival of grafted dopaminergic neurons). The use of SPECT or PET techniques for the imaging of dopamine receptor and transporter binding sites for future studies may have the added advantage that the brains would be available for immunohistochemical analysis at the end of the study.

In addition to drug-induced rotation, a battery of motor tests can be used to assess the effects of the grafted cells. The performance of complex, sensorimotor tasks requires controlled synaptic dopamine release. We found evidence for the loss of TH+ neurites between one and five weeks, a phenomenon which could have different causes including graft rejection and lack of target-derived neurotrophic factors. In order to optimise functional integration of grafted TH+ cells, strategies should be developed to prevent neurite degeneration and/or stimulate neurite outgrowth in these cells. Strategies to improve anatomical and functional integration of the grafted dopaminergic neurons may include: **1)** application of neurotrophic factors such as glial derived neurotrophic factor (Lin et al., 1993; Hudson et al., 1995) to minimise the neurite loss observed; **2)** promoting the penetration of grafted TH+ fibres into the host tissue. A better understanding of the molecular interactions between the host and graft tissue at the graft border especially the inhibitory environment of the glial scar (Petit et al., 2002; Barker et al., 1996) would be needed to achieve this objective and **3)** a multitarget transplantation strategy should lead to increased dopaminergic reinnervation of the other basal ganglia structures and hence improved functional effects (Mukhida et al., 2001).

Chapter 5: Summary

Background: Transplantation of foetal ventral mesencephalic cells has been studied in rat models of Parkinson's disease and parkinsonian patients. Difficulties in obtaining sufficient donor brain tissue have limited the clinical application of this therapy and shifted the focus towards the use of embryonic stem cells. Undifferentiated mouse ES cells differentiate into functional dopaminergic neurons after grafting in hemiparkinsonian rats but induce the formation of tumours, a problem which might be circumvented by grafting pre-differentiated ES cells.

Aim: The aim of this thesis was to study the fate of pre-differentiated mouse embryonic stem cells transplanted in adult rats with 6-hydroxydopamine-induced hemiparkinsonism.

Methods: Mouse ES cells were differentiated on a PA6-feeder for 14 days – 25 – 30% of the obtained neurons were positive for tyrosine hydroxylase – labelled with PKH26 and grafted as a suspension in the corpora striata of hemiparkinsonian adult rats with or without adjunctive cyclosporine A immunosuppression. Rats were challenged with amphetamine and apomorphine pre- and (when possible) post-grafting to assess the extent of the lesion and functional effects of the grafted cells. The survival and integration of the grafted cells and the host responses were analysed at different time points (up to five weeks) post-grafting using histochemistry, immunohistochemistry and in vitro receptor autoradiography.

Results: Mouse ES cell-derived, in vitro-differentiated dopaminergic neurons survive intrastriatal transplantation in hemiparkinsonian adult rats, express tyrosine hydroxylase and vesicular monoamine transporter (both of which are involved in dopaminergic neuro-transmission) and alleviate amphetamine-induced rotation in graft recipients. In the absence of immunosuppressive treatment, there is a strong activation of the host immune response and grafts are rejected. Cyclosporine A immunosuppression improves the survival of grafted

dopaminergic neurons but is associated with several adverse side effects including reduced spontaneous motor activity, increased risk of tumour formation and increased morbidity. Grafted dopaminergic neurons lose neurites over time and demonstrate limited reinnervation of the host striatum. There was a differential pattern of vascularisation between immunosuppressed and non-immunosuppressed graft recipients but no indication of a direct relationship between transplant vascularisation and the viability of grafted dopaminergic neurons. The number of striatal D1 receptor binding sites was not altered by denervation and/or the grafting of dopamine-producing cells. In contrast, denervation induced a loss of dopamine transporter binding in the ipsilateral striatum. This loss was not reversed by pre-differentiated mouse embryonic stem cell grafts at five weeks post grafting.

Conclusions: The results presented here demonstrate the potential of pre-differentiated embryonic stem cells for generating functional dopaminergic neurons for cell replacement therapy in Parkinson's disease. In order to optimise this therapeutic approach, novel strategies should be developed to direct efficient differentiation of embryonic stem cells and to promote the survival and integration of embryonic stem cell-derived dopaminergic neurons after transplantation in host brains.

Contributions

1. ES cell differentiation:

Dr. Jan Schindehütte, PD Dr. Ahmed Mansouri

Max Planck Institute for Biophysical Chemistry, Göttingen

2. Lesion and transplantation surgery and behavioural testing:

Dr. Paul Christian Baier

Assistance: Keneuoe Hycianth Thinyane

Department of Clinical Neurophysiology

Medical School, University of Göttingen

3. Histology and receptor autoradiography:

Keneuoe Hycianth Thinyane

Technical assistance: Simone Lüert

Susanne Bauch (for confocal laser scanning microscopy)

Clinical Neurobiology Laboratory

German Primate Center, Göttingen

References

Abercrombie M (1946) Estimation of nuclear population from microtome section. Anat Rec 94: 239-247.

Baier PC, Schindehutte J, Thinyane K, Flugge G, Fuchs E, Mansouri A, Paulus W, Gruss P, Trenkwalder C (2004) Behavioral changes in unilaterally 6-hydroxy-dopamine lesioned rats after transplantation of differentiated mouse embryonic stem cells without morphological integration. Stem Cells 22: 396-404.

Bain G, Kitchens D, Yao M, Huettner JE, Gottlieb DI (1995) Embryonic stem cells express neuronal properties in vitro. Dev Biol 168: 342-357.

Barberi T, Klivenyi P, Calingasan NY, Lee H, Kawamata H, Loonam K, Perrier AL, Bruses J, Rubio ME, Topf N, Tabar V, Harrison NL, Beal MF, Moore MA, Studer L (2003) Neural subtype specification of fertilization and nuclear transfer embryonic stem cells and application in parkinsonian mice. Nat Biotechnol 21: 1200-1207.

Barker CF, Billingham RE (1977) Immunologically privileged sites. Adv Immunol 25: 1-54.

Barker RA, Dunnett SB (1999) Functional integration of neural grafts in Parkinson's disease. Nat Neurosci 2: 1047-1048.

Barker RA, Dunnett SB, Faissner A, Fawcett JW (1996) The time course of loss of dopaminergic neurons and the gliotic reaction surrounding grafts of embryonic mesencephalon to the striatum. Exp Neurol 141: 79-93.

Beal MF (2001) Experimental models of Parkinson's disease. Nat Rev Neurosci 2: 325-334.

Beresford IJ, Davenport AP, Sirinathsinghji DJ, Hall MD, Hill RG, Hughes J (1988) Experimental hemiparkinsonism in the rat following chronic unilateral infusion of MPP+ into

the nigrostriatal dopamine pathway--II. Differential localization of dopamine and cholecystokinin receptors. Neuroscience 27: 129-143.

Betarbet R, Sherer TB, Greenamyre JT (2002) Animal models of Parkinson's disease. Bioessays 24: 308-318.

Bjorklund A, Lindvall O (2000) Cell replacement therapies for central nervous system disorders. Nat Neurosci 3: 537-544.

Bjorklund A, Stenevi U, Schmidt RH, Dunnett SB, Gage FH (1983) Intracerebral grafting of neuronal cell suspensions. II. Survival and growth of nigral cell suspensions implanted in different brain sites. Acta Physiol Scand Suppl 522: 9-18.

Bjorklund LM, Sanchez-Pernaute R, Chung S, Andersson T, Chen IY, McNaught KS, Brownell AL, Jenkins BG, Wahlestedt C, Kim KS, Isacson O (2002) Embryonic stem cells develop into functional dopaminergic neurons after transplantation in a Parkinson rat model. Proc Natl Acad Sci U S A 99: 2344-2349.

Blyszczuk P, Czyz J, Kania G, Wagner M, Roll U, St Onge L, Wobus AM (2003) Expression of Pax4 in embryonic stem cells promotes differentiation of nestin-positive progenitor and insulin-producing cells. Proc Natl Acad Sci U S A 100: 998-1003.

Bohlen und HO, Schober A, Krieglstein K (2004) Genes, proteins, and neurotoxins involved in Parkinson's disease. Prog Neurobiol 73: 151-177.

Booij J, de Bruin K, de Win MM, Lavini C, den Heeten GJ, Habraken JB (2003) Imaging of striatal dopamine transporters in rat brain with single pinhole SPECT and co-aligned MRI is highly reproducible. Nucl Med Biol 30: 643-649.

Booij J, de Bruin K, Habraken JB, Voorn P (2002) Imaging of dopamine transporters in rats using high-resolution pinhole single-photon emission tomography. Eur J Nucl Med Mol Imaging 29: 1221-1224.

Booij J, Tissingh G, Winogrodzka A, van Royen EA (1999) Imaging of the dopaminergic neurotransmission system using single-photon emission tomography and positron emission tomography in patients with parkinsonism. Eur J Nucl Med 26: 171-182.

Borlongan CV, Freeman TB, Hauser RA, Cahill DW, Sanberg PR (1996) Cyclosporine-A increases locomotor activity in rats with 6-hydroxydopamine-induced hemiparkinsonism: relevance to neural transplantation. Surg Neurol 46: 384-388.

Brownell AL, Livni E, Galpern W, Isacson O (1998) In vivo PET imaging in rat of dopamine terminals reveals functional neural transplants. Ann Neurol 43: 387-390.

Brundin P, Bjorklund A (1998) Survival of expanded dopaminergic precursors is critical for clinical trials. Nat Neurosci 1: 537.

Brundin P, Dunnett S, Bjorklund A, Nikkhah G (2001) Transplanted dopaminergic neurons: more or less? Nat Med 7: 512-513.

Brundin P, Nilsson OG, Gage FH, Bjorklund A (1985) Cyclosporin A increases survival of cross-species intrastriatal grafts of embryonic dopamine-containing neurons. Exp Brain Res 60: 204-208.

Brundin P, Widner H, Nilsson OG, Strecker RE, Bjorklund A (1989) Intracerebral xenografts of dopamine neurons: the role of immunosuppression and the blood-brain barrier. Exp Brain Res 75: 195-207.

Buehr M, Nichols J, Stenhouse F, Mountford P, Greenhalgh CJ, Kantachuvesiri S, Brooker G, Mullins J, Smith AG (2003) Rapid loss of Oct-4 and pluripotency in cultured rodent blastocysts and derivative cell lines. Biol Reprod 68: 222-229.

Caille I, Dumartin B, Bloch B (1996) Ultrastructural localization of D1 dopamine receptor immunoreactivity in rat striatonigral neurons and its relation with dopaminergic innervation. Brain Res 730: 17-31.

Casper D, Finkelstein E, Goldstein IM, Palencia D, Yunger Y, Pidel A (2003) Dopaminergic neurons associate with blood vessels in neural transplants. Exp Neurol 184: 785-793.

Castilho RF, Hansson O, Brundin P (2000) FK506 and cyclosporin A enhance the survival of cultured and grafted rat embryonic dopamine neurons. Exp Neurol 164: 94-101.

Catapano LA, Sheen VL, Leavitt BR, Macklis JD (1999) Differentiation of transplanted neural precursors varies regionally in adults striatum. Neuroreport 10: 3971-3977.

Chalon S, Emond P, Bodard S, Vilar MP, Thiercelin C, Besnard JC, Guilloteau D (1999) Time course of changes in striatal dopamine transporter and D2 receptors with specific iodinated markers in a rat model of Parkinson's disease. Synapse 31(2): 134-139

Chase TN, Oh JD, Blanchet PJ (1998) Neostriatal mechanisms in Parkinson's disease. Neurology 51: S30-S35.

Chung S, Sonntag KC, Andersson T, Bjorklund LM, Park JJ, Kim DW, Kang UJ, Isacson O, Kim KS (2002) Genetic engineering of mouse embryonic stem cells by Nurr1 enhances differentiation and maturation into dopaminergic neurons. Eur J Neurosci 16: 1829-1838.

Cicchetti F, Brownell AL, Williams K, Chen YI, Livni E, Isacson O (2002) Neuroinflammation of the nigrostriatal pathway during progressive 6-OHDA dopamine

degeneration in rats monitored by immunohistochemistry and PET imaging. Eur J Neurosci 15: 991-998.

Clarkson ED, Zawada WM, Adams FS, Bell KP, Freed CR (1998) Strands of embryonic mesencephalic tissue show greater dopamine neuron survival and better behavioral improvement than cell suspensions after transplantation in parkinsonian rats. Brain Res 806: 60-68.

Cochen V, Ribeiro MJ, Nguyen JP, Gurruchaga JM, Villafane G, Loc'h C, Defer G, Samson Y, Peschanski M, Hantraye P, Cesaro P, Remy P (2003) Transplantation in Parkinson's disease: PET changes correlate with the amount of grafted tissue. Mov Disord 18: 928-932.

Cortes R, Camps M, Gueye B, Probst A, Palacios JM (1989) Dopamine receptors in human brain: autoradiographic distribution of D1 and D2 sites in Parkinson syndrome of different etiology. Brain Res 483: 30-38.

Czyz J, Wiese C, Rolletschek A, Blyszczuk P, Cross M, Wobus AM (2003) Potential of embryonic and adult stem cells in vitro. Biol Chem 384: 1391-1409.

Dauer W, Przedborski S (2003) Parkinson's disease: mechanisms and models. Neuron 39: 889-909.

Dawson TM, Dawson VL, Gage FH, Fisher LJ, Hunt MA, Wamsley JK (1991) Functional recovery of supersensitive dopamine receptors after intrastriatal grafts of fetal substantia nigra. Exp Neurol 111: 282-292.

De Long MR, (2000) The basal ganglia. In: Kandel R, Schwartz JH, Jessell TM, (eds.). Principles of Neural Science. New York: McGraw-Hill.

Deacon T, Dinsmore J, Costantini LC, Ratliff J, Isacson O (1998) Blastula-stage stem cells can differentiate into dopaminergic and serotonergic neurons after transplantation. Exp Neurol 149: 28-41.

Depino AM, Earl C, Kaczmarczyk E, Ferrari C, Besedovsky H, del Rey A, Pitossi FJ, Oertel WH (2003) Microglial activation with atypical proinflammatory cytokine expression in a rat model of Parkinson's disease. Eur J Neurosci 18: 2731-2742.

Doetschman TC, Eistetter H, Katz M, Schmidt W, Kemler R (1985) The in vitro development of blastocyst-derived embryonic stem cell lines: formation of visceral yolk sac, blood islands and myocardium. J Embryol Exp Morphol 87: 27-45.

Drukker M, Katz G, Urbach A, Schuldiner M, Markel G, Itskovitz-Eldor J, Reubinoff B, Mandelboim O, Benvenisty N (2002) Characterization of the expression of MHC proteins in human embryonic stem cells. Proc Natl Acad Sci U S A 99: 9864-9869.

Duan WM, Brundin P, Grasbon-Frodl EM, Widner H (1996) Methylprednisolone prevents rejection of intrastriatal grafts of xenogeneic embryonic neural tissue in adult rats. Brain Res 712: 199-212.

Duan WM, Westerman M, Flores T, Low WC (2001) Survival of intrastriatal xenografts of ventral mesencephalic dopamine neurons from MHC-deficient mice to adult rats. Exp Neurol 167: 108-117.

Duan WM, Widner H, Brundin P (1995) Temporal pattern of host responses against intrastriatal grafts of syngeneic, allogeneic or xenogeneic embryonic neuronal tissue in rats. Exp Brain Res 104: 227-242.

Dunnett SB (1991) Transplantation of embryonic dopamine neurons: what we know from rats. J Neurol 238: 65-74.

Dunnett SB (1994) Behavioural consequences of neural transplantation. J Neurol 242: S43-S53.

Dunnett SB (1995) Functional repair of striatal systems by neural transplants: evidence for circuit reconstruction. Behav Brain Res 66: 133-142.

Dunnett SB, Bjorklund A (1999) Prospects for new restorative and neuroprotective treatments in Parkinson's disease. Nature 399: A32-A39.

Dusart I, Marty S, Peschanski M (1991) Glial changes following an excitotoxic lesion in the CNS--II. Astrocytes. Neuroscience 45: 541-549.

Dusart I, Nothias F, Roudier F, Besson JM, Peschanski M (1989) Vascularization of fetal cell suspension grafts in the excitotoxically lesioned adult rat thalamus. Brain Res Dev Brain Res 48: 215-228.

Emgard M, Karlsson J, Hansson O, Brundin P (1999) Patterns of cell death and dopaminergic neuron survival in intrastriatal nigral grafts. Exp Neurol 160: 279-288.

Englund U, Fricker-Gates RA, Lundberg C, Bjorklund A, Wictorin K (2002) Transplantation of human neural progenitor cells into the neonatal rat brain: extensive migration and differentiation with long-distance axonal projections. Exp Neurol 173: 1-21.

Fawcett J (1994) Astrocytes and axon regeneration in the central nervous system. J Neurol 242: S25-S28.

Fawcett JW, Asher RA (1999) The glial scar and central nervous system repair. Brain Res Bull 49: 377-391.

Feldmann SF, Meyer JS, Quenzer LF (eds.) (1997) In principles of neuropsychopharmacology. Sunderland, MA; Sinauer Associates Inc.

Finkelstein DI, Stanic D, Parish CL, Tomas D, Dickson K, Horne MK (2000) Axonal sprouting following lesions of the rat substantia nigra. Neuroscience 97: 99-112.

Finsen BR, Sorensen T, Castellano B, Pedersen EB, Zimmer J (1991) Leukocyte infiltration and glial reactions in xenografts of mouse brain tissue undergoing rejection in the adult rat brain. A light and electron microscopical immunocytochemical study. J Neuroimmunol 32: 159-183.

Fisher LJ, Gage FH (1993) Grafting in the mammalian central nervous system. Physiol Rev 73: 583-616.

Fraichard A, Chassande O, Bilbaut G, Dehay C, Savatier P, Samarut J (1995) In vitro differentiation of embryonic stem cells into glial cells and functional neurons. J Cell Sci 108 (Pt 10): 3181-3188.

Freed C, Revay R, Vaughan RA, Kriek E, Grant S, Uhl GR, Kuhar MJ (1995) Dopamine transporter immunoreactivity in rat brain. J Comp Neurol 359: 340-349.

Freed CR, Greene PE, Breeze RE, Tsai WY, DuMouchel W, Kao R, Dillon S, Winfield H, Culver S, Trojanowski JQ, Eidelberg D, Fahn S (2001) Transplantation of embryonic dopamine neurons for severe Parkinson's disease. N Engl J Med 344: 710-719.

Freed CR, Leehey MA, Zawada M, Bjugstad K, Thompson L, Breeze RE (2003) Do patients with Parkinson's disease benefit from embryonic dopamine cell transplantation? J Neurol 250 Suppl 3: III44-III46.

Freed WJ, Poltorak M, Becker JB (1990) Intracerebral adrenal medulla grafts: a review. Exp Neurol 110: 139-166.

Gasser T (2003) Overview of the genetics of parkinsonism. Adv Neurol 91: 143-152.

Geny C, Naimi-Sadaoui S, Jeny R, Belkadi AM, Juliano SL, Peschanski M (1994) Long-term delayed vascularization of human neural transplants to the rat brain. J Neurosci 14: 7553-7562.

Giovanni A, Sieber BA, Heikkila RE, Sonsalla PK (1994) Studies on species sensitivity to the dopaminergic neurotoxin 1-methyl-4-phenyl-1,2,3,6-tetrahydropyridine. Part 1: Systemic administration. J Pharmacol Exp Ther 270: 1000-1007.

Graham WC, Crossman AR, Woodruff GN (1990) Autoradiographic studies in animal models of hemi-parkinsonism reveal dopamine D2 but not D1 receptor supersensitivity. I. 6-OHDA lesions of ascending mesencephalic dopaminergic pathways in the rat. Brain Res 514: 93-102.

Haas SJ, Bauer P, Rolfs A, Wree A (2000) Immunocytochemical characterization of in vitro PKH26-labelled and intracerebrally transplanted neonatal cells. Acta Histochem 102: 273-280.

Hagell P, Piccini P, Bjorklund A, Brundin P, Rehncrona S, Widner H, Crabb L, Pavese N, Oertel WH, Quinn N, Brooks DJ, Lindvall O (2002) Dyskinesias following neural transplantation in Parkinson's disease. Nat Neurosci 5: 627-628.

Hayes GM, Woodroofe MN, Cuzner ML (1987) Microglia are the major cell type expressing MHC class II in human white matter. J Neurol Sci 80: 25-37.

Hersch SM, Ciliax BJ, Gutekunst CA, Rees HD, Heilman CJ, Yung KK, Bolam JP, Ince E, Yi H, Levey AI (1995) Electron microscopic analysis of D1 and D2 dopamine receptor proteins in the dorsal striatum and their synaptic relationships with motor corticostriatal afferents. J Neurosci 15: 5222-5237.

Hudson J, Granholm AC, Gerhardt GA, Henry MA, Hoffman A, Biddle P, Leela NS, Mackerlova L, Lile JD, Collins F, . (1995) Glial cell line-derived neurotrophic factor augments midbrain dopaminergic circuits in vivo. Brain Res Bull 36: 425-432.

Isacson O, Bjorklund LM, Schumacher JM (2003) Toward full restoration of synaptic and terminal function of the dopaminergic system in Parkinson's disease by stem cells. Ann Neurol 53 Suppl 3: S135-S146.

Isovich E, Mijnster MJ, Flugge G, Fuchs E (2000) Chronic psychosocial stress reduces the density of dopamine transporters. Eur J Neurosci 12: 1071-1078.

Jenner P (2003) Dopamine agonists, receptor selectivity and dyskinesia induction in Parkinson's disease. Curr Opin Neurol 16 Suppl 1: S3-S7.

Jensen MB, Finsen B, Zimmer J (1997) Morphological and immunophenotypic microglial changes in the denervated fascia dentata of adult rats: correlation with blood-brain barrier damage and astroglial reactions. Exp Neurol 143: 103-116.

Jeon BS, Jackson-Lewis V, Burke RE (1995) 6-Hydroxydopamine lesion of the rat substantia nigra: time course and morphology of cell death. Neurodegeneration 4: 131-137.

Kandel R, Schwartz JH, Jessell TM, (eds.) (2000) Principles of Neural Science. New York: McGraw-Hill.

Kawasaki H, Mizuseki K, Nishikawa S, Kaneko S, Kuwana Y, Nakanishi S, Nishikawa SI, Sasai Y (2000) Induction of midbrain dopaminergic neurons from ES cells by stromal cell-derived inducing activity. Neuron 28: 31-40.

Kim JH, Auerbach JM, Rodriguez-Gomez JA, Velasco I, Gavin D, Lumelsky N, Lee SH, Nguyen J, Sanchez-Pernaute R, Bankiewicz K, McKay R (2002) Dopamine neurons derived from embryonic stem cells function in an animal model of Parkinson's disease. Nature 418: 50-56.

Kohutnicka M, Lewandowska E, Kurkowska-Jastrzebska I, Czlonkowski A, Czlonkowska A (1998) Microglial and astrocytic involvement in a murine model of Parkinson's disease induced by 1-methyl-4-phenyl-1,2,3,6-tetrahydropyridine (MPTP). Immunopharmacology 39: 167-180.

Kordower JH, Freeman TB, Olanow CW (1998) Neuropathology of fetal nigral grafts in patients with Parkinson's disease. Mov Disord 13 Suppl 1: 88-95.

Kordower JH, Freeman TB, Snow BJ, Vingerhoets FJ, Mufson EJ, Sanberg PR, Hauser RA, Smith DA, Nauert GM, Perl DP, . (1995) Neuropathological evidence of graft survival and striatal reinnervation after the transplantation of fetal mesencephalic tissue in a patient with Parkinson's disease. N Engl J Med 332: 1118-1124.

Kordower JH, Goetz CG, Freeman TB, Olanow CW (1997) Dopaminergic transplants in patients with Parkinson's disease: neuroanatomical correlates of clinical recovery. Exp Neurol 144: 41-46.

Kordower JH, Rosenstein JM, Collier TJ, Burke MA, Chen EY, Li JM, Martel L, Levey AE, Mufson EJ, Freeman TB, Olanow CW (1996) Functional fetal nigral grafts in a patient with

Parkinson's disease: chemoanatomic, ultrastructural, and metabolic studies. J Comp Neurol 370: 203-230.

Kreutzberg GW (1996) Microglia: a sensor for pathological events in the CNS. Trends Neurosci 19: 312-318.

Kullberg S, Aldskogius H, Ulfhake B (2001) Microglial activation, emergence of ED1-expressing cells and clusterin upregulation in the aging rat CNS, with special reference to the spinal cord. Brain Res 899: 169-186.

Larsson LC, Duan WM, Widner H (1999) Discordant xenografts: different outcome after mouse and rat neural tissue transplantation to guinea-pigs. Brain Res Bull 49: 367-376.

Lawrence JM, Huang SK, Raisman G (1984) Vascular and astrocytic reactions during establishment of hippocampal transplants in adult host brain. Neuroscience 12: 745-760.

Lee SH, Lumelsky N, Studer L, Auerbach JM, McKay RD (2000) Efficient generation of midbrain and hindbrain neurons from mouse embryonic stem cells. Nat Biotechnol 18: 675-679.

Leigh K, Elisevich K, Rogers KA (1994) Vascularization and microvascular permeability in solid versus cell-suspension embryonic neural grafts. J Neurosurg 81: 272-283.

Lin LF, Doherty DH, Lile JD, Bektesh S, Collins F (1993) GDNF: a glial cell line-derived neurotrophic factor for midbrain dopaminergic neurons. Science 260: 1130-1132.

Lindvall O (1994) Clinical application of neuronal grafts in Parkinson's disease. J Neurol 242: S54-S56.

Lindvall O, Hagell P (2002) Cell replacement therapy in human neurodegenerative disorders. Clinical Neuroscience Research 2:86 – 92.

Liu J, Lauder JM (1992) Serotonin promotes region-specific glial influences on cultured serotonin and dopamine neurons. Glia 5: 306-317.

Lotharius J, Brundin P (2002) Pathogenesis of Parkinson's disease: dopamine, vesicles and alpha-synuclein. Nat Rev Neurosci 3: 932-942.

Luthman J, Fredriksson A, Sundstrom E, Jonsson G, Archer T (1989) Selective lesion of central dopamine or noradrenaline neuron systems in the neonatal rat: motor behavior and monoamine alterations at adult stage. Behav Brain Res 33: 267-277.

Mahalik TJ, Clayton GH (1991) Specific outgrowth from neurons of ventral mesencephalic grafts to the catecholamine-depleted striatum of adult hosts. Exp Neurol 113: 18-27.

Marshall JF, Navarrete R, Joyce JN (1989) Decreased striatal D1 binding density following mesotelencephalic 6-hydroxydopamine injections: an autoradiographic analysis. Brain Res 493: 247-257.

Marty S, Dusart I, Peschanski M (1991) Glial changes following an excitotoxic lesion in the CNS--I. Microglia/macrophages. Neuroscience 45: 529-539.

Mijnster MJ, Isovich E, Flugge G, Fuchs E (1999) Localization of dopamine receptors in the tree shrew brain using [3H] - SCH23390 and [125I]-epidepride. Brain Res 841: 101-113.

Morizane A, Takahashi J, Takagi Y, Sasai Y, Hashimoto N (2002) Optimal conditions for in vivo induction of dopaminergic neurons from embryonic stem cells through stromal cell-derived inducing activity. J Neurosci Res 69: 934-939.

Mukhida K, Baker KA, Sadi D, Mendez I (2001) Enhancement of sensorimotor behavioral recovery in hemiparkinsonian rats with intrastriatal, intranigral, and intrasubthalamic nucleus dopaminergic transplants. J Neurosci 21: 3521-3530.

Nakashima H, Kawamura K, Date I (1988) Immunological reaction and blood-brain barrier in mouse-to-rat cross-species neural graft. Brain Res 475: 232-243.

Nikkhah G, Bentlage C, Cunningham MG, Bjorklund A (1994) Intranigral fetal dopamine grafts induce behavioral compensation in the rat Parkinson model. J Neurosci 14: 3449-3461.

Nirenberg MJ, Chan J, Liu Y, Edwards RH, Pickel VM (1996) Ultrastructural localization of the vesicular monoamine transporter-2 in midbrain dopaminergic neurons: potential sites for somatodendritic storage and release of dopamine. J Neurosci 16: 4135-4145.

Nutt JG, Carter JH, Sexton GJ (2004) The dopamine transporter: importance in Parkinson's disease. Ann Neurol 55: 766-773.

Olanow CW, Brin MF (2001) Surgical therapies for Parkinson's disease. A physician's perspective. Adv Neurol 86: 421-433.

Olanow CW, Goetz CG, Kordower JH, Stoessl AJ, Sossi V, Brin MF, Shannon KM, Nauert GM, Perl DP, Godbold J, Freeman TB (2003) A double-blind controlled trial of bilateral fetal nigral transplantation in Parkinson's disease. Ann Neurol 54: 403-414.

Olanow CW, Kordower JH, Freeman TB (1996) Fetal nigral transplantation as a therapy for Parkinson's disease. Trends Neurosci 19: 102-109.

Olsson M, Bentlage C, Wictorin K, Campbell K, Bjorklund A (1997) Extensive migration and target innervation by striatal precursors after grafting into the neonatal striatum. Neuroscience 79: 57-78.

Ostenfeld T, Caldwell MA, Prowse KR, Linskens MH, Jauniaux E, Svendsen CN (2000) Human neural precursor cells express low levels of telomerase in vitro and show diminishing cell proliferation with extensive axonal outgrowth following transplantation. Exp Neurol 164: 215-226.

Pakzaban P, Isacson O (1994) Neural xenotransplantation: reconstruction of neuronal circuitry across species barriers. Neuroscience 62: 989-1001.

Paxinos G, Watson C, (1998) The Rat Brain in Stereotaxic Coordinates. Fourth Edition; FL; Academic Press.

Petit A, Quenneville N, Vallee A, Pierret P, Doucet G (2002) Differences in host serotonin innervation of intrastriatal grafts are not determined by a glial scar or chondroitin sulfate proteoglycans. Exp Neurol 177: 61-74.

Piccini P, Brooks DJ, Bjorklund A, Gunn RN, Grasby PM, Rimoldi O, Brundin P, Hagell P, Rehncrona S, Widner H, Lindvall O (1999) Dopamine release from nigral transplants visualized in vivo in a Parkinson's patient. Nat Neurosci 2: 1137-1140.

Poltorak M, Freed WJ (1989) Immunological reactions induced by intracerebral transplantation: evidence that host microglia but not astroglia are the antigen-presenting cells. Exp Neurol 103: 222-233.

Polverini PJ, Cotran PS, Gimbrone MA, Jr., Unanue ER (1977) Activated macrophages induce vascular proliferation. Nature 269: 804-806.

Rascol O, Payoux P, Ory F, Ferreira JJ, Brefel-Courbon C, Montastruc JL (2003) Limitations of current Parkinson's disease therapy. Ann Neurol 53 Suppl 3: S3-12.

Rodriguez-Pallares J, Guerra MJ, Labandeira-Garcia JL (2003) Elimination of serotonergic cells induces a marked increase in generation of dopaminergic neurons from mesencephalic precursors. Eur J Neurosci 18: 2166-2174.

Rosenstein JM (1995) Why do neural transplants survive? An examination of some metabolic and pathophysiological considerations in neural transplantation. Exp Neurol 133: 1-6.

Saucedo-Cardenas O, Quintana-Hau JD, Le WD, Smidt MP, Cox JJ, De Mayo F, Burbach JP, Conneely OM (1998) Nurr1 is essential for the induction of the dopaminergic phenotype and the survival of ventral mesencephalic late dopaminergic precursor neurons. Proc Natl Acad Sci U S A 95: 4013-4018.

Savasta M, Dubois A, Feuerstein C, Manier M, Scatton B (1987) Denervation supersensitivity of striatal D2 dopamine receptors is restricted to the ventro- and dorsolateral regions of the striatum. Neurosci Lett 74: 180-186.

Savasta M, Mennicken F, Chritin M, Abrous DN, Feuerstein C, Le Moal M, Herman JP (1992) Intrastriatal dopamine-rich implants reverse the changes in dopamine D2 receptor densities caused by 6-hydroxydopamine lesion of the nigrostriatal pathway in rats: an autoradiographic study. Neuroscience 46: 729-738.

Sawamoto K, Nakao N, Kakishita K, Ogawa Y, Toyama Y, Yamamoto A, Yamaguchi M, Mori K, Goldman SA, Itakura T, Okano H (2001) Generation of dopaminergic neurons in the adult brain from mesencephalic precursor cells labeled with a nestin-GFP transgene. J Neurosci 21: 3895-3903.

Sawamoto K, Nakao N, Kobayashi K, Matsushita N, Takahashi H, Kakishita K, Yamamoto A, Yoshizaki T, Terashima T, Murakami F, Itakura T, Okano H (2001) Visualization, direct isolation, and transplantation of midbrain dopaminergic neurons. Proc Natl Acad Sci U S A 98: 6423-6428.

Schierle GS, Hansson O, Leist M, Nicotera P, Widner H, Brundin P (1999) Caspase inhibition reduces apoptosis and increases survival of nigral transplants. Nat Med 5: 97-100.

Schmitz Y, Schmauss C, Sulzer D (2002) Altered dopamine release and uptake kinetics in mice lacking D2 receptors. J Neurosci 22: 8002-8009.

Schwarting RK, Huston JP (1996) The unilateral 6-hydroxydopamine lesion model in behavioral brain research. Analysis of functional deficits, recovery and treatments. Prog Neurobiol 50: 275-331.

Schwarz SC, Schwarz J, Sautter J, Oertel WH (1998) Effects of macrophage migration inhibitory factor and macrophage migration stimulatory factor on function and survival of foetal dopaminergic grafts in the 6-hydroxydopamine rat model of Parkinson's disease. Exp Brain Res 120: 95-103.

Shin JJ, Fricker-Gates RA, Perez FA, Leavitt BR, Zurakowski D, Macklis JD (2000) Transplanted neuroblasts differentiate appropriately into projection neurons with correct neurotransmitter and receptor phenotype in neocortex undergoing targeted projection neuron degeneration. J Neurosci 20: 7404-7416.

Snyder-Keller AM, Carder RK, Lund RD (1989) Development of dopamine innervation and turning behavior in dopamine-depleted infant rats receiving unilateral nigral transplants. Neuroscience 30: 779-794.

Stanic D, Finkelstein DI, Bourke DW, Drago J, Horne MK (2003) Timecourse of striatal re-innervation following lesions of dopaminergic SNpc neurons of the rat. Eur J Neurosci 18: 1175-1188.

Stanic D, Parish CL, Zhu WM, Krstew EV, Lawrence AJ, Drago J, Finkelstein DI, Horne MK (2003) Changes in function and ultrastructure of striatal dopaminergic terminals that regenerate following partial lesions of the SNpc. J Neurochem 86: 329-343.

Studer L (2001) Stem cells with brainpower. Nat Biotechnol 19: 1117-1118.

Studer L, Tabar V, McKay RD (1998) Transplantation of expanded mesencephalic precursors leads to recovery in parkinsonian rats. Nat Neurosci 1: 290-295.

Takeshima T, Shimoda K, Sauve Y, Commissiong JW (1994) Astrocyte-dependent and -independent phases of the development and survival of rat embryonic day 14 mesencephalic, dopaminergic neurons in culture. Neuroscience 60: 809-823.

Thomson JA, Itskovitz-Eldor J, Shapiro SS, Waknitz MA, Swiergiel JJ, Marshall VS, Jones JM (1998) Embryonic stem cell lines derived from human blastocysts. Science 282: 1145-1147.

Ungerstedt U (1968) 6-Hydroxy-dopamine induced degeneration of central monoamine neurons. Eur J Pharmacol 5: 107-110.

Wobus AM, Holzhausen H, Jakel P, Schoneich J (1984) Characterization of a pluripotent stem cell line derived from a mouse embryo. Exp Cell Res 152: 212-219.

Yurek DM (1997) Intranigral transplants of fetal ventral mesencephalic tissue attenuate D1-agonist-induced rotational behavior. Exp Neurol 143: 1-9.

Zawada WM, Zastrow DJ, Clarkson ED, Adams FS, Bell KP, Freed CR (1998) Growth factors improve immediate survival of embryonic dopamine neurons after transplantation into rats. Brain Res 786: 96-103.

Zetterstrom RH, Williams R, Perlmann T, Olson L (1996) Cellular expression of the immediate early transcription factors Nurr1 and NGFI-B suggests a gene regulatory role in several brain regions including the nigrostriatal dopamine system. Brain Res Mol Brain Res 41: 111-120.

Zigmond MJ, Abercrombie ED, Berger TW, Grace AA, Stricker EM (1990) Compensations after lesions of central dopaminergic neurons: some clinical and basic implications. Trends Neurosci 13: 290-296.

Zigmond MJ, Abercrombie ED, Stricker EM (1990) Partial damage to nigrostriatal bundle: compensatory changes and the action of L-dopa. J Neural Transm Suppl 29: 217-232.

Acknowledgements

I thank Dr. Jan Schindehütte and PD. Dr. Ahmed Mansouri for the supply of embryonic stem cells and Dr. Christian Baier who performed and provided guidance in performing stereotactic surgery and behavioural testing.

The support and guidance of the following people made this work possible:

Prof. Dr. Eberhard Fuchs

PD. Dr. Gabriele Flügge

Prof. Dr. Friedrich-Wilhelm Schürmann

Prof. Dr. Walter Paulus

Simone Lüert was involved in all aspects of this project and I am truly grateful for her excellent technical assistance and support throughout this period. Steffi Gleisberg provided expertise advice on receptor autoradiography and Susanne Bauch support with laser scanning microscopy. Andreas Heutz provided the computer know-how -- thanks.

Curriculum Vitae

Keneuoe Hycianth Thinyane was born on March 12, 1976 in Leribe, Lesotho. She obtained her bachelor of pharmacy degree (B.Pharm) from the University of the Western Cape, South Africa in 2000. In 2000 she was accepted into the Msc/PhD/MD-PhD Neurosciences Program at the University of Göttingen, Germany and is since 2001 working on a doctoral thesis entitled „Transplantation of mouse embryonic stem-cell derived dopaminergic neurons in a unilateral 6-hydroxydopamine lesion rat model of Parkinson's disease – characterisation of the fate of the engrafted cells and the host responses".

Publication List

Articles

1. P.C. Baier, J. Schindehutte, K. Thinyane, G. Flugge, E. Fuchs, A. Mansouri, W. Paulus, P. Gruss and C. Trenkwalder. Behavioral changes in unilaterally 6-hydroxy-dopamine lesioned rats after transplantation of differentiated mouse embryonic stem cells without morphological integration. Stem Cells 22 (3):396-404, 2004.
2. Keneuoe Thinyane, Paul Christian Baier, Jan Schindehütte, Ahmed Mansouri, Walter Paulus, Claudia Trenkwalder, Gabriele Flügge, Eberhard Fuchs. Fate of Pre-Differentiated Mouse Embryonic Stem Cells Transplanted in Unilaterally 6-Hydroxydopamine-Lesioned Rats: Histological Characterisation of the Grafted Cells (in preparation).

Abstracts

1. J. Schindehuette, P.C. Baier, K. Thinyane, E. Fuchs, W. Paulus, C. Trenkwalder, P. Gruss. Transplantation of dopaminergic neurons derived from murine embryonic stem cells in unilaterally 6-OHDA lesioned rats. 32nd Society for Neuroscience (SfN) Annual Meeting; November 2 – 7, 2002; Orlando, USA.
2. K. Thinyane, P.C. Baier, J. Schindehütte, C. Trenkwalder, E. Fuchs, W. Paulus, P. Gruss, G. Flügge. Transplantation of differentiated murine embryonic stem cells in a 6-hydroxy-dopamine rat model of Parkinson's disease. 3rd International Symposium on Neurorepair and Neuroprotection; May 3 – 10, 2003; Magdeburg, Germany.
3. K. Thinyane, P.C. Baier, J. Schindehuette, G. Flugge, E. Fuchs, W. Paulus, P. Gruss, C. Trenkwalder. Transplantation of differentiated murine embryonic stem cells in a 6-hydroxydopamine rat model for Parkinson's disease. 29th Göttingen Neurobiology Meeting; June 12 – 15, 2003; Göttingen, Germany.

4. K. Thinyane, P.C. Baier, J. Schindehütte, F.W. Schuermann, C. Trenkwalder, E. Fuchs, W. Paulus, P. Gruss, G. Flügge. Transplantation of differentiated mouse embryonic stem cells in 6-OHDA-lesioned rats. 33rd Society for Neuroscience (SfN) Annual Meeting; November 8 – 12, 2003; New Orleans, USA.